REPORT DOCUMENTATION PAGE

Form Approved OMB No. 0704-0188

1. AGENCY USE ONLY *(Leave blank)*	2. REPORT DATE	3. REPORT TYPE AND DATES COVERED
		Annual Feb. 20, 1991 - June 19, 1994

4. TITLE AND SUBTITLE

IMPROVED GALLIUM NITRIDE AND ALUMINUM NITRIDE ELECTRONIC MATERIALS

5. FUNDING NUMBERS

F49620-91-C-0032

61102F

2305/ES

6. AUTHOR(S)

W.D. Partlow, (PI), W.J. Choyke, R.P. Devaty, John T. Yates, Jr., Karl-Heinz Bornschauer, P.J. Chen, C.C. Cheng, M.L. Colaianni, H. Gutleben, A. Hubner, S.R. Lucas, M.F. MacMillan

7. PERFORMING ORGANIZATION NAME(S) AND ADDRESS(ES)

Westinghouse STC
1310 Beulah Road
Pittsburgh, PA 15235-5098

8. PERFORMING ORGANIZATION REPORT NUMBER

AFOSR-TR- 95 0263

94-9SB2-ALGAN-R1

9. SPONSORING/MONITORING AGENCY NAME(S) AND ADDRESS(ES)

Air Force Office of Scientific Research
Bolling Air Force Base
Washington, DC 20332

NE

10. SPONSORING/MONITORING AGENCY REPORT NUMBER

F49620-91C-0032

11. SUPPLEMENTARY NOTES

This document has been approved for public release and sale; its distribution is unlimited.

12a. DISTRIBUTION/AVAILABILITY STATEMENT

Unlimited

12b. DISTRIBUTION CODE

F

13. ABSTRACT *(Maximum 200 words)*

This report describes the results of a three year program to improve the quality of Group III nitride electronic materials. The effort was directed toward understanding and controlling surface-reactive chemical paths toward the growth of GaN. We demonstrated low temperature synthesis of GaN from trimethyl gallium and ammonia by two techniques: a two-step process using atomic hydrogen and electron beams, and a single step process using only an electron beam. The electron beam activation made it possible to grow GaN in patterns.

Several novel tools for the growth and processing of semiconductor materials resulted from this work. (i) A liquid N_2-cooled reflector source of atomic hydrogen was developed for chemical activation and reactive cleaning of semiconductor surfaces. (ii) An electron beam was used to stimulate the GaN synthesis reaction, providing a tool for activation of growth reactions which is an alternative to ion beams. These techniques were particularly effective in removing carbon associated with the methyl radical.

In a parallel effort we carried out cathodoluminescence and infrared reflectance studies of GaN, AlN, superlattices, heterostructures with related wideband materials, providing information on the material defects and structure. We developed a model which allows the extraction of structural information of the component materials from infrared reflectance measurements near the restrahlen region.

14. SUBJECT TERMS

15. NUMBER OF PAGES

16. PRICE CODE

17. SECURITY CLASSIFICATION OF REPORT	18. SECURITY CLASSIFICATION OF THIS PAGE	19. SECURITY CLASSIFICATION OF ABSTRACT	20. LIMITATION OF ABSTRACT
Unrestricted	Unrestricted	Unrestricted	

CLASSIFIED BY:

DECLASSIFY ON:

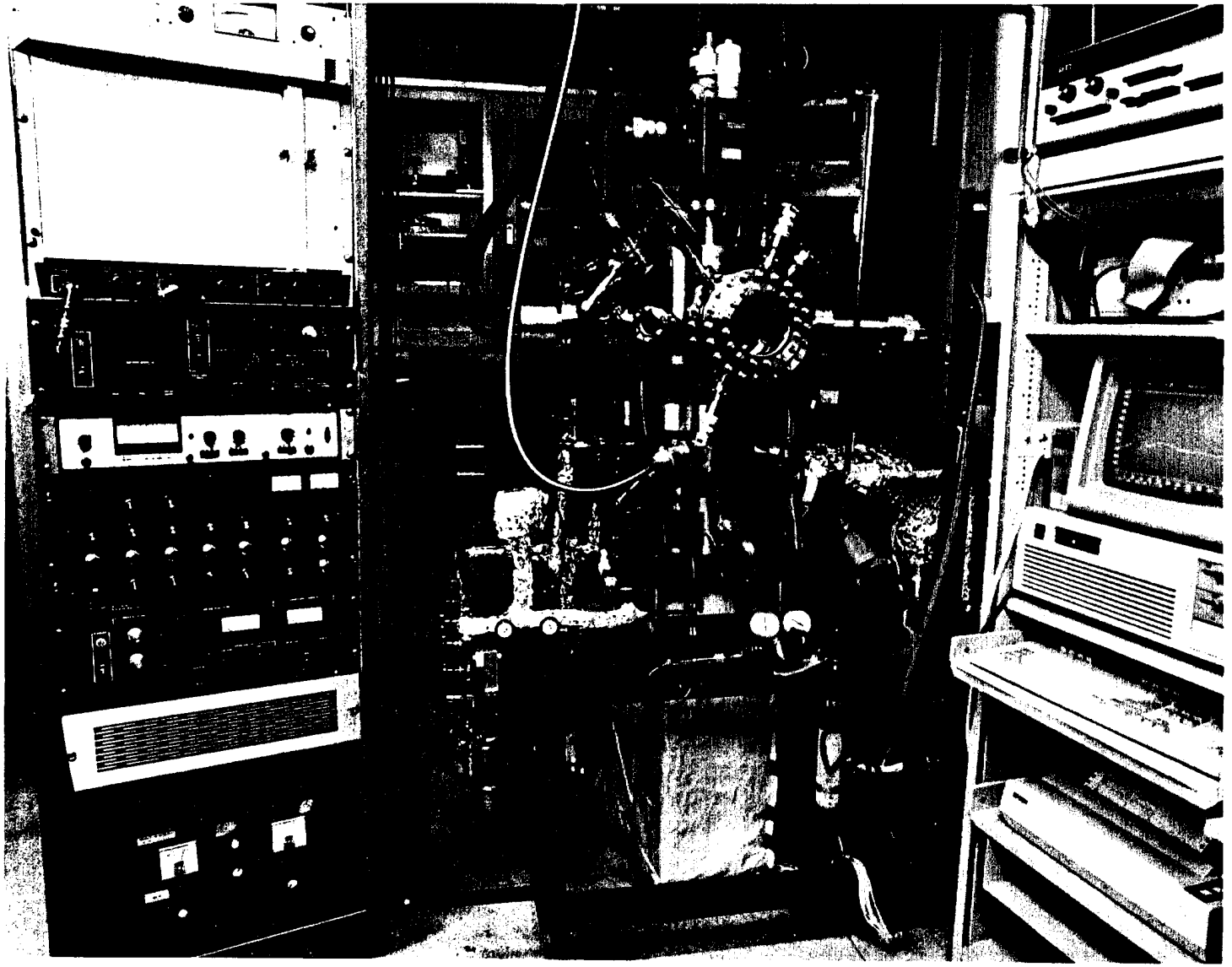

Photograph of the UHV vacuum chamber, analytical tools, and associated electronics used on the study of the synthesis of GaN from alkyl surface reactions.

IMPROVED GALLIUM NITRIDE AND ALUMINUM NITRIDE ELECTRONIC MATERIALS

W. D. Partlow (P. I.), W. J. Choyke, R. P. Devaty,
John T. Yates, Jr., K.-H. Bornscheuer, P. J. Chen, C. C. Cheng,
M. L. Colaianni, H. Gutleben, A. Hubner, S. R. Lucas, M. F. MacMillan

ABSTRACT

This report describes the results of a three year program to improve the quality of Group III nitride electronic materials. The effort was directed toward understanding and controlling surface-reactive chemical paths toward the growth of GaN. We demonstrated low temperature synthesis of GaN from tri-methyl gallium and ammonia by two techniques: a two-step processes using atomic hydrogen and electron beams, and a single step process using only an electron beam. The electron beam activation made it possible to grow GaN in patterns.

Several novel tools for the growth and processing of semiconductor materials resulted from this work. (i) A liquid N_2-cooled reflector source of atomic hydrogen was developed for chemical activation and reactive cleaning of semiconductor surfaces. (ii) An electron beam was used to stimulate the GaN synthesis reaction, providing a tool for activation of growth reactions which is an alternative to ion beams. These techniques were particularly effective in removing carbon associated with the methyl radical.

In a parallel effort we carried out cathodoluminescence and infrared reflectance studies of GaN, AlN, superlattices, and heterostructures with related wideband materials, providing information on the material defects and structure. We developed a model which allows the extraction of structural information of the component materials from infrared reflectance measurements near the restrahlen region.

1. OVERVIEW

The body of this report consists of an executive summary of the program results, presenting our objectives, results, and conclusions in a manner that is readable by technical individuals that are not necessarily experts in surface science, semiconductor material growth, or characterization. The surface chemistry work is presented in Section 2, and the characterization work is presented in Section 3. It is described in much greater detail in the articles that we have published, or submitted for publication in the scientific literature. We provide references to the articles that are now in print, and we have included copies of key articles not yet in print as appendices to this report.

A complete list of the publications and patent disclosures that were produced on this program is provided in Section 4.

2. SURFACE-CHEMICAL SYNTHESIS OF GaN

The objective of this effort was to develop non-thermal paths to the synthesis and growth of Group III nitrides. We concentrated on the reaction of trimethyl gallium: $Ga(CH_3)_3$ with ammonia: NH_3. It is important to use non-thermal synthesis routes with GaN because of its chemical instability at high temperatures[1]. The high equilibrium vapor pressure of nitrogen over hot GaN makes conventional melt or solution growth impossible at pressures below about 15 kbar. The presence of ammonia in the vapor improves the situation considerably[2], but it is widely believed that the nitrogen instability leads to a high level of defects in thermally activated growth of GaN. Super-reactive species, such as nitrogen ions have been provided at the GaN growth surfaces to counteract this effect[3,4,5], and promising results using these approaches have been reported.

As an alternative to these, our approach uses highly reactive atomic hydrogen and electron beams to activate the reaction, specifically excluding ion beams. We believe that our approach has the potential for less collisional disturbance of the growing surface because of the low mass of the electrons (a

3 keV electron has about an order of magnitude less momentum than a 10 eV nitrogen ion). The techniques developed here proved to be extremely effective in removing the carbon that is associated with the methyl radicals of the trimethyl gallium.

By carrying out our experiments at low temperatures in the 100 K range, we have been able to characterize the process kinetics, providing a high degree of understanding that cannot be obtained by other techniques. This includes obtaining the parameters necessary for predicting the process characteristics at more practical growth temperatures in the 900K range, high enough to obtain the surface mobilities needed for good epitaxial growth, but low enough to avoid loss of nitrogen.

The following subsections contain descriptions of the experimental apparatus and methods, the description and characterization of the cooled, low-energy atomic hydrogen source developed on the program, and a discussion of the key experiments in which we removed the methyl radicals from adsorbed layers of trimethyl gallium and converted the resulting layers to GaN.

2.1. Experimental Apparatus

A schematic of the experimental apparatus developed and used for this work is shown in Fig. 2.1. It contains:

a. A multicapillary array molecular doser which provides a calibrated beam of collimated molecules to the surface. It is equipped with a shutter for kinetic uptake measurements;
b. A quadrupole mass spectrometer for collecting species desorbed from the surface. It is housed in a differentially pumped shield, with an aperture that admits gas desorbed from the the central region of the sample, discriminating against desorption from extraneous locations. It is equipped with a bias shield to prevent escape of the electrons from the ion source;
c. An Auger electron spectrometer for surface analysis, and for providing an electron beam for stimulating surface reactions;

d. A reverse view LEED apparatus for structural characterization;

e. A cryogenically cooled reflector source of atomic hydrogen, which is provides a low energy beam of H without the high radiant flux that usually accompanies filament-dissociated H sources.

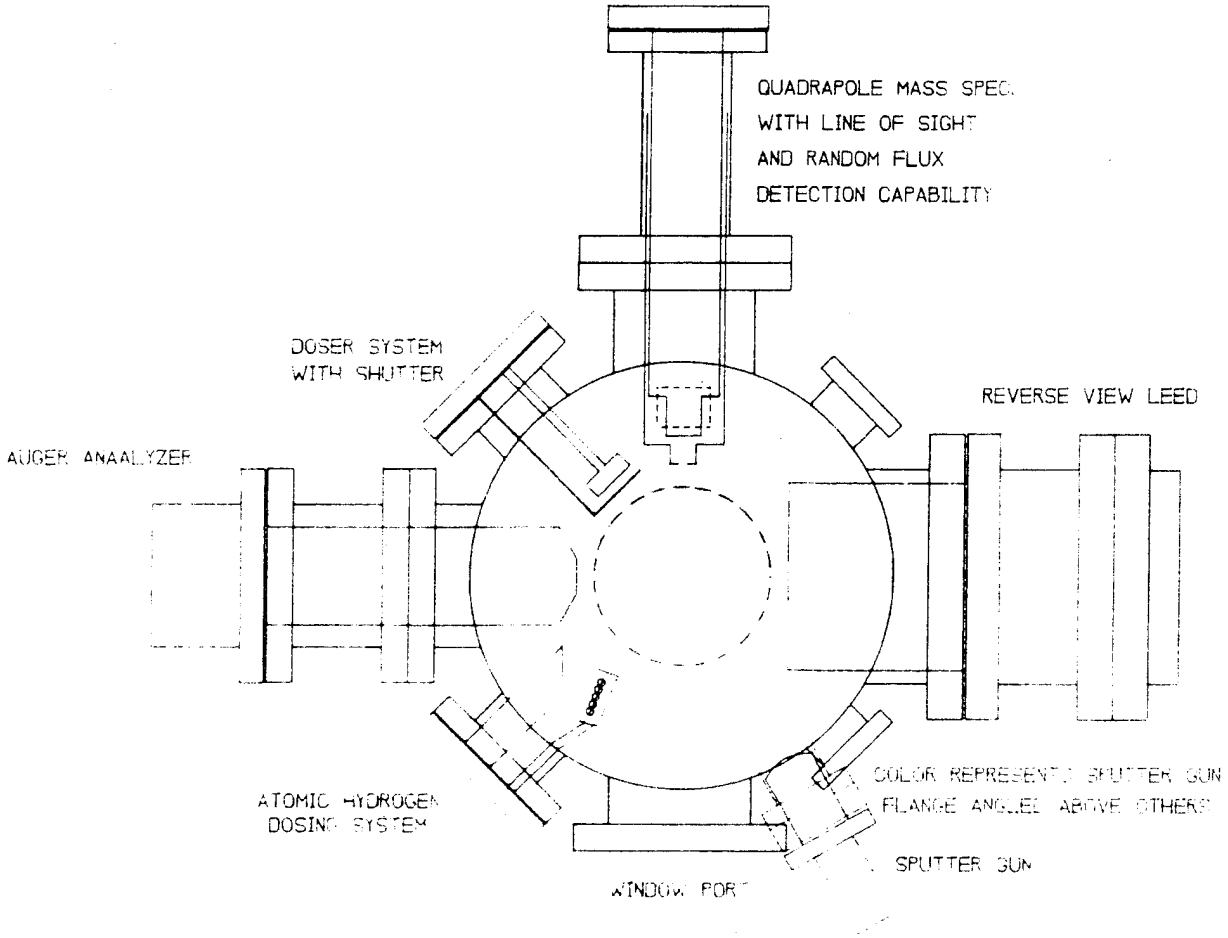

Fig. 2.1Schematic of the UHV surface chemistry apparatus at the University of Pittsburgh used for the study of synthesis of GaN from alkyls.

The steel UHV system is pumped by a 270 l/s in pump, a 150 l/s turbo pump, and a titanium sublimation pump. It achieves a base pressure of $5X10^{-11}$ Torr. This apparatus provides the capability for control and characterization of surface synthesis reactions by introducing known fluxes of neutral species to the sample surface, measuring the kinetics of the adsorption of these species on the surface, measuring surface kinetics by mass spectroscopy of desorbed

species, introducing reactive H and electron beams to activate chemical reactions, and monitoring the composition and character of the surface species to determine the results of the reactions. A photograph of the apparatus is shown as the frontispiece of this report.

2.2. Reflector Atomic Hydrogen Source

This tool was invented[6] on the program to solve the problems caused by excessive sample heating from the hot tungsten filament used to dissociate molecular hydrogen into atomic hydrogen. It takes advantage of the fact that the reflectivity of a cooled Pyrex glass surface is high for atomic hydrogen, but low for optical and infrared radiation, the main mechanism of sample heating. The recombination of atomic H on Pyrex has been reported[7] to be in the range of 10^{-3} to 10^{-4}, while the reflectance of optical and near infrared radiation from the first surface is about 4%. The Pyrex was cooled to about 120 K to avoid possible evolution of impurities due to the incident atomic H. A schematic diagram of the source is shown in Fig. 2.2. It consists of a flat spiral tungsten filament located at that exit of a stainless steel effusive dosing arrangement, shielded from direct line-of-sight exposure to the sample.

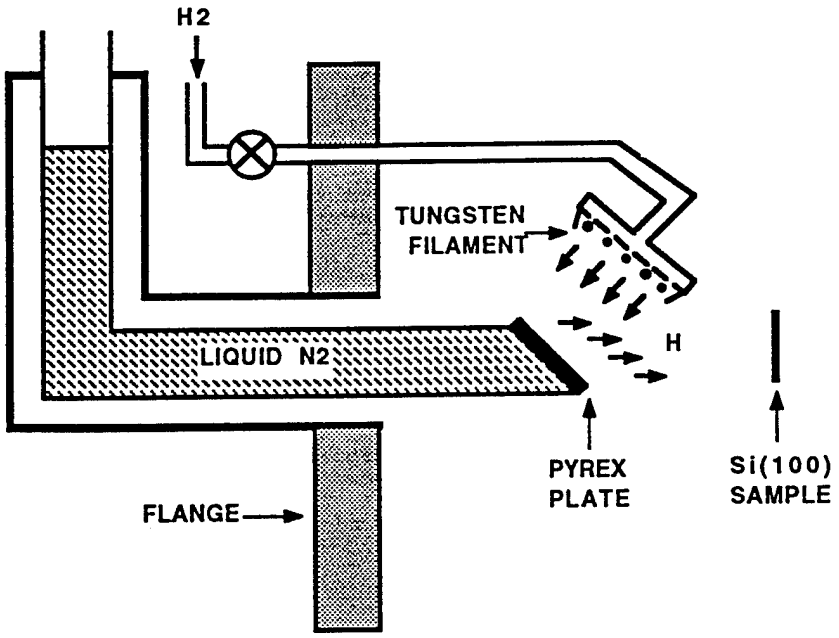

Fig. 2.2 Schematic diagram of the reflector atomic hydrogen source.

We calibrated the source by using a Si(100) crystal surface as a collector, employing temperature programmed desorption of H_2 to measure the amount of atomic H received by the crystal. The temperature dependence of the atomic H production rate as a function of temperature is shown in Fig. 2.3. The data show that above a filament temperature of about 2000 K, the production rate of H reaches a plateau, in agreement with the results of Koehler et. al.[8]. We therefore selected a filament temperature of 1800 K for out experiments, producing a reproducible rate of atomic H generation.

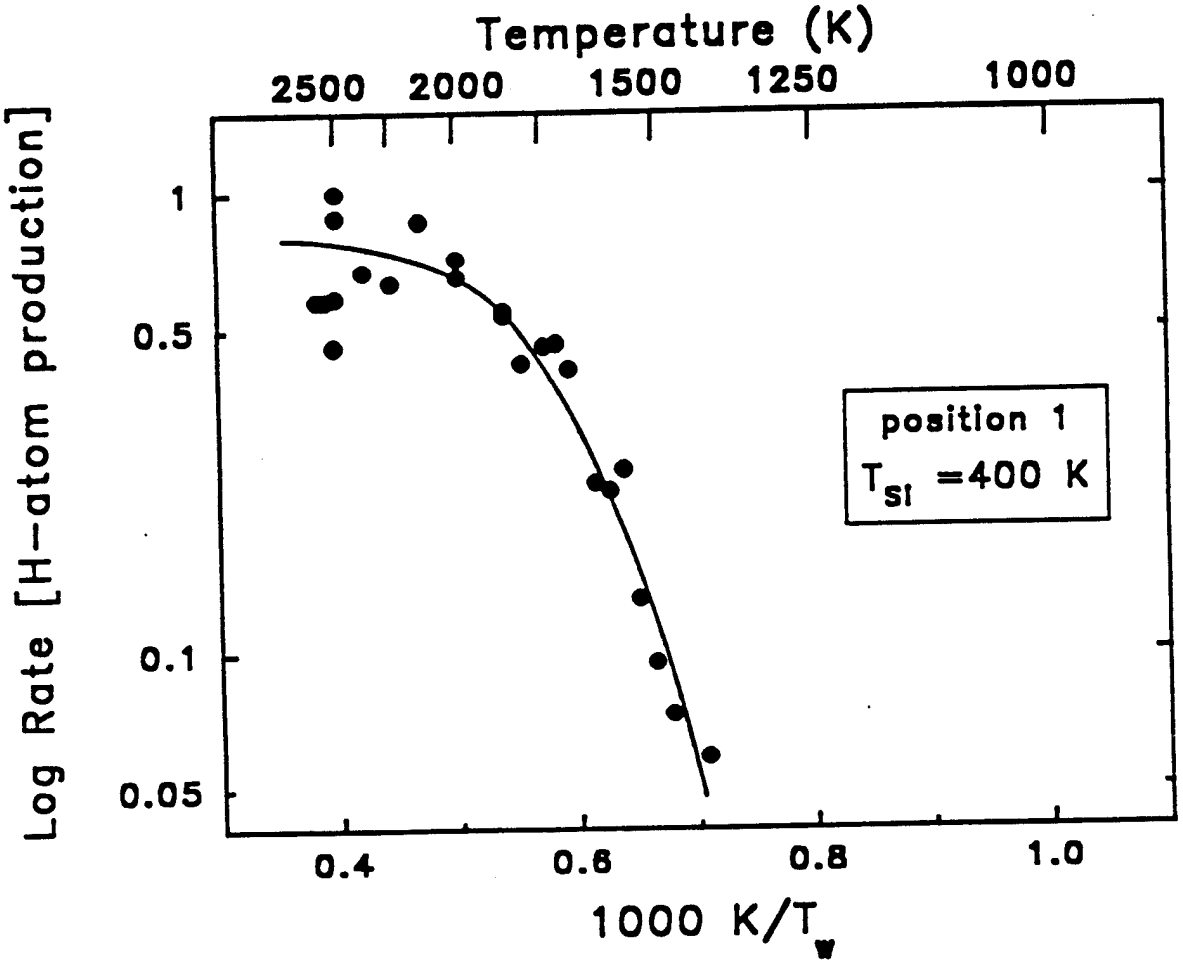

Fig. 2.3 Efficiency of atomic hydrogen production on the tungsten filament of the cooled atomic hydrogen source.

A photograph of the prototype of the atomic H source is shown in Fig. 2.4, showing it rugged and practical construction, and compatibility with standard

UHV systems. We believe that the cool, clean atomic H beams produced by this source would be useful for many applications for surface cleaning where surface damage, heating, and impurities must be minimized.

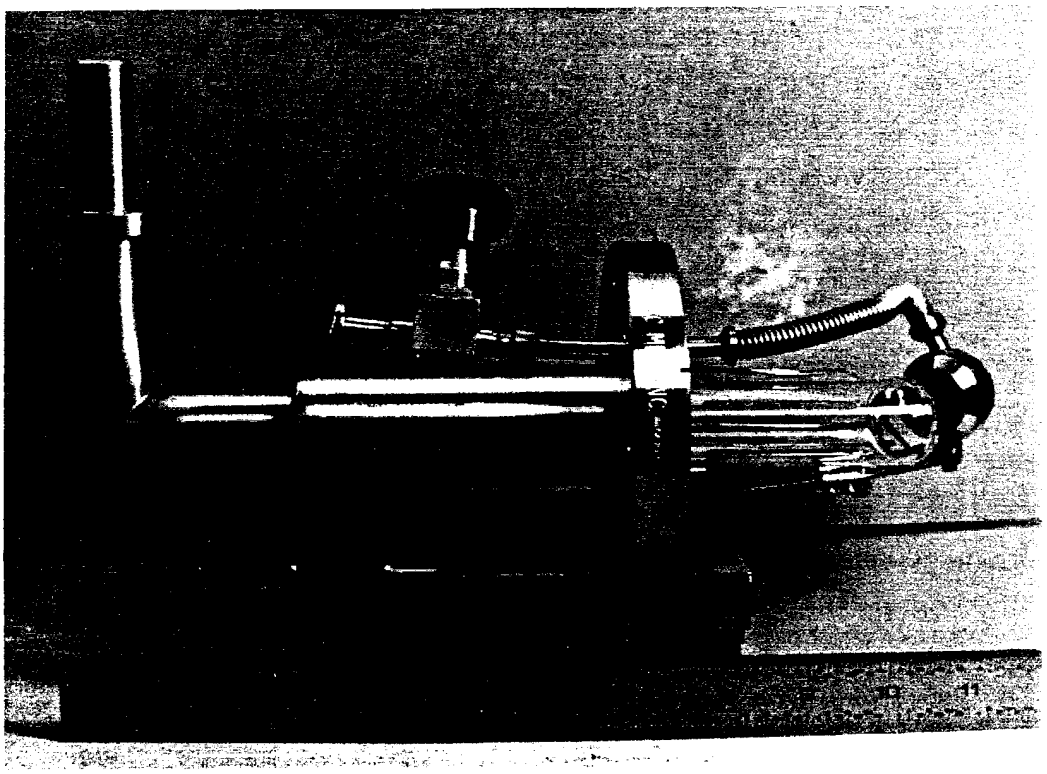

Fig. 2.4. Photograph of the prototype cooled reflector-atomic H source used in this work.

2.3. Decomposition of $Ga(CH_3)_3$-Derived Layers By Atomic H

We used atomic H from our cooled reflector source to deplete the carbon from layers produced by adsorption of $Ga(CH_3)_3$ on SiO_2 surfaces[9]. It is known[10] that $Ga(CH_3)_3$ partially dissociates on SiO_2 surfaces to form $Ga(CH_3)_2$, so we designate this first layer as $Ga(CH_3)_x$. The dissociation is postulated to occur on the surface Si-O-Si groups. Using temperature programmed desorption, we have observed that from this monolayer , $Ga(CH_3)_2$ (m/e = 99) desorbs at its maximum rate at 155 K, as shown on the bottom desorption spectrum of Fig 2.5. For this monolayer coverage, almost no $Ga(CH_3)_3$ (m/e = 114) is seen to desorb.

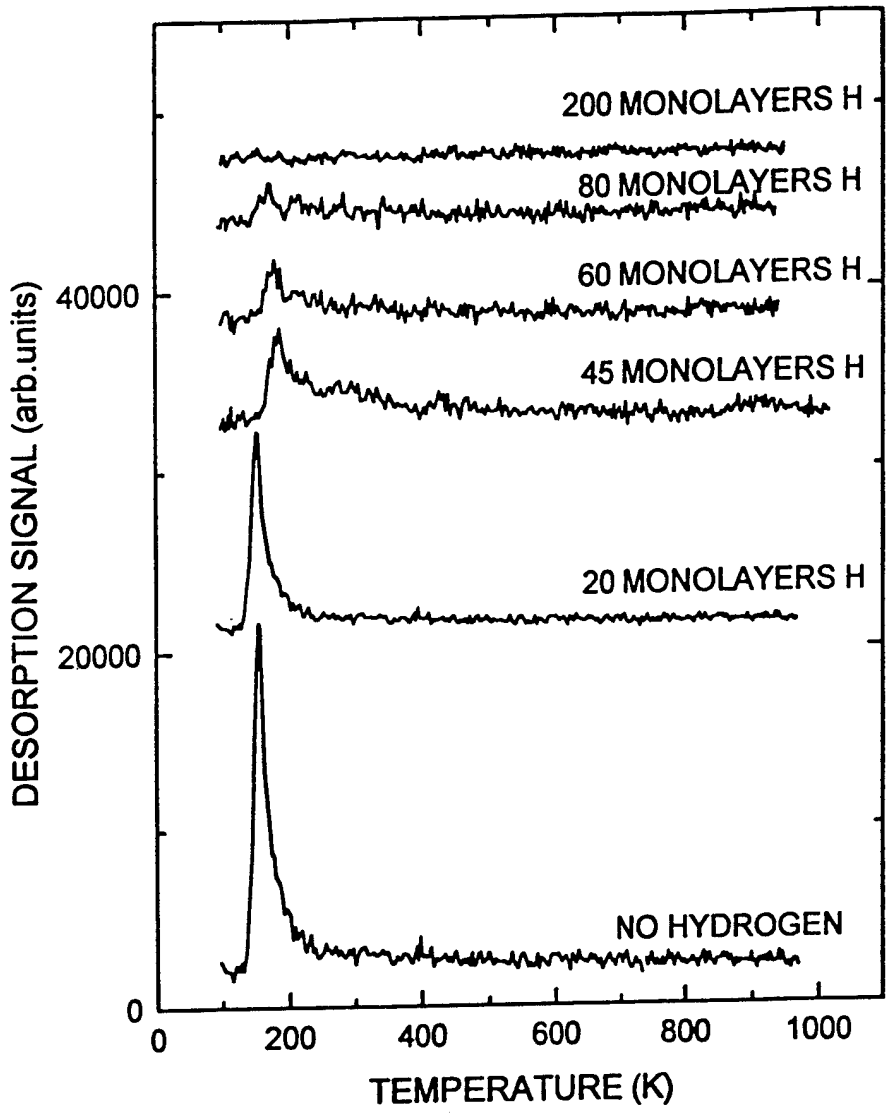

Fig. 2.5. Depletion of m/e = 99 thermal desorption product following various atomic H exposures at 108 K Complete loss of this product is observed for approximately 100 monolayers of atomic H exposure.

Upon exposing the surface at 108 K to various doses of atomic H, it is evident that the $Ga(CH_3)_x$ is depleted from the surface, and after about 100-200 monolayers of atomic H exposure it is completely removed. This conclusion is substantiated by the similar behavior seen in the the Ga^+ fragment (m/e = 69), as shown in Fig. 2.6. Subsequent Auger spectroscopy measurements indicate that after exposure of the surface with atomic hydrogen, elemental Ga remains

up to temperatures of 800 K. These results show that atomic H activates a major modification of the layers derived from $Ga(CH_3)_3$ adsorption, and the final product appears to be devoid of C. The kinetic experiments described in the following section show that this is indeed the case.

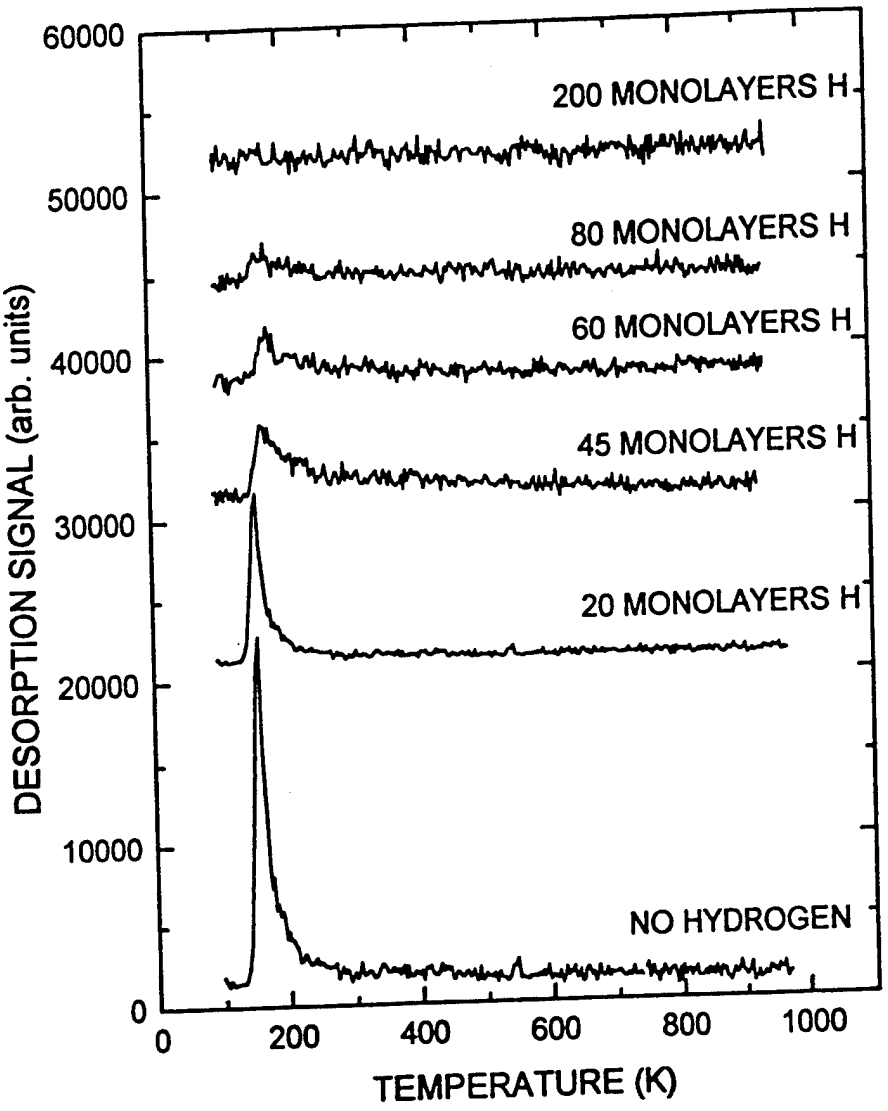

Fig. 2.6. Depletion of the m/e = 69 thermal desorption product following various atomic H exposures at 108 K. Complete loss of this product is observed for approximately 100 monolayers of atomic H exposure.

2.4. Kinetics of Extraction of CH_3 by Atomic H

Three experiments to examine the kinetics of CH_3 extraction by atomic H were performed in the temperature range of 97 K to 138 K. Auger spectroscopy was employed to monitor both the C(KLL) and the Ga(LMM) intensities following various exposures to atomic H. Each measurement was made after moving the crystal so that a fresh region of the crystal was exposed. The left hand side of Fig. 2.7 shows the Auger measurements. It is seen that the C is depleted efficiently by atomic H exposure, and to within experimental error, it is totally depleted after about 100 monolayers exposure of atomic H, in agreement with the measurements described above.

The behavior of the Ga (LMM) Auger signal during exposure to atomic H is also consistent. Initially, a slight decrease in the Ga(LMM) signal is observed. This is followed by an overall increase as the CH_3 groups are removed. The slow increase in Ga(LMM) is due to a reduction of the screening of primary and Auger electrons, as expected from the reduction in the surface coverage of CH_3 groups.

The right hand side of Fig. 4 presents the C(KLL) Auger intensity in a semilog plot as a function of exposure to atomic H. The linear behavior observed is indicative of a CH_3-extraction reaction which is first order in the surface coverage of CH_3 groups. The slope of the first order plots is independent of substrate temperature over the 41 K range investigated. From these slopes, and estimated errors, an activation energy for the H-induced extraction process is determined to be 0 (+0.09, -0.02) kcal/mole.

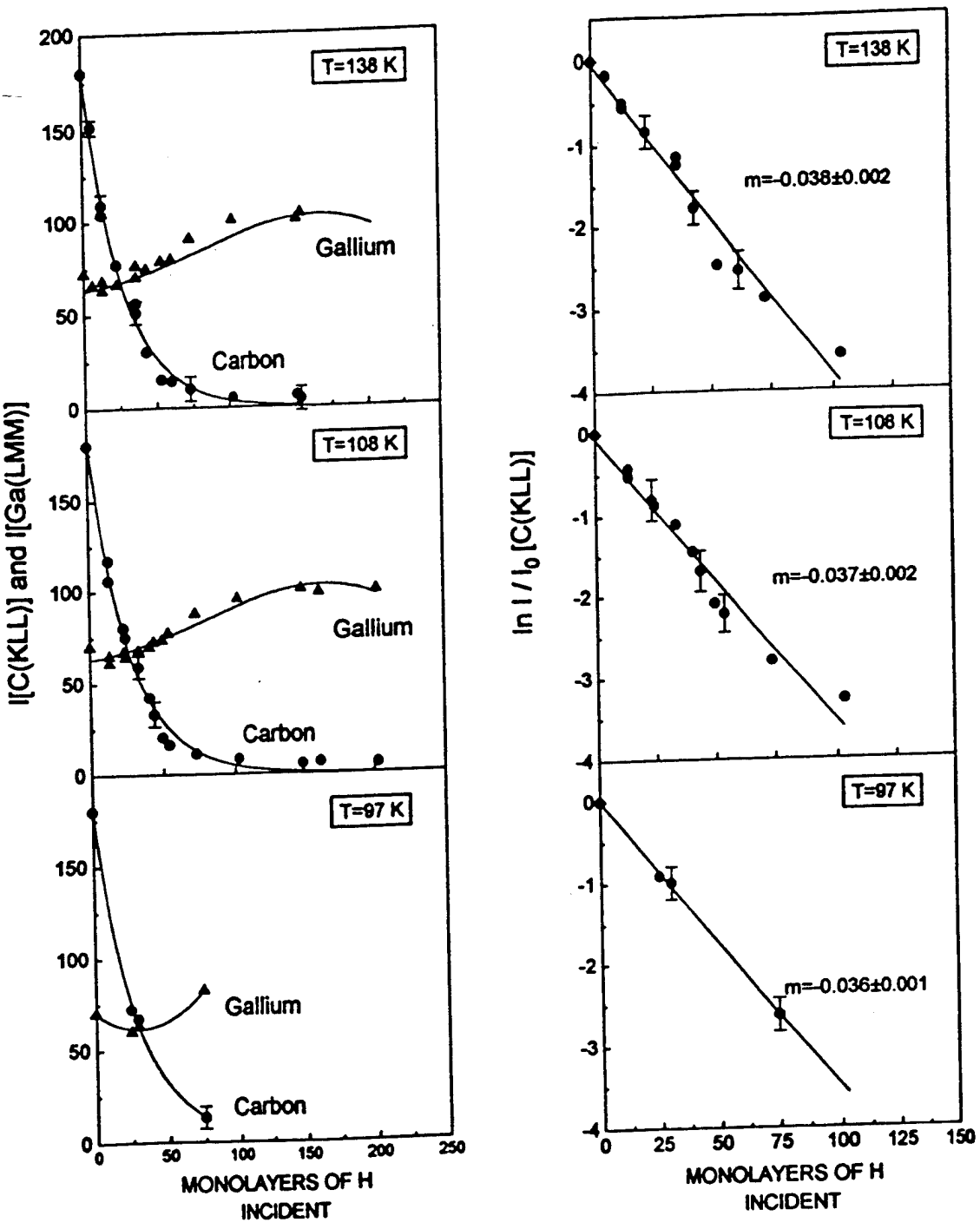

Fig. 2.7 Kinetics of extraction of CH_3 by atomic H from one monolayer of $Ga(CH_3)_x$ on SiO_2/Si(100) at three temperatures. The behavior of both the C(KLL) and the Ga(LMM) Auger intensities are shown on the left. On the right, semilog plots of the c(KLL) Auger signals are shown.

2.5. Electron Beam Conversion of H-Stripped Layers to GaN

We demonstrated the synthesis of GaN monolayers from the $Ga(CH_3)_3$-derived layers that had been stripped of carbon with atomic H. The chamber was backfilled with NH_3 to produce a steady state coverage of NH_3 on the surface. Since metallic Ga does not react with NH_3 at our sample temperatures, the nitriding reaction must be activated, and we selected an electron beam for this purpose. The central portion of the sample was exposed to electron bombardment with the electron beam from the Auger spectrometer, and a dot of GaN was produced in this location. This was verified by the shape of the Auger N(KLL) signal (which will be discussed later in this section) , and by the thermal desorption characteristics: the dot did not change significantly upon heating to 900K, while the unreacted region around the dot essentially vanished. The entire process is summarized in Fig. 2.8. This demonstration proved the basic feasibility of the process for producing GaN, but the process is complicated, and difficult to envision as a practical growth technique. In the following sections, we describe a much more practical process in which the carbon stripping and the nitridation is done in one step with an electron beam.

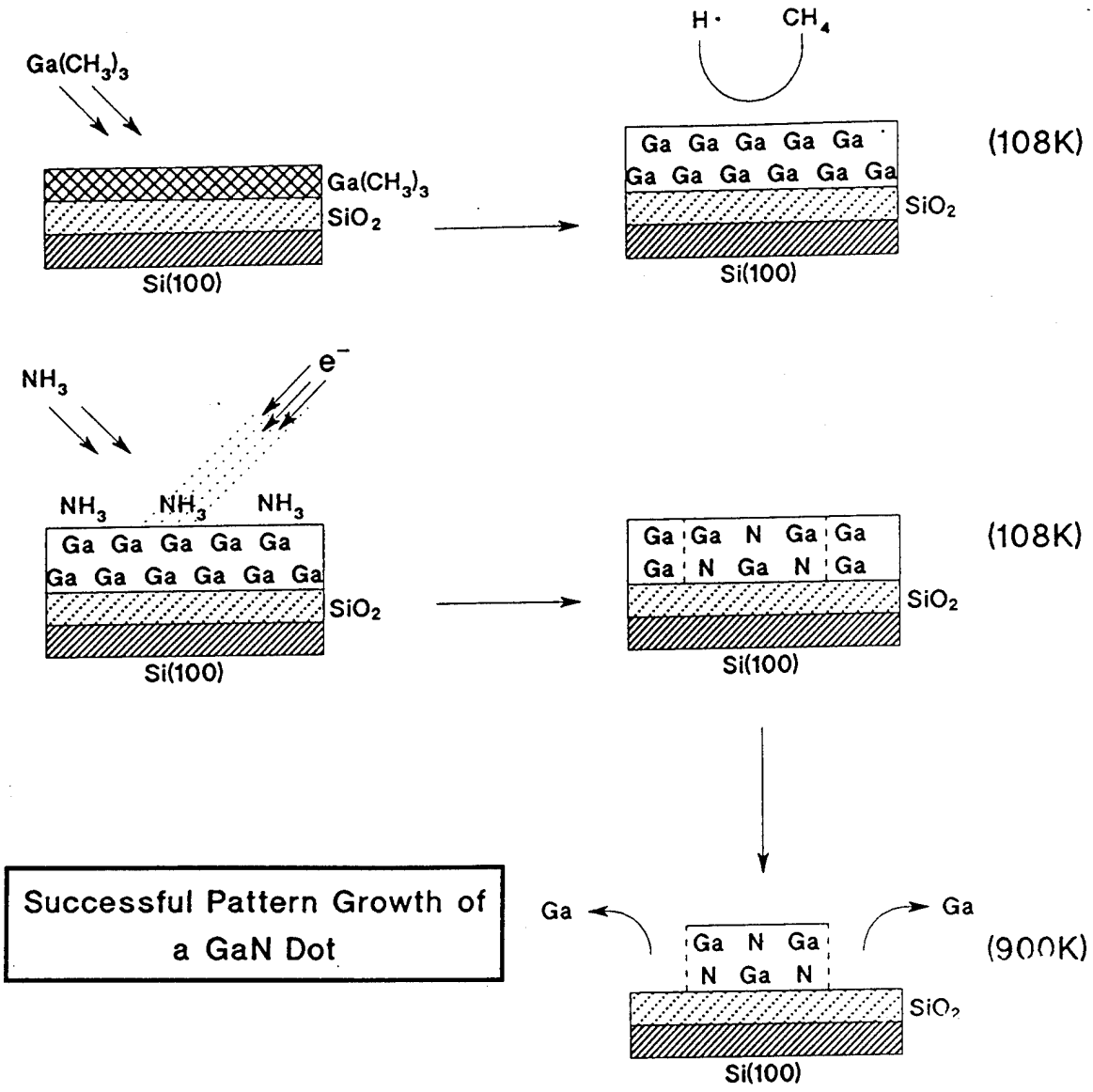

Fig. 2.8, Schematic representation of the two-step process for forming monolayers of GaN.

2.6. Electron-Induced Reactions of NH_3 With $Ga(CH_x)$

Building on the demonstrated ability of atomic H to break the Ga-CH_3 bond, we carried out experiments[11] in which the source of atomic H was the electron bombardment of adsorbed NH_3 in the presence of an adsorbed monolayer of $Ga(CH_3)x$. This was done by backfilling the vacuum chamber with NH_3 immediately following adsorption of $Ga(CH_3)_3$ on a SiO_2 surface, and subjecting the mixed layer to the electron beam. The results of the experiment for three NH_3 pressures is shown in Fig. 2.9. On the left side of the figure, the decrease in the C(KLL) Auger intensity, compared to control experiments with no NH_3, is shown for increasing exposure to electrons. The rate of CH_3 removal increases monotonically with the pressure of NH_3, and hence the coverage of NH_3 and with the supply of atomic H produced from the adsorbed NH_3. Linear semilogarithmic plots, shown in the right side of Fig. 2.9, indicate that the kinetics of removal of CH_3 groups are first order in the surface coverage of CH_3 groups. A cross section, QP_{NH_3}, for the removal process, was determined from these plots. As expected, it was observed to increase for increasing ammonia pressure, P_{NH_3}, which increased the NH_3 coverage.

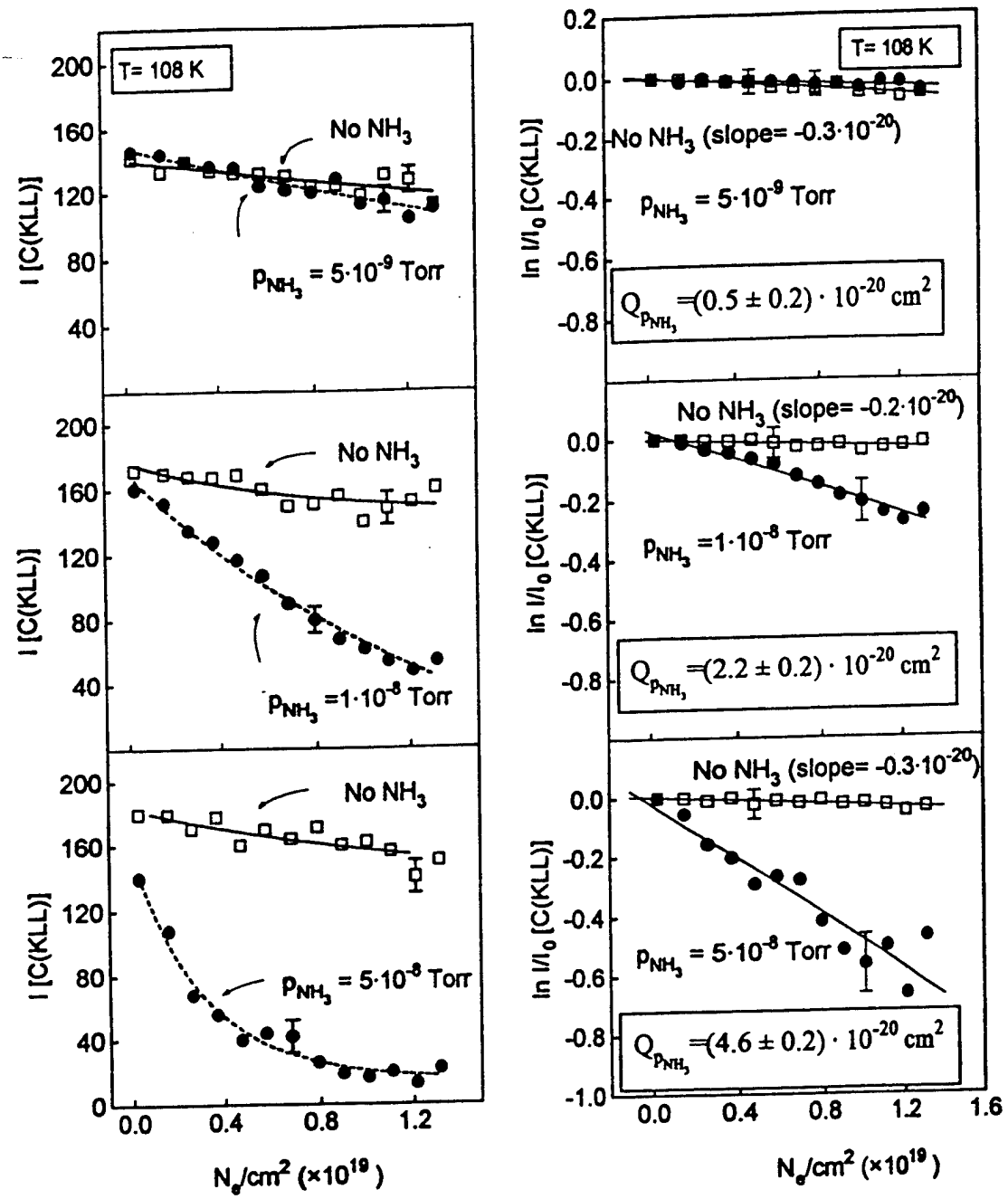

Fig. 2.9. Electron-induced reaction of NH_3 with $Ga(CH_3)_x/SiO_2$. Shown is the C(KLL) Auger signal (left side) and its normalized natural logarithm (right side) versus the number of electrons per cm^2.

Confirming that the CH_3 groups were being preferentially removed from the $Ga(CH_3)_x$ monolayer by the use of atomic H produced from adsorbed NH_3, Fig. 2.10 shows the behavior of the Ga(LMM) Auger intensity for the same experiment that is shown in Fig. 2.9. On the left side of Fig. 2.10, the Ga(LMM) intensity is plotted versus the fluence of electrons. A semilogarithmic lot of the Ga behavior is shown on the right side. It is seen that within experimental errors, the small rate of loss of Ga(LMM) intensity in the electron beam does not change when the NH_3 pressure is raised to 5×10^{-8} Torr. A comparison of the rate of carbon loss and the rate of Ga loss (Figs. 2.9 and 2.10) for the same pressure of NH_3 shows that the rate of loss of carbon is comparatively high as a result of the interaction of the electron beam in the presence of adsorbed NH_3. Control experiments in a background of N_2, monitoring both C and Ga, indicated that no measurable depletion effect exists as a result of the presence of N_2. Thus the CH_3 removal process, using electron beam excitation, is correlated with the presence of species containing hydrogen, namely, NH_3.

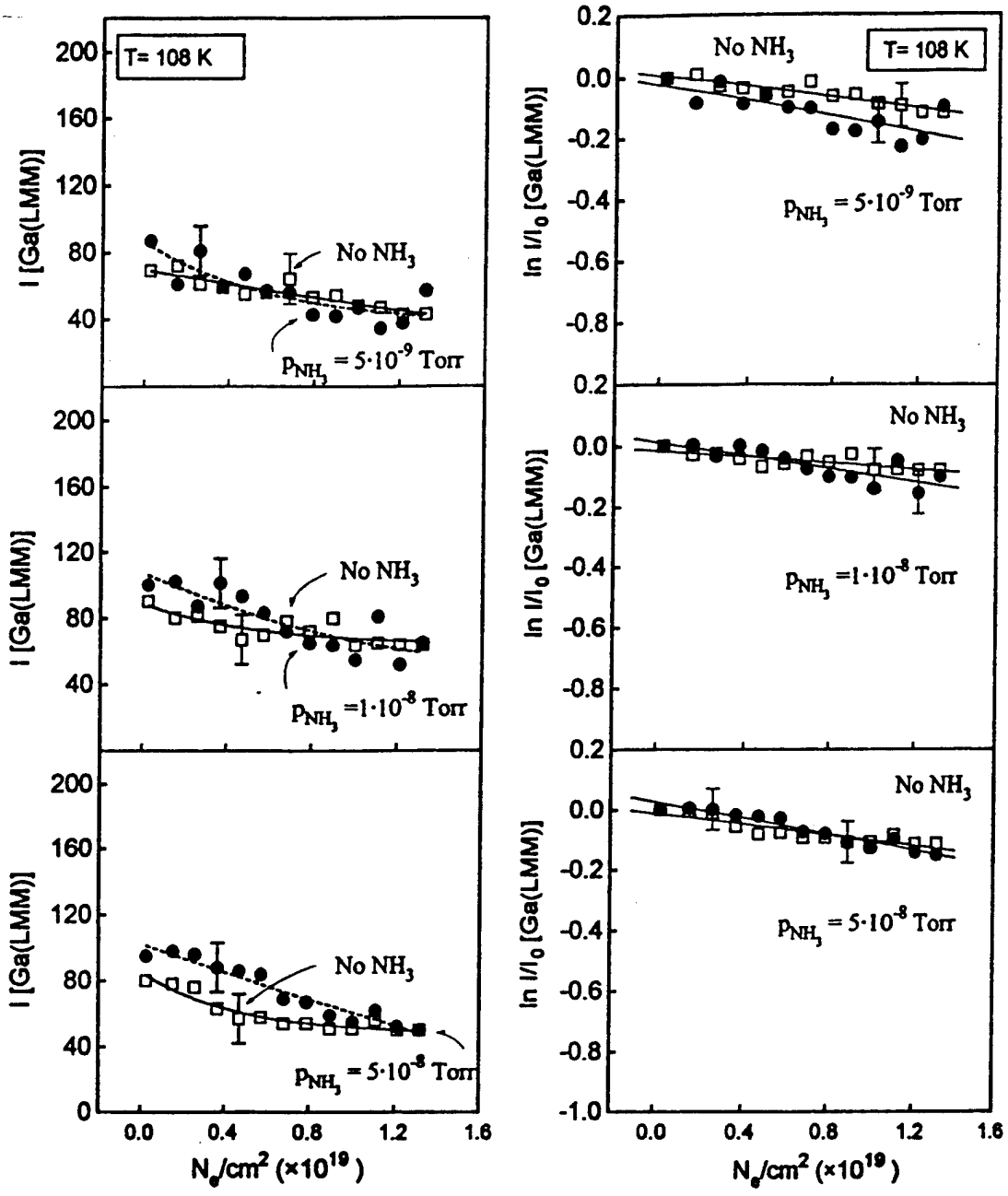

Fig. 2.10. The Ga(LMM) Auger signal(left side) and its normalized natural logarithm (right side) versus the number of electrons per cm^2 for the electron-induced reaction of NH_3 with $Ga(CH_3)_x/SiO_2$.

2.7. Direct Formation of GaN Patterns with an Electron Beam

Utilizing the capability of the electron beam to both strip the carbon and activate the nitridation we produced GaN dots in a single step process as shown schematically in Fig. 2.11. The reaction described in the Sect. 2.6 was carried out in a localized region in the center of the substrate, producing GaN in the area exposed to the beam. As before, we found that heating the sample to 900 K resulted in removal of the species from the non-irradiated regions, and the stable GaN remained.

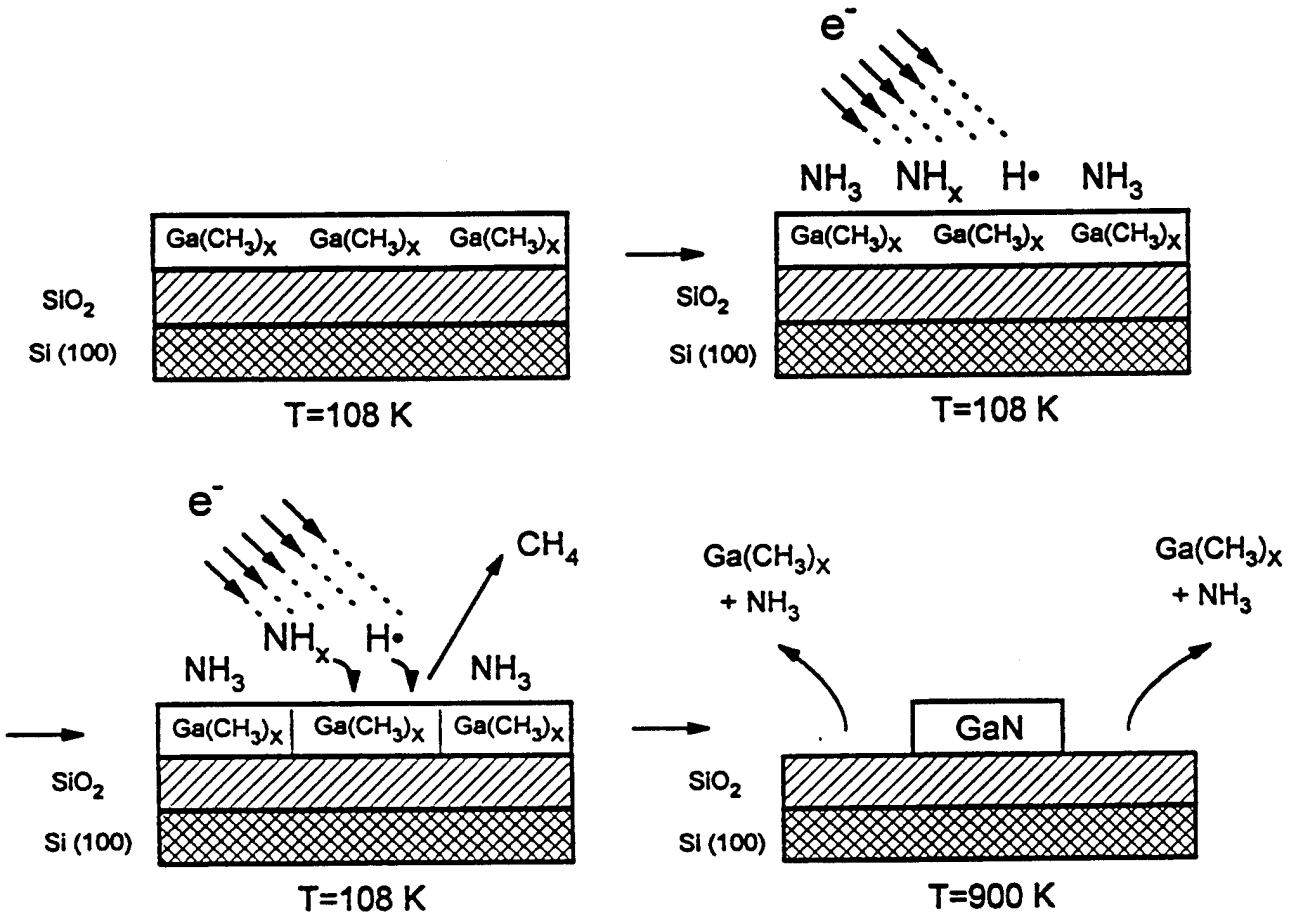

Fig. 2.11. Schematic diagram of the mechanisms for GaN production by an electron-induced reaction of adsorbed $Ga(CH_3)_3$ with NH_3 at 108 K.

The data supporting this picture are shown in Fig. 2.12. The left side shows three schematics of the layer structure at key points in the process, while the right side shows that Auger spectra for each . The top row shows the Auger spectrum of the adsorbed $Ga(CH_3)_x$. Following electron exposure in ambient NH_3, the second row shows that C has been removed , only N and Ga signals are seen. Upon heating to 300 K, the lower spectra show that the N and Ga signals are unchanged in the irradiated area, but are greatly reduced elsewhere, indicating that the stable GaN produced in the center is unaffected, but the volatile unreacted species have desorbed.

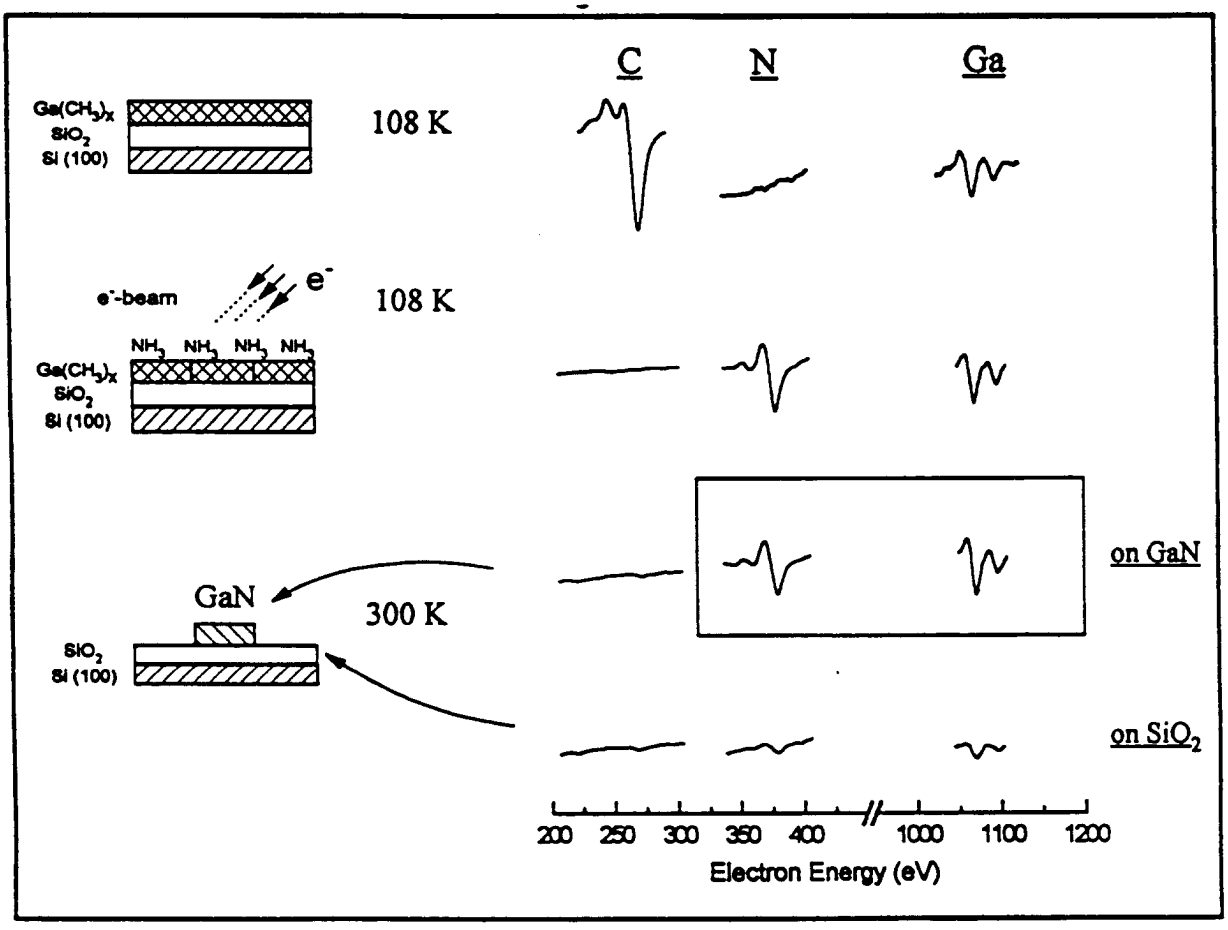

Fig. 2.12. Monolayer GaN synthesis on SiO_2 by an electron-induced reaction of $Ga(CH_3)_x$ with NH_3 at 108 K.

We repeated the procedure shown in Fig 2.11 a second time to grow another layer of GaN on the dot. We see in Fig 2.13 that almost complete removal of carbon has been achieved by the electron beam + NH_3 treatment, and prominent N and Ga features are observed to remain in the irradiated region following heating to 900 K. By this temperature, even smaller residual signals are seen on the non-irradiated regions.

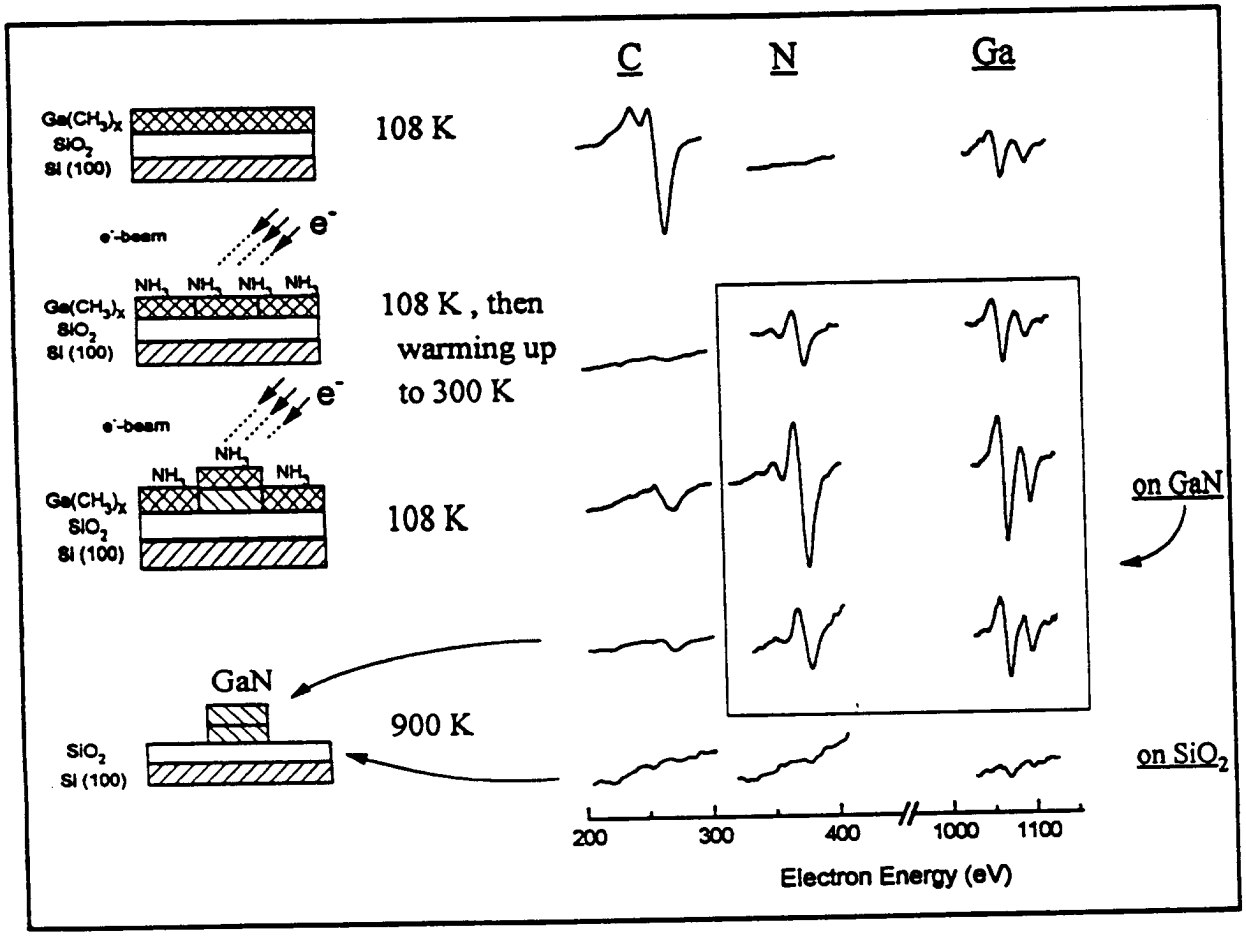

Fig. 2.13. Multilayer GaN synthesis on SiO2 by an electron-induced reaction of adsorbed $Ga(CH_3)_3$ with NH_3 at 108 K.

2.8. N(KLL) Auger Lineshape for Electron Beam-Produced GaN

The N(KLL) Auger feature of the GaN dot, both for monolayer and multilayer preparation, is shown in Fig. 2.14, along with the Auger line from a thick layer of GaN and from a thick layer of Si_3N_4. For a film of GaN produced at the one monolayer level, both GaN and Si_3N_4 will be observed by Auger spectroscopy, since Si_3N_4 is also made by the electron beam on the SiO_2 substrate. With increasing thickness of the GaN film, the N(KLL) Auger lineshape will approach that of GaN, but as long as the thickness of the GaN film is of the order of the escape depth of the Auger electrons, about 10Å, there will be a contribution from the underlying Si_3N_4 also, as seen in Fig. 2.14. This may contribute to the lack of exact agreement in the N(KLL) Auger lineshape with that measured for the GaN standard. The data of Fig. 2.14 indicate that the multilayer Auger line shape more closely agrees with the lineshape for bulk GaN than does the monolayer GaN lineshape (as expected).

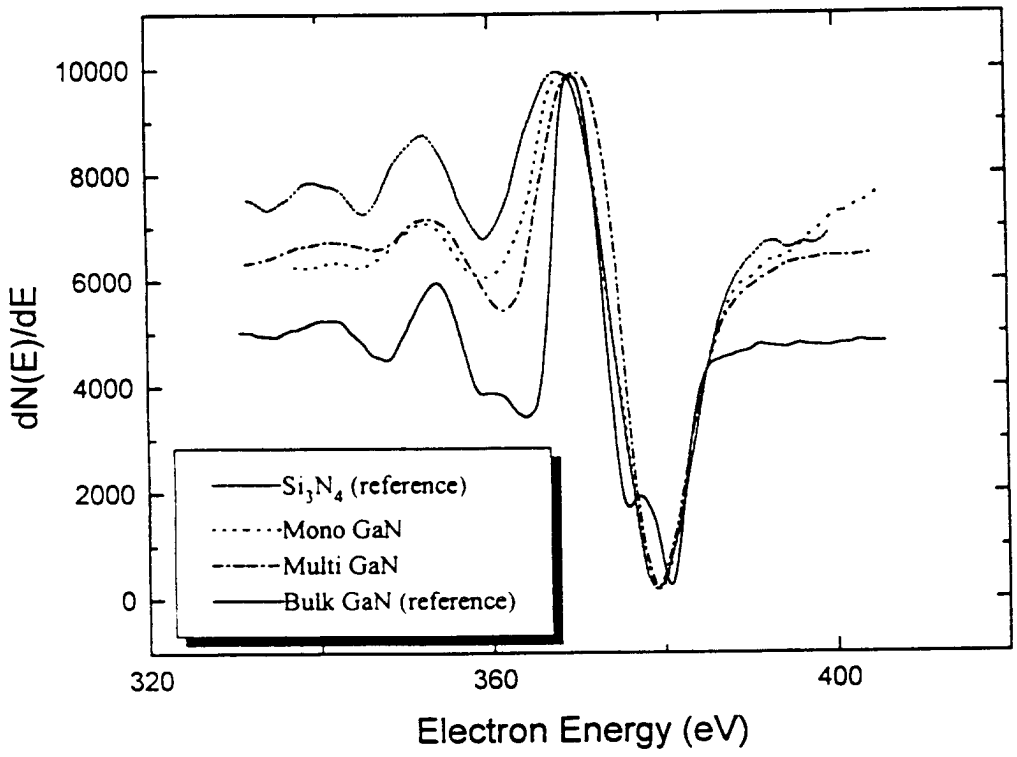

Fig. 2.14. Normalized and superimposed lineshapes of the N(KLL) Auger signal with increasing thickness of the GaN film. Comparisons to reference thick films of GaN and Si_3N_4 are given.

2.9. Growth of a GaN Line with the Electron Beam

The procedure to produce a dot of GaN was modified to produce a line , and the Auger profile perpendicular to the line was acquired as shown in Fig. 2.15. It was grown at 108 K without subsequent heating, so that both $Ga(CH_3)_x$ and NH_3 remained adsorbed outside of the line. The C(KLL) Auger signal is seen to be small on the GaN line, but high off the line, while the N(KLL) Auger signal shows the opposite behavior. The data are arbitrarily fitted to a Gaussian profile for smoothing, but it is not the the actual functional dependence.

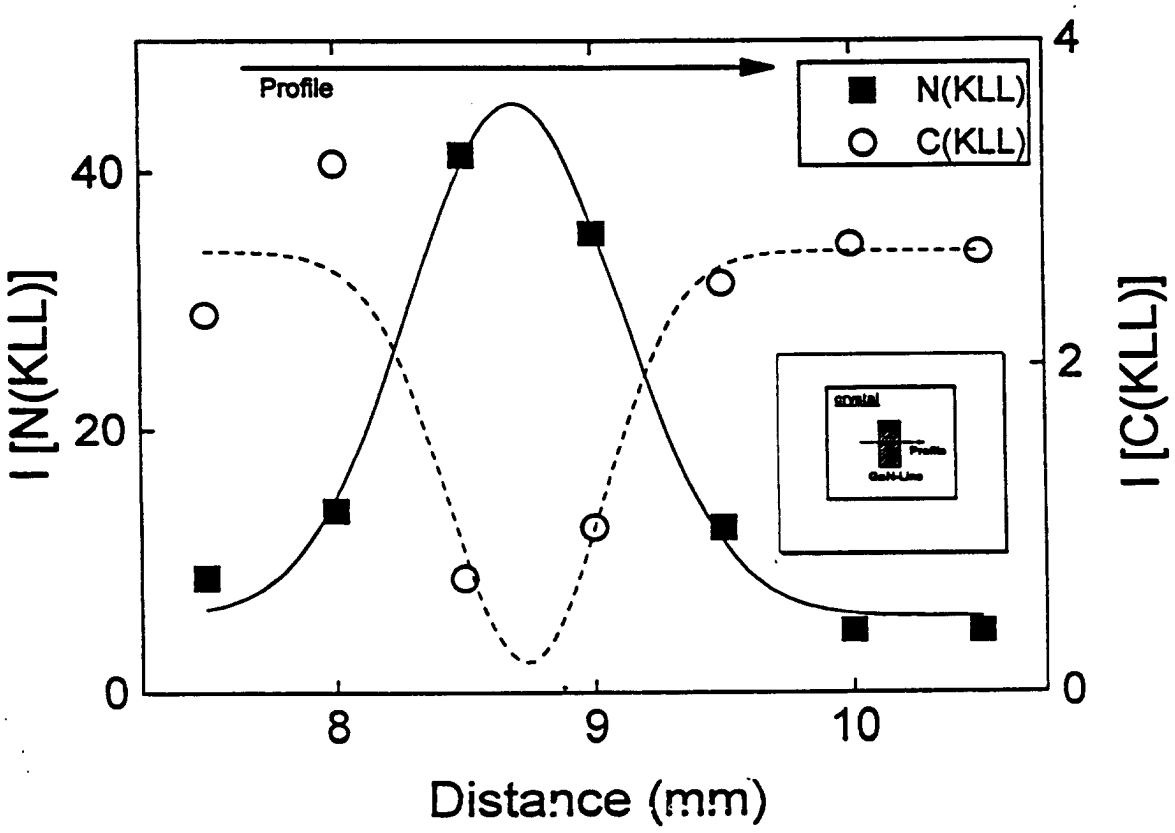

Fig. 2.15. Profiles of C(KLL) and N(KLL) Auger signals taken across a GaN line grown by electron beam reaction of NH_3 with $Ga(CH_3)_x/SiO_2$.

2.10. Discussion

2.10.1. Mechanism of Ga-CH_3 Bond Breaking by Atomic Hydrogen

As this experimental work was being carried out, a theoretical understanding of the interaction of atomic hydrogen with metal alkyls was achieved by Hiraoka and Mashita, using ab-initio methods[12]. Their study was directed toward the understanding of the reaction of atomic H with $Al(CH_3)_3$, and they employed the $H_2Al(CH_3)$ molecule as a model for the trimethylaluminum. Fig. 2.16 illustrates important facts about the attack of atomic H on the Al-CH_3 bond, as deduced by the ab-initio calculations. A hydrogen atom attacks the Al center in the $H_2Al(CH_3)$ molecule, producing a stable $H_3Al(CH_3)$ intermediate species, with an energy of -3.0 kcal/mol compared to the reactants. This local minimum energy state can then undergo two reactions. Reaction channel a leads to the dissociation of the Al-C bond, producing a CH_3 radical which leaves. The activation energy for reaction a is only 1.9 kcal/mole. An alternate chemical route is the production of a transition complex via reaction channel b. Here the hydrogen atom inserts into the Al-C bond, also causing the bond to break, and producing a CH_4 molecule. The activation energy for this process is calculated to be 12.7 kcal/mole. This overall reaction is exothermic by 21.7 kcal/mole.

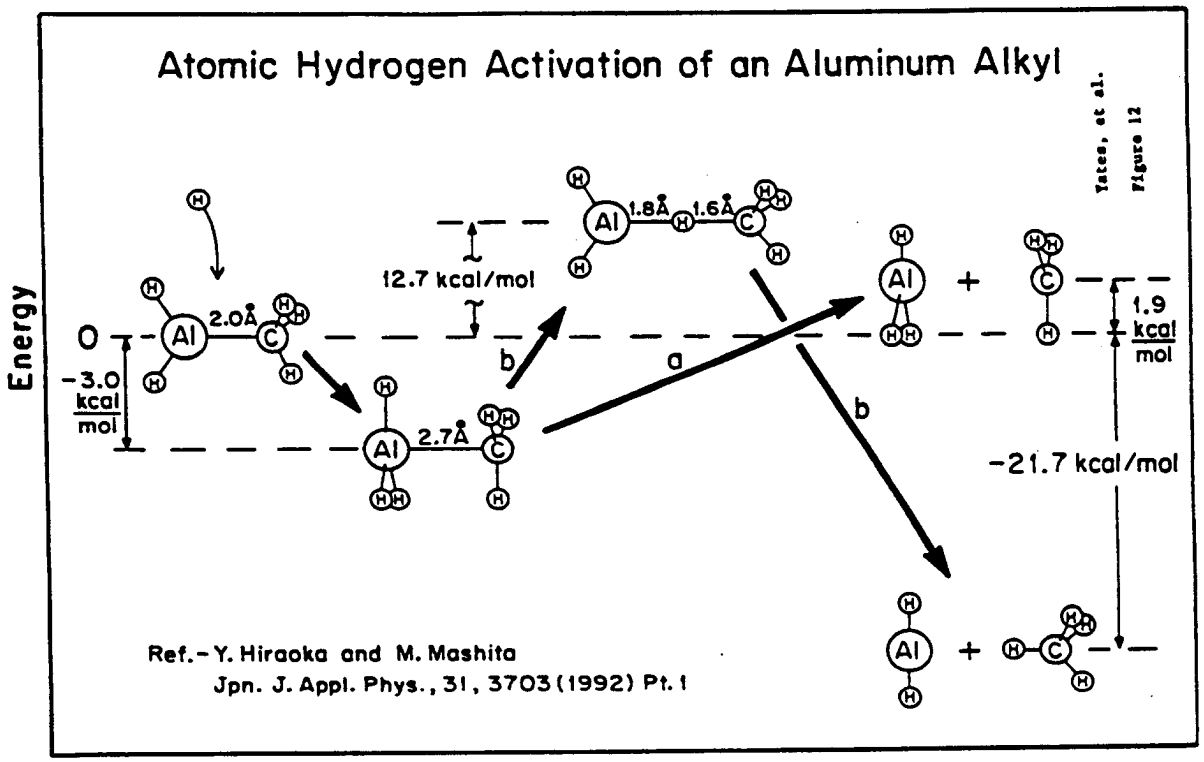

Fig 2.16. Atomic hydrogen activation of an aluminum alkyl from ab-initio calculations.

It is likely that similar reactions exist for $Ga(CH_3)_x$ species when interaction with atomic hydrogen occurs. From our measurements, it is not possible to determine whether reaction channel **a** or **b** is most favored, but both of them involve the scission of the metal-carbon bond and the loss of carbon, either as CH_3 or as CH_4. Further support for the attack of atomic H on the metal atom can be found in recent studies[13] by Downs et al., where, under hydrogenation conditions, $Ga(CH_3)_3$ is converted to a digallium molecule containing two bridging hydrogen atoms as shown in Fig. 2.17. This molecule, whose structure has been determined by electron diffraction, represents the first definitive structural characterization of a compound containing two Ga atoms linked by a hydrogen bridge. The digallium molecule is stable to 290 K. The ab-initio

calculations and the structural verification of the replacement of a Ga-CH_3 bond by a bridging H atom leaves little doubt that similar chemistry may be achieved by the exposure of surface species containing Ga-CH_3 bonds to atomic H, as demonstrated in the research reported here. In both cases, attack of the metal atom by atomic H occurs with the elimination of the Ga-CH_3 bond. The low activation energy calculated for the CH_3 elimination compared to CH_4 elimination, in the case of the aluminum compound, may indicate that CH_3 elimination is the favorable kinetic route for the Ga-CH_3 system.

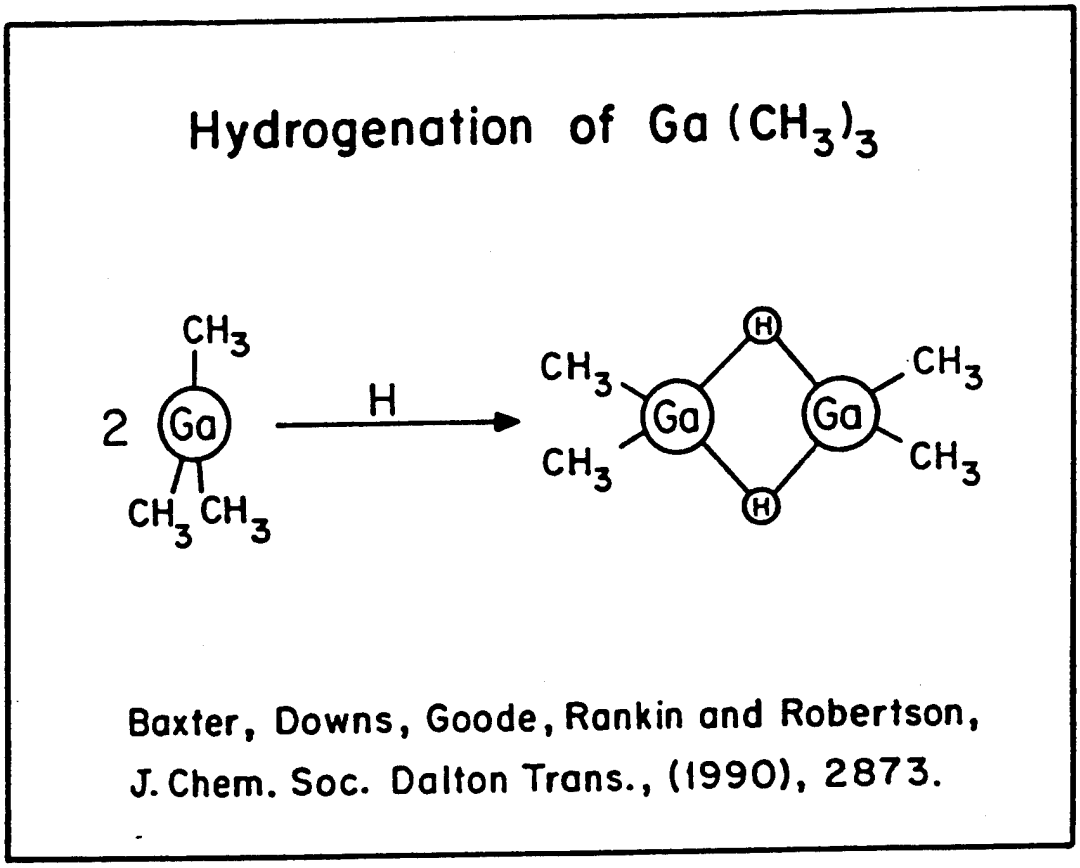

Fig. 2.17. Reaction scheme leading to the displacement of CH_3 groups from $Ga(CH_3)_3$ under hydrogenation conditions.

2.10.2. Relationship to MOCVD Production of III-V Compounds

This new reaction, involving H atom insertion into Ga-CH_3 bonds, could be very important in MOCVD of MBE processes in which atomic H is present. The reaction can occur both in the gas phase and on the growing film surface, and probably applies to all of the Group III metal alkyls containing CH_3, C_2H_5, etc. alkyl groups. Although our studies were carried out at about 100 K in order to be able to retain high coverages of $Ga(CH_3)_x$ on the substrate for investigation, the findings apply directly to deposition processes carried out at higher temperatures, where high surface coverage is provided by high equilibrium pressures of the of the reactants in the case of CVD, or by beams in the case of MBE.

2.10.3. The Electron-Induced Reaction of NH3 with $Ga(CH_3)_x/SiO_2$

The ability of electron impact dissociation to produce H atoms from the NH_3 molecule was employed as a method of producing a GaN film in the region irradiated by the electron beam. Assuming first-order kinetics for the electron impact induced reaction, the cross section for carbon depletion QP_{NH_3}, was evaluated from the slopes of Fig. 2.9, according to the general equation:

$$N_C = N_C^0 \exp[-(jt/e)QP_{NH_3}]. \qquad (1)$$

Here N_C and N_C^0 are the coverage of carbon atoms at time t and at time 0, respectively, j is the electron current density, and e is the elementary charge. The cross section, QP_{NH_3}, is dependent on the pressure of NH_3 because of the dependence of the rate of electron-induced reaction on the steady state coverage of NH_3 achieved under dynamic conditions. The cross section QP_{NH_3} for depletion of carbon is of the order of 5×10^{-20} cm^2 at $P_{NH_3} = 5 \times 10^{-8}$ Torr.

Under the conditions of this experiment, each electron has an efficiency of order 5×10^{-6} for causing a CH_3 extraction process[9]. This is due to two inefficient processes working in series:

$$NH_3 + e^- \rightarrow NH_x + H \qquad (2)$$

$$H + Ga(CH_3)_x \rightarrow HGa(CH_3)_{x-1} + CH_3 \text{ or } CH_4 \qquad (3)$$

If e_1 is the efficiency to produce one H per electron in reaction (2), and e_2 is the efficiency of CH_3 extraction by the atomic H thus produced, as described by reaction (2), then the overall process efficiency is $e_1 \times e_2$, which we know to be about 5×10^{-6}. We know from Sect. 2.6 that e_2 is about 10^{-2}, so we can determine that e_1 is about 5×10^{-4}. This corresponds to an electron impact dissociation cross section of order 5×10^{-19} cm^{-1} for breaking the N-H bond in adsorbed NH_3 by electron impact with 3 kV electrons, assuming a steady state coverage of NH_3 to be about $10^{15}/cm^2$.

2.10.4. Growth of GaN

To summarize, the experiments described in this report indicate that GaN can be grown using electron impact of NH_3 to produce atomic H, which then reacts with Ga-CH_3 moieties, displacing the CH_3 group. The production of GaN was substantiated by the following experimental results:

a. Carbon is removed by the action of the H atoms produced by electron bombardment.
b. Gallium and nitrogen are thermally fixed in the dot or line which has been subjected to the electron-stimulated reaction conditions.
c. Gallium and nitrogen are not thermally fixed outside of the irradiated area, where reaction conditions are not provided.
d. The GaN produced is thermally stable to 900K.
e. The N(KLL) Auger line shape can be explained by the production of a GaN layer over a Si_3N_4 layer, which is also produced on the SiO_2-coated substrate.

2.10.5. Conclusions

The following conclusions can be reached from this work:

a. The reaction between the Ga-CH_3 bond and atomic H occurs near 100 K with the elimination of carbon either as CH_3 and/or CH_4. This process occurs with zero activation energy in accordance with theoretical expectations.

b. The efficiency of the reaction per incident H atom is of the order of 10^{-2}. The CH_3 extraction is first order in CH_3 coverage on the surface.

c. Using an electron beam, incident on adsorbed NH_3, atomic H may be generated in the irradiated region of the surface. This atomic hydrogen may also be used to activate the Ga-CH_3 bond and GaN may be then produced.

d. This new synthesis method offers the possibility of achieving low temperature growth of GaN films on suitably matched substrates, thus reducing nitrogen vacancies that result from its thermal instability. This technique may result in less carbon contamination from growth from alkyl precursors, and the ability to grow in patterns defined by an electron beam may find novel applications.

e. These findings are very likely to apply in a general way to the production of III-V compound semiconductor films from Group III metal alkyls and group V hydrides.

2.10.6. Acknowledgements

The authors wish to acknowledge Dr. D. K. Wickenden, Applied Physics Laboratory, Johns Hopkins University, for supplying the GaN/Al_2O_3 sample used for reference Auger spectral measurements.

3. CHARACTERIZATION OF GROUP III NITRIDES

Materials characterization experiments consisted of cathodoluminescence (CL) measurements which provided information on the electronic properties of Group III nitride layers, and infrared reflectance measurements which provided insight into their structural properties[14]. We collaborated with nine laboratories around the world, providing important material data feedback to both growth groups and device groups.

Significant features near the band edge, which have strong dependence on the character and the purity of the materials, are easily measured by CL. Fig 3.1 shows the spectrum of a GaN film deposited on a sapphire substrate with a GaN buffer layer, in which three sharp free exciton (FE) peaks were identified in a cryogenic CL measurement. Dopants and impurities can be detected and identified by CL. Fig 3.2 shows a peak associated with silicon in a doped GaN film grown on SiC.

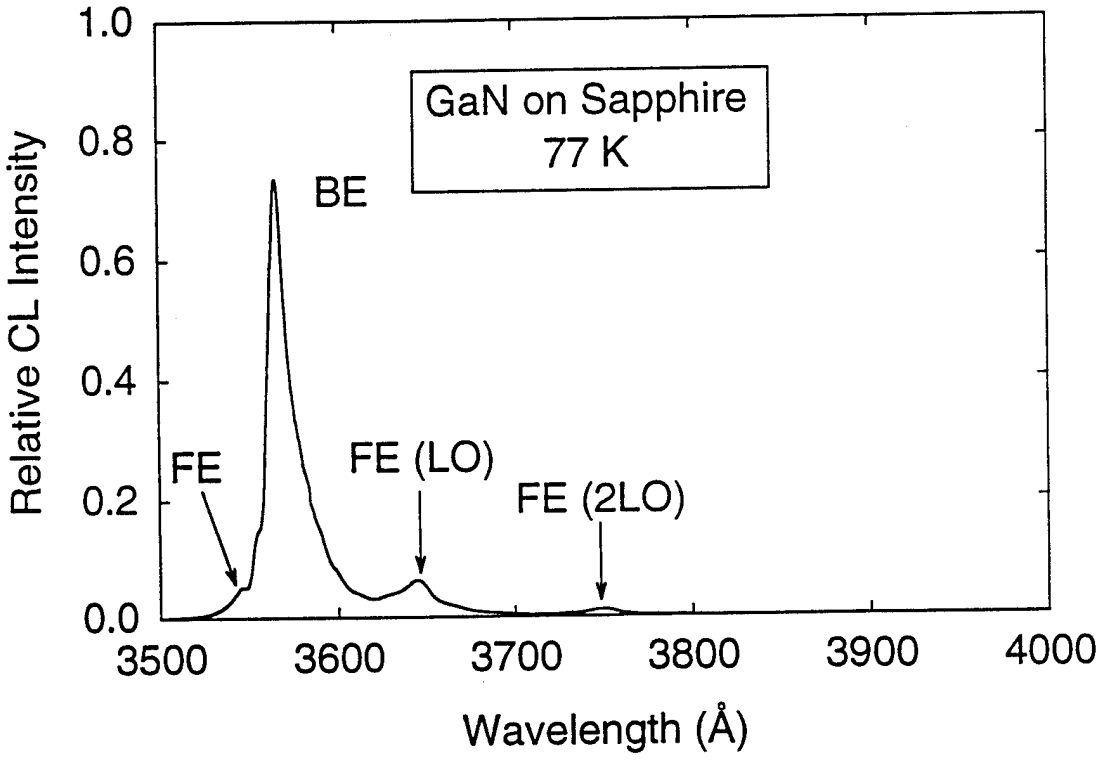

Fig. 3.1. Cathodoluminescence of a 4.48 μm thick GaN film deposited on a sapphire substrate with a GaN buffer layer.

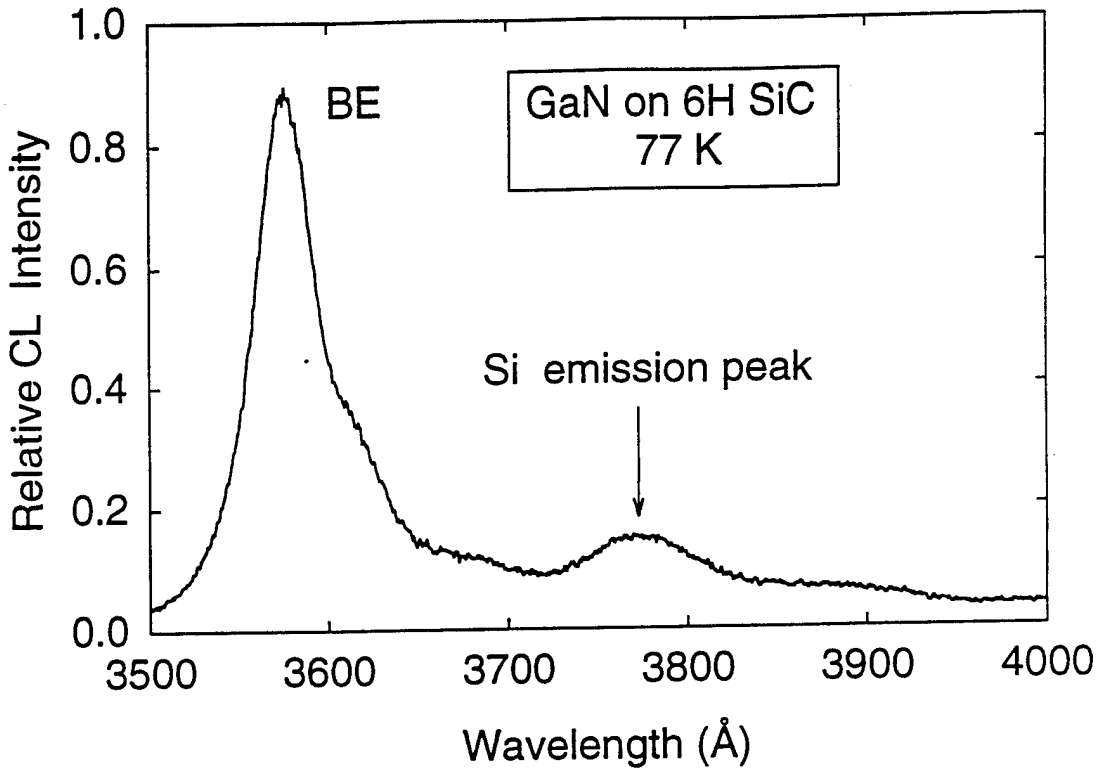

Fig. 3.2. Cathodoluminescence of a 0.5 μm thick GaN film doped with silicon, deposited on a (0001) 6H SiC substrate.

We developed a Lorentz oscillator model[15] of the infrared reflectance of AlN layers on substrates such as SiC and Si. The model takes into account film and substrate anisotropy and non-normal incidence rays, and requires only bulk material parameters. Comparison of infrared reflectance measurements to the model provides information on the thickness, orientation, and quality of epitaxial AlN films. As an example, Fig. 3.3 shows the IR reflectance of a GaN film on a sapphire substrate, along with the spectrum predicted by the model. Comparison to the model made it possible to identify the vibrational modes that give rise to the spectral features.

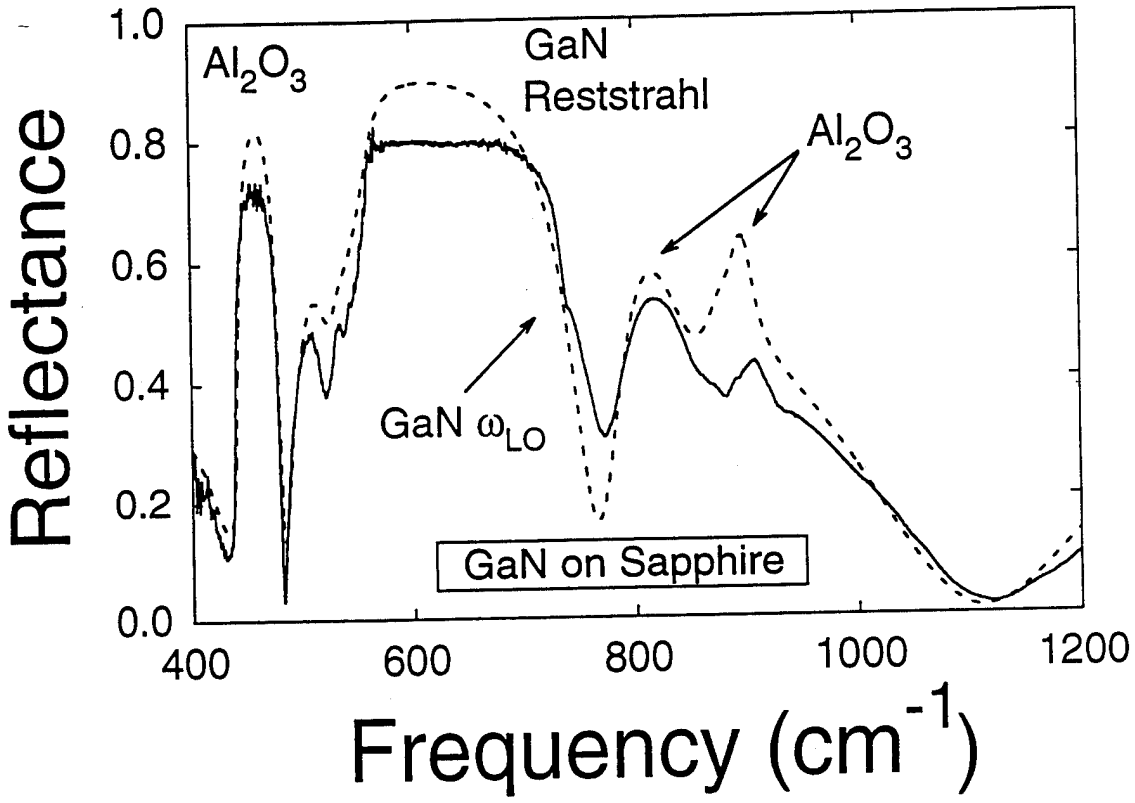

Fig. 3.3. Reflectance of a 4.52 μm thick GaN film on a sapphire substrate. The solid line represents the data, and the dashed line is the calculated spectrum.

4. PUBLICATIONS AND PATENT DISCLOSURES

4.1. Refereed Journal Articles and Proceedings

1. M. L. Colaianni , P. J. Chen, H. Gutleben, and J, T, Yates, Jr., "Vibrational Studies of CH3I on Si(100)-(2X1): Adsorption and Decomposition of the Methyl Species", Chem Phys. Lett. **191**, 561 (1992).
2. K. H. Bornschauer, S. R. Lucas, W. J. Choyke, W. D. Partlow, and J. T. Yates, Jr., "Reflector Atomic Hydrogen Source - A method for Producing Pure Atomic Hydrogen in Ultrahigh Vacuum", J. Vac. Sci. Technol. A, **11 No. 5**, 2822, (1993).
3. M. F. MacMillan, R. P. Devaty, and W. J. Choyke, "Thin Aluminum Nitride Films on Various Substrates", Applied Physics Letters **62,** 750 (1993).
4. S. R. Lucas, W. D. Partlow, W. J, Choyke, and J. T. Yates, Jr., "Ga-CH_3 Bond Scission by Atomic H- The Depletion of Surface Carbon From a Gallium Alkyl Film of Silicon Oxide" Submitted to J. Vac. Sci. Technol., April, 1994.
5. A. Hubner, S. R. Lucas, W. D. Partlow, W. J, Choyke, J. A. Schaefer, and J. T. Yates, Jr., "GaN Patterned Film Synthesis - Carbon Depletion by Hydrogen Atoms Produced From NH_3 Activated by Electron Impact", Submitted to J. Vac. Sci. Technol., April, 1994.
6. J. T. Yates, Jr., A. Hubner, S. R. Lucas, W. D. Partlow, J. A. Schaefer, and W. J, Choyke, "Activation of the Ga-CH_3 Bond Using Atomic Hydrogen- A Possible Route to III-V Semiconductor Films with Low Carbon Levels", Submitted to Applied Surface Science, May, 1994
7. M. F. MacMillan, R. P. Devaty, W. J. Choyke, A. Khan, M. E. Lin, H. Morkoc, W. A. Bryden, T. J. Kistenmacher, and S. Nakamura, "Cathodoluminescence and FTIR Reflectance of Thin AlN and GaN Films", to be published in Proceedings of the ICSCRM-93 Conference, Institute of Physics.

4.2. Presentations at Conferences

1. W. J. Choyke, M. F. MacMillan, and R. P. Devaty, "LTCL and FTIR Reflectivity of AlN Films on SiC and Si Substrates", Workshop on Wide Bandgap Nitrides, St. Louis, MO, April 13, 1992.
2. M. F. MacMillan, R. P. Devaty, W. J. Choyke, A. Khan, M. E. Lin, H. Morkoc, W. A. Bryden, T. J. Kistenmacher, and S. Nakamura, "Cathodoluminescence and FTIR Reflectance of Thin AlN and GaN Films"
3. J. T. Yates, Jr., A. Hubner, S. R. Lucas, W. D. Partlow, J. A. Schaefer, and W. J, Choyke, "Activation of the Ga-CH3 Bond Using Atomic Hydrogen- A Possible Route to III-V Semiconductor Films with Low Carbon Levels", International ALE Conference, Sendai, Japan, May, 1994
4. J. T. Yates, Jr., W. J, Choyke, W. D. Partlow, S. R. Lucas, and A. Hubner , New Method to Produce Carbon-Free GaN Films", Submitted to Workshop on Wide Bandgap Nitrides, St. Louis, MO, October, 1994.

4.3. Patent Disclosures

1. "Reflector Atomic Hydrogen Source", K. H. Bornschauer, S. R. Lucas, W. J. Choyke, W. D. Partlow, and J. T. Yates, Jr., April, 1993.
2. "Patterned Film Growth of Pure Gallium Nitride, GaN Using Electron Beam Activation", A. Hubner, S. R. Lucas, W. D. Partlow, W. J, Choyke, J. A. Schaefer, and J. T. Yates, Jr., April, 1994.

5. REFERENCES

1. J. Karpinski, J. Jun, and S. Porowski, "Equilibrium pressure of N_2 over GaN and high pressure solution growth of GaN", J. Cryst. Growth **66**, 1 (1984)
2. C. D. Thurmond and R. A. Logan, "The equilibrium pressure of N_2 over GaN", J. Electrochem. Soc.: Solid State Science and Technology **119 No. 5**, 622 (1972).

3. M. J. Paisley, Z. Sitar, J. B. Posthill, and R. F. Davis, J. Vac. Sci. Technol. A **7**, 701 (1989).
4. S. Strite, J. Ruan, Z. Li, N. Manning, A. Salvador, H. Chen, David J. Smith, W. J. Choyke, and H. Morkoc, J. Vac. Sci. Technol. B **9**, 1924 (1991).
5. M. Rubin, N. Newman, J. S. Chan, T. C. Fu, and J. T. Ross, Appl. Phys. Lett. **64(1)**, 64 (1994).
6. K. H. Bornschauer, S. R. Lucas, W. J. Choyke, W. D. Partlow, and J. T. Yates, Jr., "Reflector Atomic Hydrogen Source - A method for Producing Pure Atomic Hydrogen in Ultrahigh Vacuum", J. Vac. Sci. Technol. A, **11 No. 5**, 2822, (1993).
7. B. J. Wood and H. Wise, J. Chem. Phys. **29**, 1416 (1958).
8. B. G. Koehler, C. H. Mak, D. A. Arthur, P. A. Coon, and S. M. George, J. Chem. Phys. **89**, 1709 (1988).
9. S. R. Lucas, W. D. Partlow, W. J, Choyke, and J. T. Yates, Jr., "Ga-CH_3 Bond Scission by Atomic H- The Depletion of Surface Carbon From a Gallium Alkyl Film of Silicon Oxide" Submitted to J. Vac. Sci. Technol., April, 1994.
10. B. A. Morrow and R. A. McFarlane, J. Phys. Chem. **90**, 3192 (1986).
11. A. Hubner, S. R. Lucas, W. D. Partlow, W. J, Choyke, J. A. Schaefer, and J. T. Yates, Jr., "GaN Patterned Film Synthesis - Carbon Depletion by Hydrogen Atoms Produced From NH_3 Activated by Electron Impact", Submitted to J. Vac. Sci. Technol., April, 1994.
12. Y. S. Hiraoka and M Mashita, Jpn. J. Appl. Phys. **31**, 3703 (1992).
13. P. L. Baxter, A. J. Downs, M. J. Goode, D. W. H. Rankin, and H. Robertson, J. Chem. Soc. Dalton Trans. 2873 (1990).
14. "Cathodoluminescence and FTIR Reflectance of Thin AlN and GaN Films", M. F. MacMillan, R. P. Devaty, W. J. Choyke, A. Khan, M. E. Lin, H. Morkoc, W. A. Bryden, T. J. Kistenmacher, and S. Nakamura, to be published in Proceedings of the ICSCRM-93 Conference, Institute of Physics.
15. M. F. MacMillan, R. P. Devaty, and W. J. Choyke, "Infrared Reflectance of Thin Aluminum Nitride Films on Various Substrates", Applied Physics Letters **62,** 750 (1993).

6. APPENDIX 1:

"Ga-CH_3 Bond Scission by Atomic H- The Depletion of Surface Carbon From a Gallium Alkyl Film of Silicon Oxide", S. R. Lucas, W. D. Partlow, W. J, Choyke, and J. T. Yates, Jr., Submitted to J. Vac. Sci. Technol., April, 1994.

Submitted to: J. Vac. Sci. Technol.

Date: 18 April 1994

$Ga-CH_3$ Bond Scission by Atomic H- The Depletion of Surface Carbon From a Gallium Alkyl Film on Silicon Dioxide

S.R. Lucas, W.D. Partlow,† W.J. Choyke,‡ and J.T. Yates, Jr.

Surface Science Center
Department of Chemistry
University of Pittsburgh
Pittsburgh, PA 15260

†Westinghouse Science and Technology Center
‡University of Pittsburgh, Physics Department

Ga-CH_3 Bond Scission by Atomic H- The Depletion of Surface Carbon From a Gallium Alkyl Film on Silicon Dioxide

S.R. Lucas, W.D. Partlow,† W.J. Choyke,‡ and J.T. Yates, Jr.

Surface Science Center
Department of Chemistry
University of Pittsburgh
Pittsburgh, PA 15260

Abstract

It is shown that atomic hydrogen is an effective reagent for the extraction of CH_3 groups from an adsorbed monolayer produced from trimethylgallium adsorption on SiO_2. The reaction is first-order in CH_3 surface concentration and proceeds with zero activation energy in the 100 K temperature region. The efficiency for the extraction process is about 10^{-2} per atomic H collision with the surface. These results show that the Ga-CH_3 bond may be broken by insertion of hydrogen atoms and that either CH_3 or CH_4 is eliminated by the process. The results indicate that atomic hydrogen is an effective agent for removal of carbon (present as CH_3) during III-V film growth processes. The extraction of CH_3 by atomic H occurs on the surface, but in MOCVD processes a similar reaction with metal alkyl species may also occur in the gas phase. Excellent agreement with the theoretical calculations of Hiraoka and Mashita for the interaction of atomic H with $AlH_2(CH_3)$ molecules is found.

1. Introduction

The III-V compounds, in particular the wide band gap nitrides, are very attractive semiconductors for light emission applications in the blue and UV wavelengths at high temperatures [1]. The effort to produce high quality films of III-V compounds can be traced back to the 1960's where much work was initiated in an attempt to better understand compounds such as GaN, InN, and AlN. The earliest GaN samples studied were in the form of powder samples or small crystals [2]. The most prevalent technique for growing these samples was to place metallic Ga in a zone furnace and to flow NH_3 over it [2] or to use a gallium phosphide or gallium arsenide [3a] or a gallium subchloride [3b] source for transport of Ga into the furnace. Another common growth technique was the use of reactive sputtering. This method employed Ar ions to sputter a Ga film in the presence of a nitrogen plasma [4]. The GaN produced by these methods was suitable to investigate and characterize many of its properties; however, material good enough for electronic applications was still elusive. Heteroepitaxial growth was finally realized by the use of CVD (chemical vapor deposition) techniques [1]. This permitted the production of high quality films where the principal problems dealt with finding suitable substrates for a good lattice match, elimination of very high background n-type carrier concentrations thought to be due to nitrogen vacancies, and the incorporation of dopants. The problem of a proper substrate lattice match that is also thermally compatible with the GaN thin film is being investigated by the use of substrate materials such as SiC, ZnO, and MgO [1]. The production of stoichiometric GaN is still a major obstacle for producing electronic grade films. Lower growth temperatures that might allow better nitrogen incorporation from more reactive nitrogen-containing precursors are being considered [5].

The growth of these nitrides, in thin film form using MOCVD (metal organic chemical vapor deposition) and MBE (molecular beam epitaxy), is now widespread and many variations of these two techniques are in use and are just beginning to be understood. In particular the thermal decomposition of trimethylgallium, $Ga(CH_3)_3$, (TMG) [6], in the presence of NH_3 can be used for GaN film production. This type of process is known to leave carbon behind [7-10] which can be deleterious to III-V semiconductor films.

The use of incoming hydrogen atoms from the gas phase to extract certain absorbates has been experimentally demonstrated to be effective on both semiconductor [11-13] and metal surfaces [14-18]. In many cases this H atom induced extraction process is thought to occur by an Eley-Rideal mechanism where energy accomodation between the incoming H atom and the surface does not occur. We show that atomic hydrogen, (containing 52 kcal/g atom of internal energy compared to 1/2 mole of H_2), is an effective reagent for CH_3 abstraction from the Ga-CH_3 moiety at low temperatures, and that the process occurs without thermal activation. It is possible that either CH_3 radicals or that $CH_4(g)$ is the product in this hydrogen atom abstraction reaction. This reaction may serve as a basis for reducing carbon contamination of GaN (and other III-V semiconductor films) made by MOCVD methods [19].

II. Experimental

The experiments were performed in a stainless steel ultrahigh vacuum (UHV) chamber pumped by a 150 l/s turbo pump, a 270 l/s diode ion pump and a titanium sublimation pump. The base pressure attained was 1×10^{-10} Torr. The chamber is equipped with a differentially pumped UTI-100C quadrupole mass spectrometer (QMS) having an axially oriented aperture of 4.7 mm diameter. The

aperture is biased at -125 V to retard emission of stray electrons from the QMS ion source. This instrument may be employed in two modes of operation. They are: (1) for residual gas analysis, a large aperture on the side of the cylindrical shield surrounding the QMS may be opened to the ultrahigh vacuum system; (2) for temperature programmed desorption (TPD) measurements the aperture is reproducibly located 0.2 mm from the front of the substrate containing the adsorbed layer, collecting a large fraction of the desorbing gas from the central region of the substrate [20]. The vacuum system also contains a single pass CMA Auger spectrometer which was operated with a 0.3 mm diameter electron beam (3 kV, 3.0 μA), a reverse view LEED apparatus and a multicapillary array doser system for deposition of TMG at a known absorbate flux [20-21]. A unique source of atomic hydrogen was employed in this work [22]. Hydrogen molecules are directed in an effusive beam to a pancake spiral W filament at 1800 K, housed in a cylindrical metal radiation shield. The local pressure of H_2 at the W filament is ~ 50 times higher then the pressure due to the random flux of H_2 inside the chamber from the admitted H_2, producing a large yield of atomic H. A portion of this atomic H exits from the end of the shield and is efficiently reflected from a pyrex glass plate at ~ 77 K. A fraction of the reflected atomic H flux is incident on the substrate. This indirect method for delivering atomic H to the surface eliminates almost all radiation heating of the substrate.

The rate of adsorption of atomic H on a Si(100) substrate at 600 K may be employed as a method to estimate the rate of impingement of atomic H on the surface [22-24]. Figure 1 shows the rate of buildup of hydrogen coverage on Si(100)-(2x1) maintained at 600 K following exposure to atomic H. The desorbing H_2 from the Si(100) surface is measured by TPD [23]. It is observed that the hydrogen coverage rises almost linearly to a break point, indicating adsorption by a process involving a constant sticking coefficient, S_H. For

purposes of calibration, we assume in this region of coverage that $S_H = 1$, and that at the saturation point, a saturated monohydride surface phase (6.8×10^{14} H/cm^2 = 1 monolayer (ML)) has been produced [23-24]. This saturation point corresponds to a value of the pressure of H_2 multiplied by time and is equal to 2.0×10^{-5} Torr sec (corrected Bayard-Alpert gauge pressure sensitivity factor = 0.5 for H_2 [25]). In this case, the pressure of H_2 is a measure of the system pressure during dosing, not the true local pressure of hydrogen at the spiral filament which is ~ 50 times greater. The number of H_2 molecules which have entered the H atom doser is given on the abscissa of Fig. 1. Within this framework the value of 2.0×10^{-5} Torr sec is proportional to the atomic H exposure on the surface, such that 6.8×10^{14} H/cm^2 = 1 ML = 2.0×10^{-5} Torr sec. All atomic hydrogen doses in the experiments described here are referenced to this 1 ML definition, using the background system pressure of H_2 as an index of the flux of atomic hydrogen; this definition of 1 ML H exposure is a definition useful as only a qualitative index of hydrogen atom exposure, since S_H has been assumed to be unity in the estimate, and the location of the monolayer saturation point is somewhat arbitrary.

The substrate used for this study was a SiO_2 film grown on top of a clean Si(100) crystal (13 x 13 x 1.5 mm^3; p-type; B-doped; 10 ohm/cm). The crystal containing the SiO_2 film may be cooled to ~ 95 K using liquid N_2. A temperature controller, working with a feedback thermocouple signal, allows programmed heating of the Si(100) crystal from 95 K to 1200 K [26]. The chromel-alumel (Type E) thermocouple is embedded in a slot in the edge of the Si(100) crystal, and protected from touching the inner Si surface by a double envelope of Ta foil [21]. Growth of the SiO_2 film was done by using the sputter-oxidation procedure of Chen et al. [27]. This was achieved by back filling the chamber with 2.0×10^{-5} Torr oxygen and using the argon ion sputter gun (with direct Ar admission to the gun) giving a partial pressure of 2.0×10^{-5} Torr Ar in the chamber. The ion

energy was 500 eV. Bombardment of the Si(100) surface occurred at 600 K at an ion current of 0.5 $\mu A/cm^2$ for approximately 180 minutes at several different orientations of the crystal with respect to the sputter gun to allow for uniform SiO_2 film deposition. The deposition was followed by cooling the crystal in O_2, leading to the production of a layer of SiO_2, which passivates the Si(100) surface. The SiO_2 layer thickness for the annealed film (900 K) was estimated from the attenuation of the 92 eV Si (LVV) Auger feature. This attenuation corresponds to a SiO_2 film thickness of 20 Å ± 5 Å if an electron attenuation length of 6.5 Å is employed [28]. This method provides a clean reproducible SiO_2 substrate for sequential experiments.

A collimated and calibrated multicapillary array doser (doser temperature = 300 K) was employed to reproducibly dose the substrate surface [21]. The multicapillary array doser contained a 2.2 cm diameter glass multicapillary collimator array composed of closely spaced 10 μm inside-diameter capillaries of 500 μm length. The flux from the doser was controlled by a fixed, nominally 5 μm diameter, orifice seated inside the doser by adjusting the backing pressure of TMG in the gas line. The doser conductance was measured using N_2, and on this basis the calculated effusion rate of TMG is 4.14×10^{12} TMG molecules/ Torr sec. Using the geometry of the doser and crystal [29], this effusion rate is equivalent to a flux at the SiO_2 substrate of 1.4×10^{12} TMG molecules/cm^2 Torr sec. A shutter between the doser and crystal served to start and stop the adsorption step. Recent studies have shown that essentially pure TMG may be delivered in this manner [30].

Trimethylgallium was obtained from Strem Chemicals in a stainless steel cylinder. It was further purified by freeze-pump-thaw cycles inside the stainless steel gas handling line. Typical pressures of 2.0 Torr were used behind the conductance limiting orifice of the dosing system and measured to an accuracy of

± 0.001 Torr using a Baratron capacitance manometer.

III. Experimental Results

A. Adsorption of TMG on SiO_2/Si(100)

The adsorption of TMG on SiO_2 at 97 K to the extent of approximately one monolayer was monitored in several ways. The first method employed Auger electron spectroscopy (AES) measurements at different intervals during the adsorption. Each Auger measurement was done at a different position on the SiO_2 surface during the stepwise adsorption. AES measurements of the peak-to-peak intensity of the Si(LVV) 76 eV feature shown in Fig. 2 and the C(KLL) 272 eV feature in Fig. 3 both reveal a break point at 1.4×10^{14} TMG molecules/cm^2 delivered to the SiO_2 substrate. This break point is indicative of a cross over from monolayer to multilayer adsorption likely accompanied by a decrease in sticking probability occurring near the formation of monolayer coverage. This identification of the monolayer exposure can be qualitatively checked by comparison to an ideal situation by considering the TMG molecules (modeled as 7 Å diameter disks [31]) to adsorb in a close-packed manner. This yields an estimate of 2.4×10^{14} molecules/cm^2 of TMG for the saturated monolayer, in fair agreement with the breakpoint observed at an exposure of 1.4×10^{14} molecules/cm^2.

The AES measurement conditions introduce the effect of electron stimulated desorption (ESD) into the measurement of surface coverage. The Auger signals for carbon from a monolayer of TMG are shown in Fig. 4 and for gallium in Fig. 5 as a function of the extent of bombardment by the 3 kV electron beam. The ESD effect is significant for high electron doses, but relatively

insignificant for the electron doses used here.

All AES measurements following treatment of the gallium alkyl layer with atomic H were obtained by averaging over at least three points on the substrate and were made using a standardized electron dosage schedule and working within the region of electron dosage where the carbon or gallium desorption is negligible. However, both the carbon and gallium Auger signals are likely to be from surface species which have been decomposed by the electron beam. Hence these Auger intensities are indicators of the local carbon and gallium assay following electron beam induced decomposition of the adsorbed species.

The second method used to estimate TMG monolayer exposure and coverage is based on thermal desorption data. TMG has a mass spectrometer cracking pattern consisting mainly of CH_4^+ (m/e = 16), Ga^+ (m/e = 69), $Ga(CH_3)^+$ (m/e = 84; monomethylgallium, MMG), $Ga(CH_3)_2^+$ (m/e = 99; dimethylgallium, DMG), and $Ga(CH_3)_3^+$, (m/e = 114). The TPD yield versus TMG fluence in Fig. 6 shows that no TMG (m/e = 114, TMG) starts to desorb until reaching TMG exposures corresponding approximately to the formation of the second layer based on the calibrated doser results and AES measurements.

These observations (Fig. 6) indicate that the adsorption of TMG as a monolayer on SiO_2 produces primarily DMG as a thermal desorption product. The data may indicate that DMG is produced during adsorption of TMG on the SiO_2 in the first monolayer. Morrow and McFarlane [32] in fact have found that Si-O-Si groups in the surface of SiO_2 react with TMG to produce DMG surface species. This first layer is designated $Ga(CH_3)_x$. Above the monolayer coverage, TMG remains stable during heating and desorption. Detailed information about the thermal desorption from layers produced by TMG adsorption is provided later in this paper.

B. Extraction of CH_3 Groups by Atomic Hydrogen

Exposure of atomic hydrogen to the $Ga(CH_3)_x$ monolayer on the SiO_2 surface was carried out at three different substrate temperatures (97 K, 108 K and 138 K) resulting in quantitative removal of methyl groups. The results are presented on the left-hand side of Fig. 7. The experimental points shown in all three experiments were measured following controlled exposure at constant atomic hydrogen flux, so that the relative rates of methyl removal can be accurately compared. Since each of the Auger measurements were made at points not affected by the electron beam previously, the depletion of carbon is due almost entirely to atomic H exposure. The dosage of atomic hydrogen is measured in terms of monolayers of H atoms incident as defined in the Experimental section. The data show that the C(KLL) Auger signal decreases to zero while the Ga(LMM) Auger signal undergoes relatively small changes as atomic hydrogen is incident on the adsorbed $Ga(CH_3)_x$ species. A slight decrease in the Ga(LMM) Auger intensity is observed at the start, followed by a gradual increase until all carbon is seen to be removed, and the Ga(LMM) Auger intensity then remains constant. The reason for the characteristic initial slight decrease in the Ga Auger signal during CH_3 removal is currently unknown. The increase over most of the range of the experiment is undoubtedly due to the reduction in screening of the Ga by CH_3 groups as CH_3 groups are removed by the atomic H.

The data on the right-hand side of Fig. 7 are replotted as semilogarithmic plots in accordance with first-order kinetic behavior. The linear regression analysis gives a straight line with a slope, m, that is proportional to the first-order rate constant for CH_3 removal. As seen, the slopes and hence the rate constant for

the atomic-H induced methyl extraction, over a temperature range of 41 K, is constant within the experimental errors in the rate measurement. This gives an activation energy of zero for the CH_3 extraction process. The errors in this measurement correspond to an activation energy of $0^{+0.09}_{-0.02}$ kcal/mole for the CH_3 extraction by atomic H..

C. Thermal Desorption Studies Following Atomic Hydrogen Exposure

Typical thermal desorption data are shown for the 108 K-atomic H extraction experiments in Figs. 8-9 for a starting coverage derived from one monolayer of TMG exposed to varying dosages of atomic hydrogen. In Fig. 8 it is apparent that the DMG monolayer (produced from TMG adsorption on SiO_2) is systematically depleted by atomic hydrogen dosing at 108 K, until all DMG is destroyed. Following ~ 200 monolayers of atomic H exposure, no DMG cracking product is visible upon subsequent thermal desorption. Auger spectroscopy reveals that Ga is still present as seen in Fig. 7. Supporting evidence is obtained from additional studies of the Ga^+ (m/e = 69) cracking product produced in TPD following atomic hydrogen dosing as shown in Fig. 9. Here too, depletion of $Ga(CH_3)_2$ by atomic H exposure is indicated.

The depletion of the Ga^+ (m/e = 69) cracking product due to decomposition of $Ga(CH_3)_2$ by atomic hydrogen (Fig. 9) is accompanied by the deposition of metallic Ga which is strongly bound to the SiO_2 substrate, and which desorbs at much higher temperature. Auger studies of the thermal behavior of metallic Ga produced in this manner were performed as shown in Fig. 10, indicating that the Ga layer is fairly stable over the temperature range from 100 K - 700 K. Near 900 K, the SiO_2 layer on Si becomes unstable as SiO(g) desorbs and this process may

be related to the final thermal depletion of Ga.

IV. Discussion

A. Postulated Mechanism for H Atom Extraction of CH_3 Groups

As this experimental work was being carried out, a theoretical analysis of the interaction of atomic hydrogen with the trimethylaluminum molecule was published by Hiraoka and Mashita [33]. The ab initio molecular orbital calculations indicated that the two elementary steps shown below were of low activation energy, much less than the dissociation energy of the Al-CH_3 bond.

$$AlH_2CH_3 + H \rightarrow AlH_3 + CH_3, \quad E_a = 1.9 \text{ kcal/mole} \qquad (1)$$

$$AlH_2CH_3 + H \rightarrow AlH_2 + CH_4, \quad E_a = 12.7 \text{ kcal/mole} \qquad (2)$$

In the Hiraoka-Mashita calculation, the AlH_2CH_3 molecule was taken to represent the $Al(CH_3)_3$ molecule. The Al-CH_3 bond in AlH_2CH_3 has a dissociation energy of 77.1 kcal/mole[33], to form $AlH_2 + CH_3$.

The transition state for reaction (2) was determined to be a linear $H_2Al\cdots H\cdots CH_3$ complex which is a classical H atom insertion type complex. However, a lower energy local minimum was also observed for the species of C_{3v} symmetry having the structure H_3Al-CH_3, and this minimum energy structure was postulated to form in the early stage of the progress of the reaction along the

reaction coordinate leading to either reaction (1) or reaction (2).

The chemistry of $Ga(CH_3)_3$ has been explored recently under hydrogenation conditions by others[34], finding direct evidence for the production of $(CH_3)_2Ga(\mu\text{-}H)_2Ga(CH_3)_2$ molecules which are stable at 290 K. This investigation forms the first definitive structural characterization of a compound containing two Ga atoms linked by a hydrogen bridge. In addition, evidence for trimeric or higher polymers of the form $[(CH_3)_2GaH]_n$ was also obtained[34].

The ab initio calculations[33] and the structural determination of the replacement of a Ga-CH_3 bond by a bridging H bond[34] leave little doubt that similar chemistry may be achieved by the exposure of surface species containing Ga-CH_3 bonds to atomic H, as demonstrated in the research reported here.

The ab initio calculation[33] and the direct observation of hydrogen bridging between Ga atoms which have lost a CH_3 group [34] both indicate that H atom attack of the Ga atom occurs first, followed by elimination of CH_3 with the formation of either a CH_3 radical or CH_4. Our studies do not discriminate between CH_3 and CH_4 formation for $Ga(CH_3)_x$ species, although the zero activation energy measured may suggest that CH_3 elimination is favored in $Ga(CH_3)_x$ by analogy to the result calculated theoretically for reaction (1).

B. Relationship to MOCVD Production of III-V Compounds

This new reaction, involving H atom insertion into Ga-CH_3 bonds, could be very important in MOCVD processes in which atomic H is present. The elimination of CH_3 groups from metal alkyl molecules by atomic hydrogen can occur both in the gas phase as well as on the surface of the growing film. The use of atomic H provides a facile route for the elimination of carbon from the III-V

film growth process, either by displacement of CH_3 groups and/or by the formation of CH_4. As will be shown in a subsequent paper, we have used the H atom insertion process to eliminate CH_3 groups during the growth of a GaN film, where the electron bombardment of NH_3 has served to provide a local source of H atoms[19].

V. Summary

Atomic H has been used to eliminate CH_3 groups from a monolayer film derived from $Ga(CH_3)_3$ and supported on a SiO_2 film. The following observations about this reaction have been made:

1. The reaction between $Ga(CH_3)_x$ and atomic H occurs near 100 K with the elimination of carbon either as CH_3 and/or CH_4.

2. The efficiency of the reaction per incident H atom is of order 10^{-2}. Approximately 100 monolayers of incident H result in better than 95% elimination of C, as determined using both Auger spectroscopy and thermal desorption methods.

3. The activation energy for the CH_3 extraction reaction by atomic H is zero. Based on this observation the reaction may be of the Eley-Rideal type, although other studies are needed to definitely establish the mechanism.

4. The reaction is first-order in CH_3 coverage on the surface.

5. The observation of this reaction confirms theoretical expectations based on ab initio studies of the related $AlH_2(CH_3)$ molecule, where efficient H atom insertion in the Al-C bond was found to occur via low activation energy processes.

6. This work demonstrates how mechanistic information about high temperature surface processes may often be obtained by working at low temperatures where appreciable surface coverages of reactant molecules may be maintained on the surface for kinetic investigation.

Acknowledgement

The authors acknowledge with thanks the support of this work by AFOSR under contract F49620-91-C-0032. We also thank Mr. A. Hübner for assistance in the later stages of this work. We thank Professor N.J. Cooper for useful discussions.

References

1. A comprehensive review of the current status of this area is given in S. Strite and H. Markoc, J. Vac. Sci. Technol. B 10, 1237 (1992).
2. W.C. Johnson, J.B. Parsons and M.C. Crew, J. Phys. Chem, 36, 2651 (1932).
3. 3(a) A. Addamiano, J. Electrochem. Soc., 108, 1072 (1961).
   3(b) H.P. Maruska and J.J. Tietjen, Appl. Phys. Lett, 15, 327 (1969); see also ref. 1.
4. H.J. Hovel and J.J. Cuomo, Appl. Phys. Lett, 20, 71 (1972); see also ref. 1.
5. (a) H. Okumura, S. Misawa and S. Yoshida, Appl. Phys. Lett, 59, 1058 (1991); (b) M. Rubin, N. Newman, J.S. Chan, T.C. Fu, and J.T. Ross, Appl. Phys. Lett., 64, 64 (1994)
6. A. Förster and H. Lüth, J.Vac. Sci. Technol., B7, 720 (1989).
7. T.R. Gow, F. Lee, R. Lin, A.L. Backman and R.I. Masel, Vacuum, 41, 951 (1990).
8. C.R. Flores, X.-L. Zhou and J.M. White, Surf. Sci., 261, 99 (1992).
9. T.R. Gow, R. Lin and R.I. Masel, J. of Crystal Growth, 106, 577 (1990).
10. S.P. Den Baars, B.Y. Maa, P.O. Dapkus, A.D. Danner and H.C. Lee, J. Cryst. Growth, 77, 188 (1986).
11. K. Sinniah, M.G. Sherman, L.B. Lewis, W.H. Weinberg, J.T. Yates, Jr. and K.C. Janda, Phys. Rev. Lett., 62, 567 (1989).
12. K. Sinniah, M.G. Sherman, L.B. Lewis, W.H. Weinberg, J.T. Yates, Jr. and K.C. Janda, J. Chem. Phys. 92, 5700 (1990).
13. (a) C.C. Cheng, S.R. Lucas, H. Gutleben, W.J. Choyke and J.T. Yates, Jr., J. Amer. Chem. Soc., 114, 1249 (1992); (b) J.T. Yates, Jr, C.C. Cheng, Q. Gao, M.L. Colaianni and W.J. Choyke, Thin Solid Films, 225, 150 (1993).

14. P.J. Eenshuistra, J.H.M. Bonnie, J. Los and H.J. Hopman, Phys. Rev. Lett, 60, 341 (1988).

15. R.I. Hall, I. Cadez, M. Landau, F. Pichou and C. Schermann, Phys. Rev. Lett, 60, 337 (1988).

16. K.R. Lykke and B.D. Kay, in "Laser Photoionization and Desorption Surface Analysis Techniques", N.S. Nogar, ed., SPIE: Bellingham, WA. 1990, Vol. 1208, p.18.

17. C.T. Rettner and D.J. Auerbach, Phys. Rev. Lett. 69, 383 (1992).

18. C.T. Rettner and D.J. Auerbach, Science 263, 365 (1994).

19. A. Hübner, S.R. Lucas, W.D. Partlow, W.J. Choyke, J.A. Schäfer and J.T. Yates, Jr., subsequent paper.

20. V.S. Smentkowski and J.T. Yates, Jr., J. Vac. Sci. Technol., A7, 3325 (1989).

21. M.J. Bozack, L. Muehlhoff, J.N. Russell, Jr., W.J. Choyke and J.T. Yates, Jr. J. Vac. Sci. Technol., A5, 1 (1987).

22. K.H. Bornscheuer, S.R. Lucas, W.J. Choyke, W.D. Partlow and J.T. Yates, Jr., J. Vac. Sci. Technol., A11, 2822 (1993).

23. C.C. Cheng and J.T. Yates, Jr., Phys. Rev. B 43, 4041 (1991).

24. Z.H. Lu, K. Griffiths, P.R. Norton and T.K. Sham, Phys. Rev. Lett., 68, 1343 (1992).

25. P.A. Redhead, J.P. Hobson and E.V. Kornelsen, "The Physical Basis of Ultrahigh Vacuum", Chapman and Hall, Ltd., London (1968), reprinted 1993 by American Institute of Physics, pg. 264.

26. R.J. Muha, S.M. Gates, P. Basu and J.T. Yates, Jr., Rev. Sci., Inst. 56, 613 (1985).

27. P.J. Chen, M.L. Colaianni and J.T. Yates, Jr., J. Non-Crystalline Solids, 155, 131 (1993).

28. F.J. Himpsel, F.R. McFeely, A. Taleb-Ibrahimi, J.A. Yarmoff and G. Hollinger, Phys. Rev. B. 38, 6084 (1988).
29. A. Winkler and J.T. Yates, Jr., J. Vac. Sci. Technol., A6, 2929 (1988).
30. R. Lin, L. Cadwell and R.I. Masel, J. Vac. Sci. Technol., A12, 179 (1994).
31. J.R. Durig and K.K. Chatterjee, J. Raman Spec., 11, 168 (1981).
32. B.A. Morrow and R.A. McFarlane, J. Phys. Chem., 90, 3192 (1986).
33. Y.S. Hiraoka and M. Mashita, Jpn. J. Appl. Phys., 31, 3703 (1992) Pt. 1.
34. P.L. Baxter, A.J. Downs, M.J. Goode, D.W.H. Rankin and H. Robertson, J. Chem. Soc. Dalton Trans, (1990), 2873.

Figure Captions

Figure 1. Development of hydrogen coverage on Si(100) at 600 K. The monohydride saturation coverage corresponds to 6.8×10^{14} H/cm^2 on the perfect Si(100) surface.

Figure 2. Auger spectroscopy study of the adsorption of trimethylgallium on SiO_2/Si(100) at 97 K. The attenuation of the Si(LVV) Auger intensity is followed, sampling a new position on the surface for each point. The monolayer coverage is shown at the dotted line.

Figure 3. Auger spectroscopy study of the adsorption of trimethylgallium on SiO_2/Si(100) at 97 K. The growth of the C(KLL) Auger intensity is followed, sampling a new position on the surface for each point. The monolayer coverage is shown at the dotted line.

Figure 4. Effect of prolonged electron beam exposure on the carbon Auger intensity measured for one monolayer of trimethylgallium on SiO_2/Si(100). The electron beam remains on one spot during continuous irradiation. The data show that the effect of the electron beam on the C(KLL) intensity is small during the time required to make one measurement.

Figure 5. Effect of prolonged electron beam exposure on the gallium Auger intensity measured for one monolayer of trimethylgallium on SiO_2/Si(100). The electron beam remains on one spot during continuous irradiation. The data show that the effect of the electron beam on the Ga(LMM) intensity is small during the time required to make one measurement.

Figure 6. Time integrated yields of mass spectrometer fragments from trimethylgallium-derived layers on SiO_2/Si(100). The adsorption temperature was 97 K. Above the one monolayer coverage, the desorption of TMG begins to be observed at m/e = 114. For coverages in the first monolayer, the mass spectrometer detects only DMG at m/e = 99. This suggests that the first layer may be DMG at 97 K adsorption temperature.

Figure 7. Kinetics of extraction by atomic H of CH_3 from one monolayer of $Ga(CH_3)_x$ on SiO_2/Si(100) at three temperatures. The behavior of both the C(KLL) and the Ga(LMM) Auger intensities are shown on the left. Auger intensities are measured at different spots on the surface for each point. On the right, a semilog plot of the behavior of the C(KLL) signal is shown. Within experimental error, the slope of the first order plot, m, is constant over a 41 K temperature range, indicating that atomic H extraction of CH_3 groups is non-activated.

Figure 8. Depletion of the m/e = 99 thermal desorption feature following various atomic H exposures at 108 K. Complete loss of this product is observed for approximately 100 ML of atomic H exposure.

Figure 9. Depletion of the m/e = 69 thermal desorption feature following various atomic H exposures at 108 K. Complete loss of this product is observed for approximately 100 ML of atomic H exposure. Subsequent Auger studies show that Ga remains on the surface following this treatment.

Figure 10. Thermal stability of the gallium film produced by complete removal of CH_3 groups using atomic H. Auger spectroscopy is employed for these measurements.

Lucas, et a

Figure 1

DEVELOPMENT OF HYDROGEN COVERAGE ON Si(100)

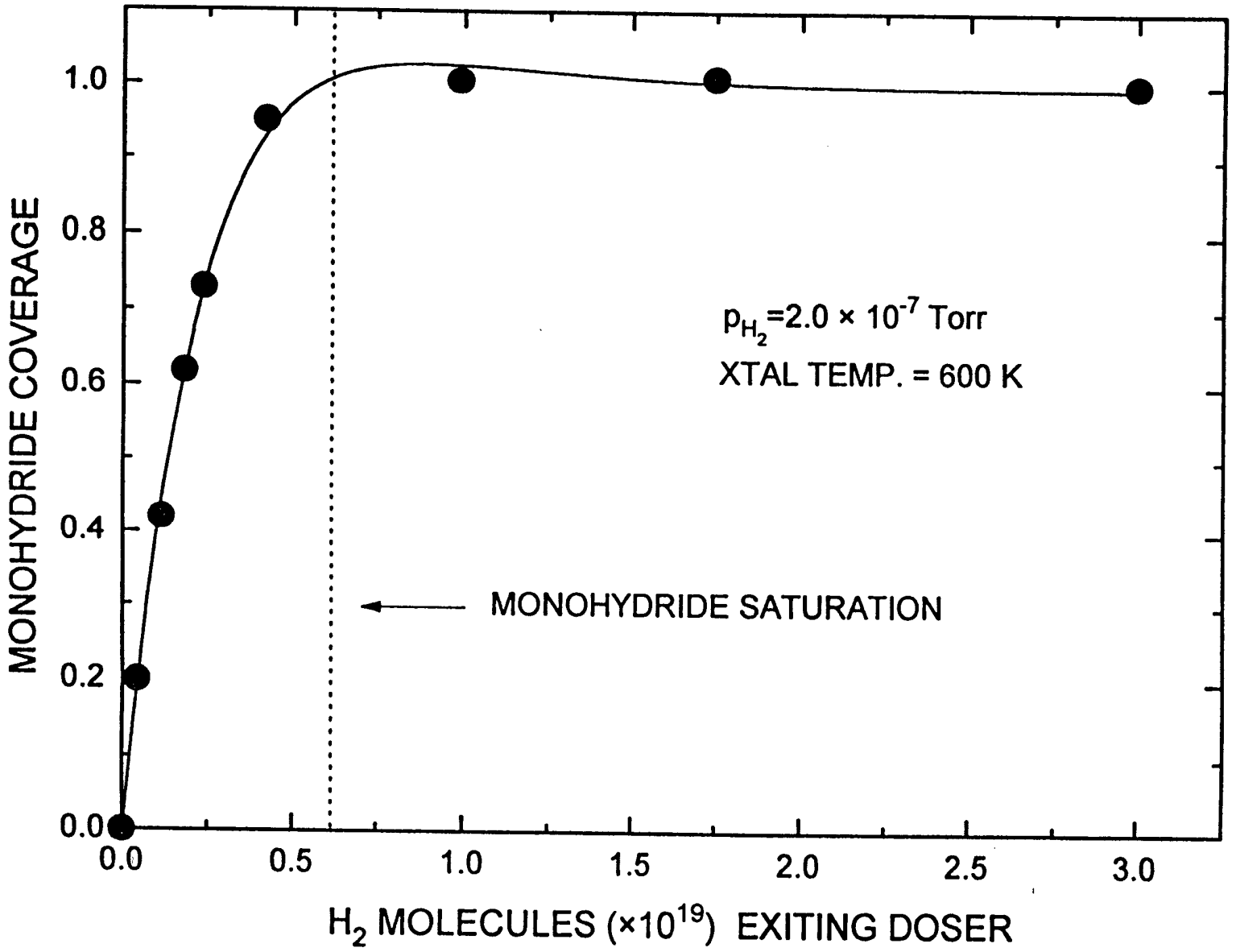

Lucas, et a

Figure 3

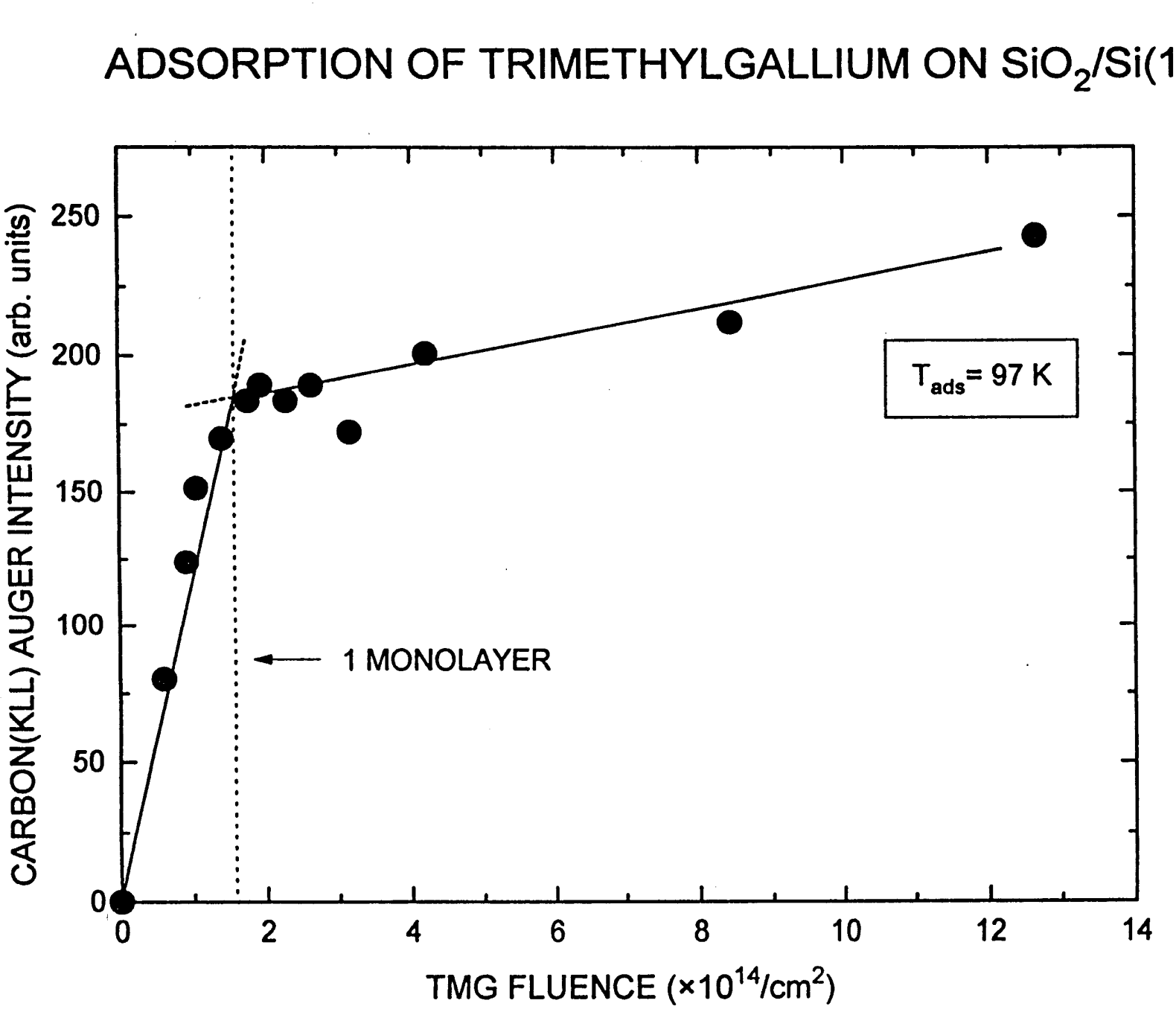

Lucas, et al
Figure 2

ADSORPTION OF TRIMETHYLGALLIUM ON SiO_2/Si(100)

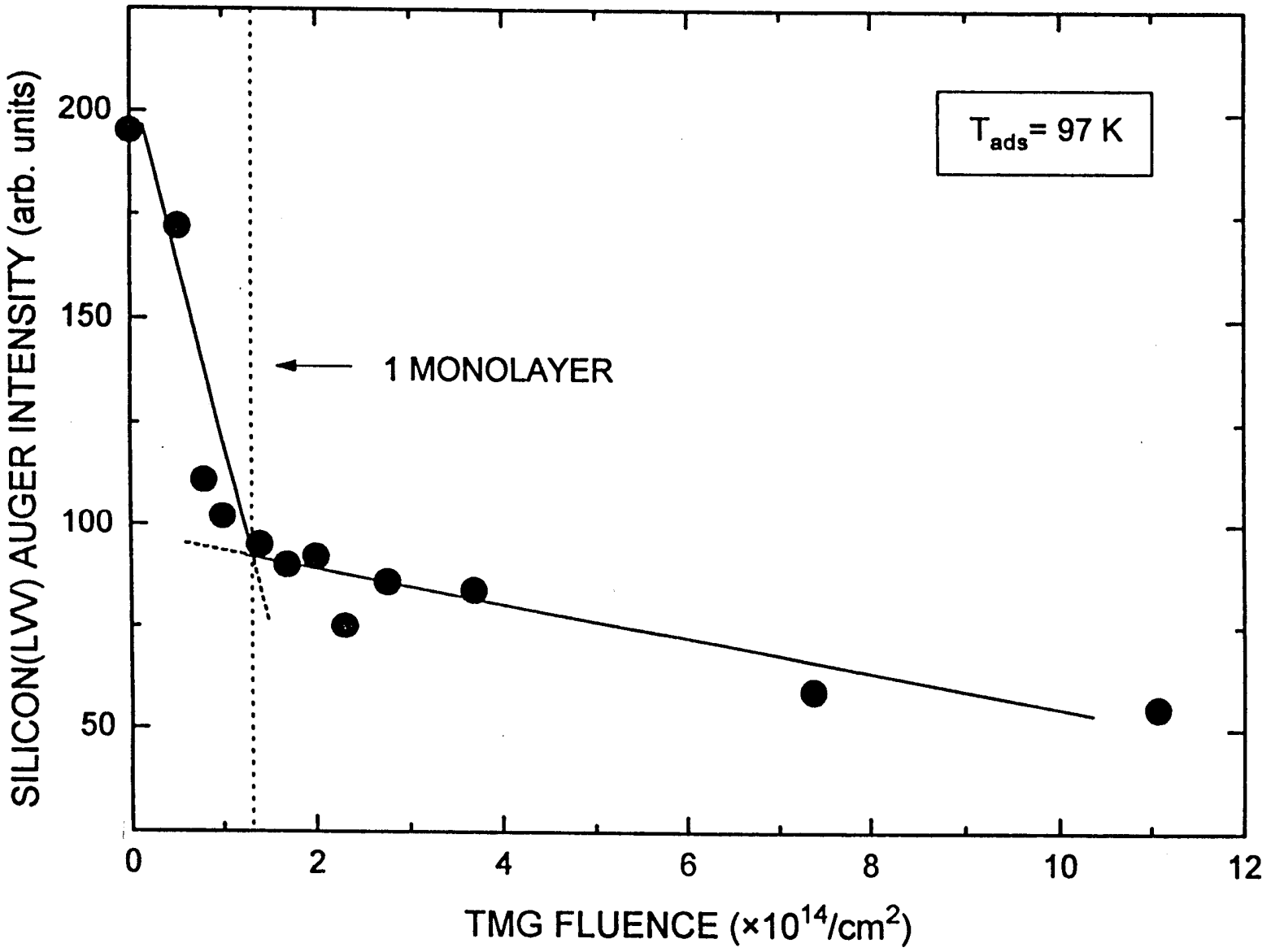

Lucas, et al

Figure 4

EFFECT OF PROLONGED ELECTRON BEAM EXPOSURE ON TMG/SiO_2

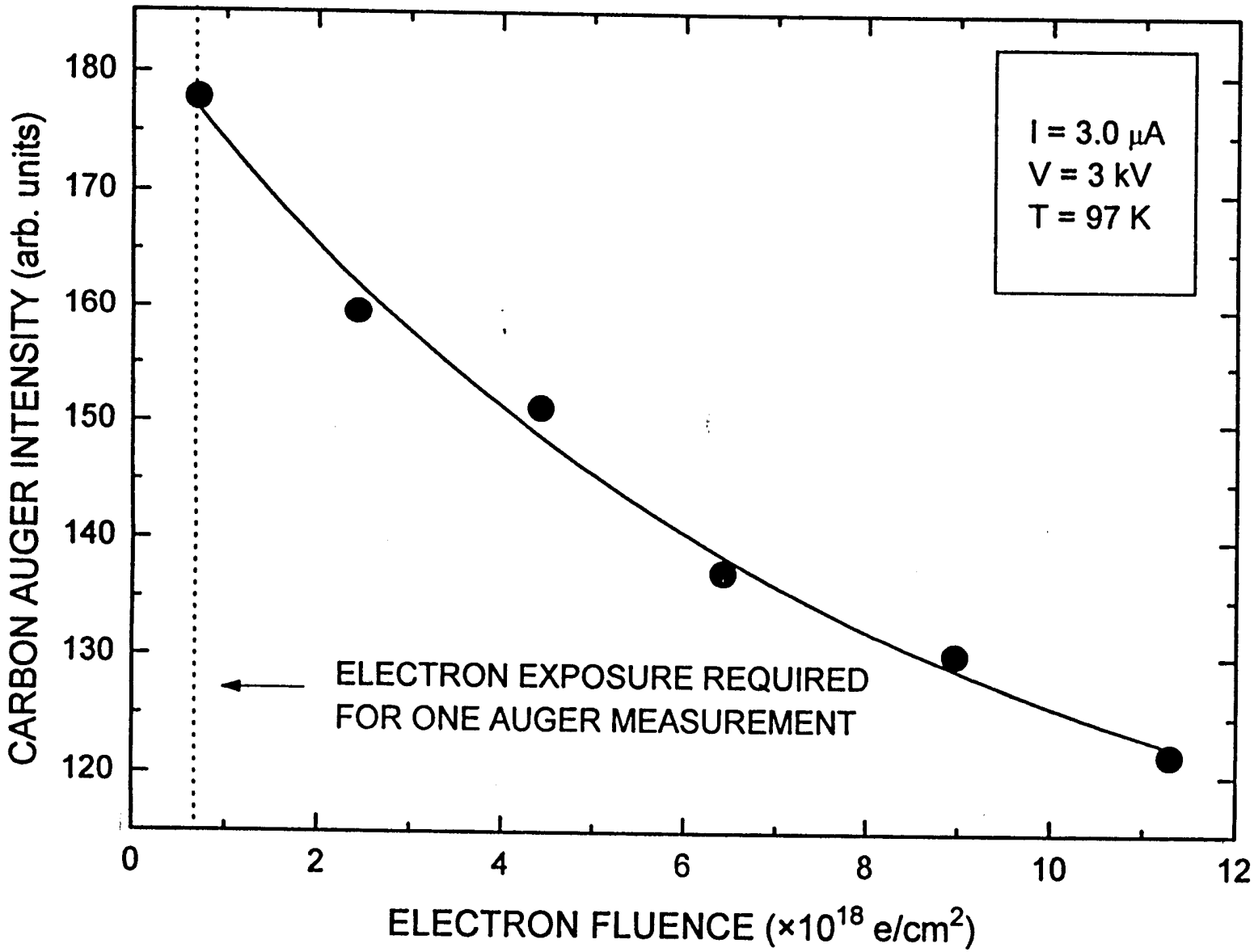

Lucas, et
Figure

EFFECT OF PROLONGED ELECTRON BEAM EXPOSURE ON TMG/SiO_2

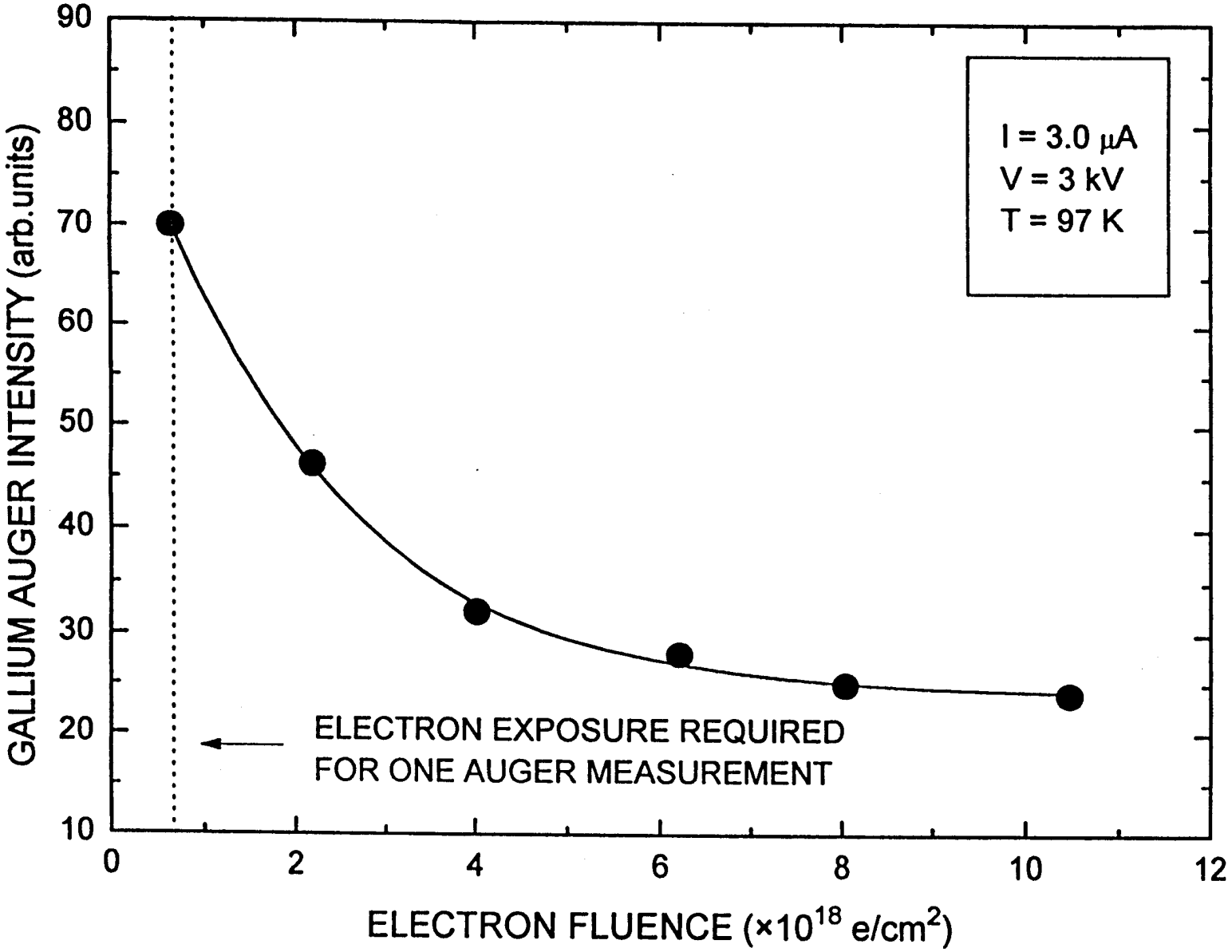

Lucas, et al

Figure 6

THERMAL DESORPTION OF m/e=99 and m/e=114 FROM SiO_2 EXPOSED TO TMG

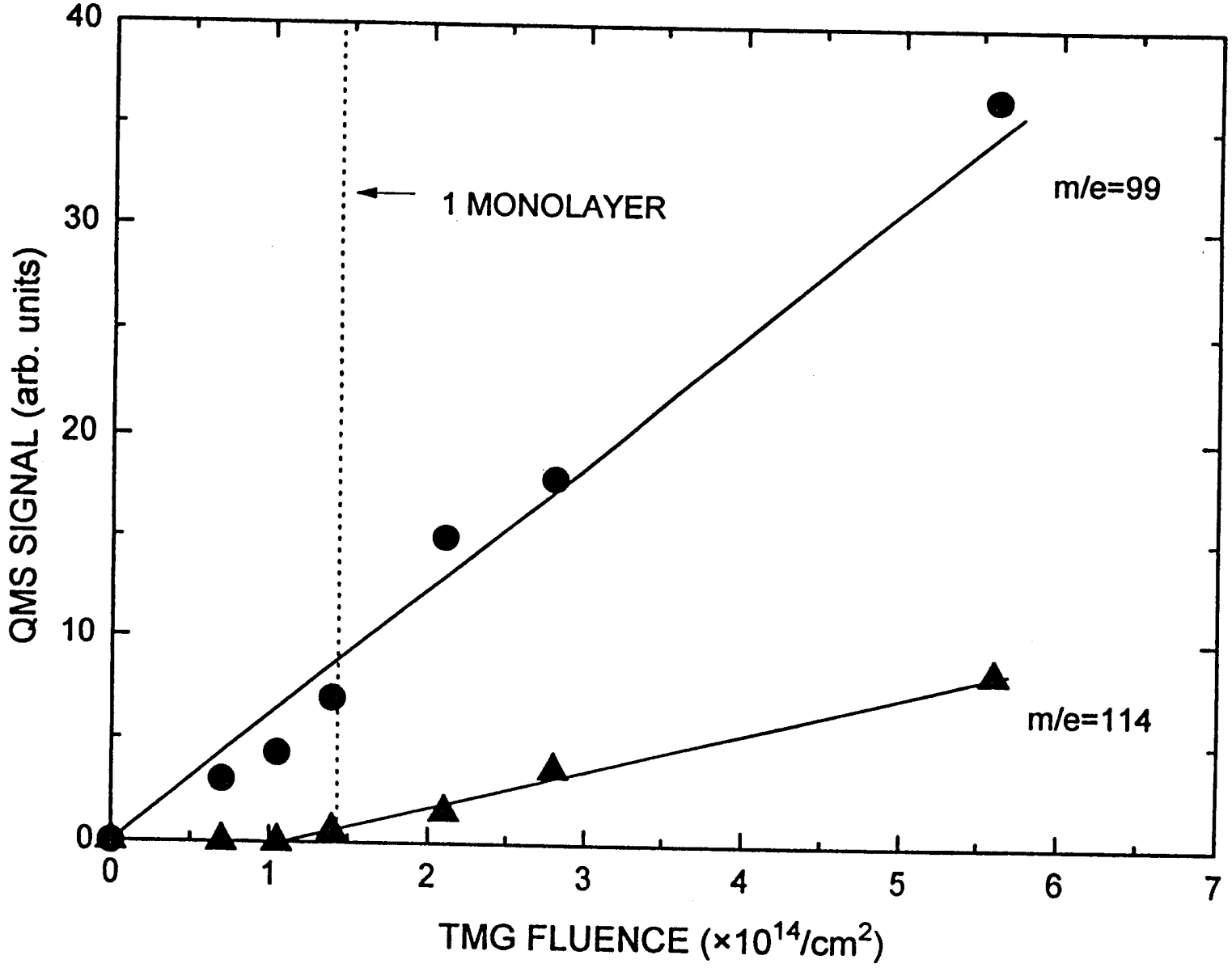

KINETICS OF EXTRACTION OF CH_3 FROM $Ga(CH_3)_X$ BY ATOMIC HYDROGEN AT DIFFERENT TEMPERATURES

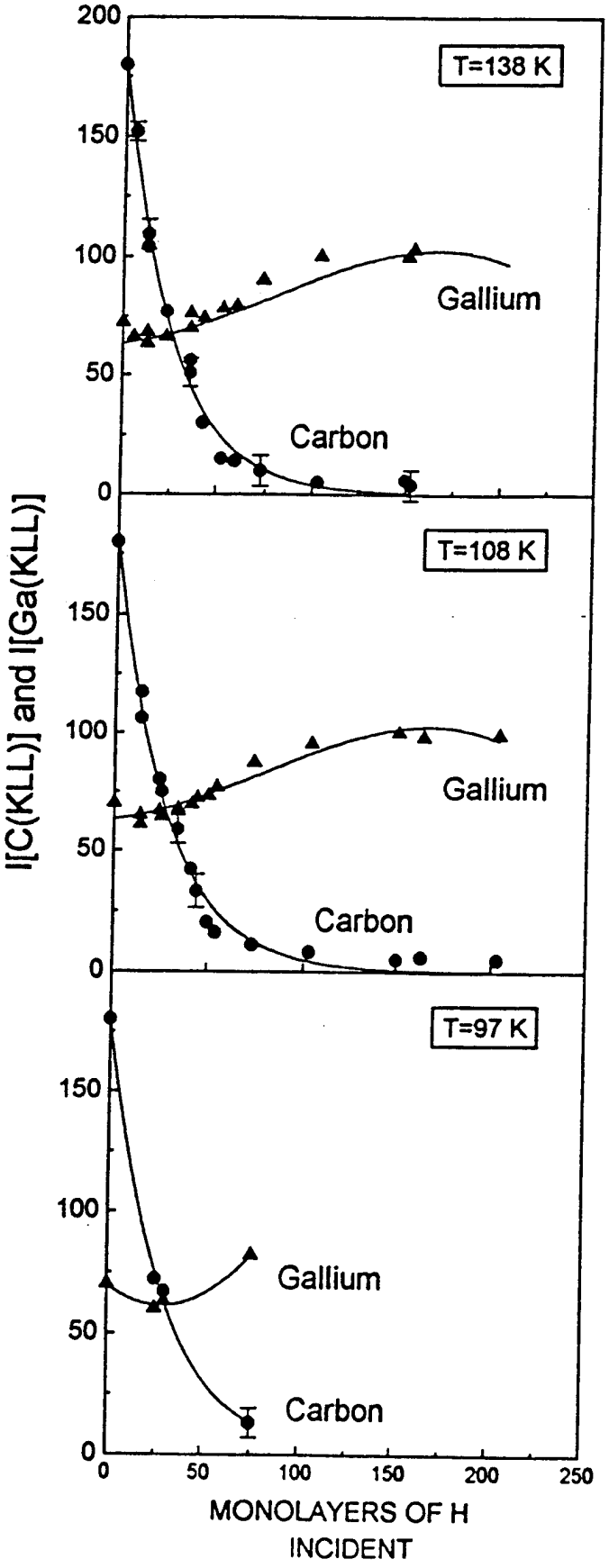

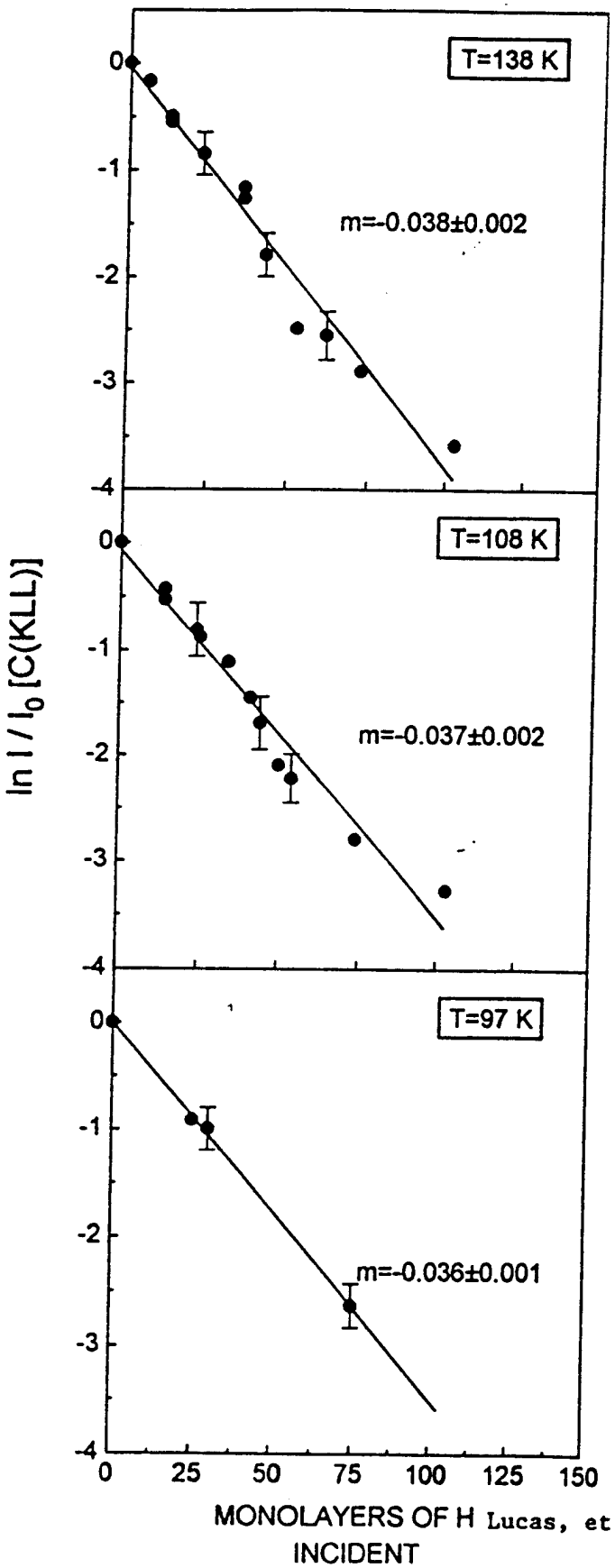

Lucas, et

Figure

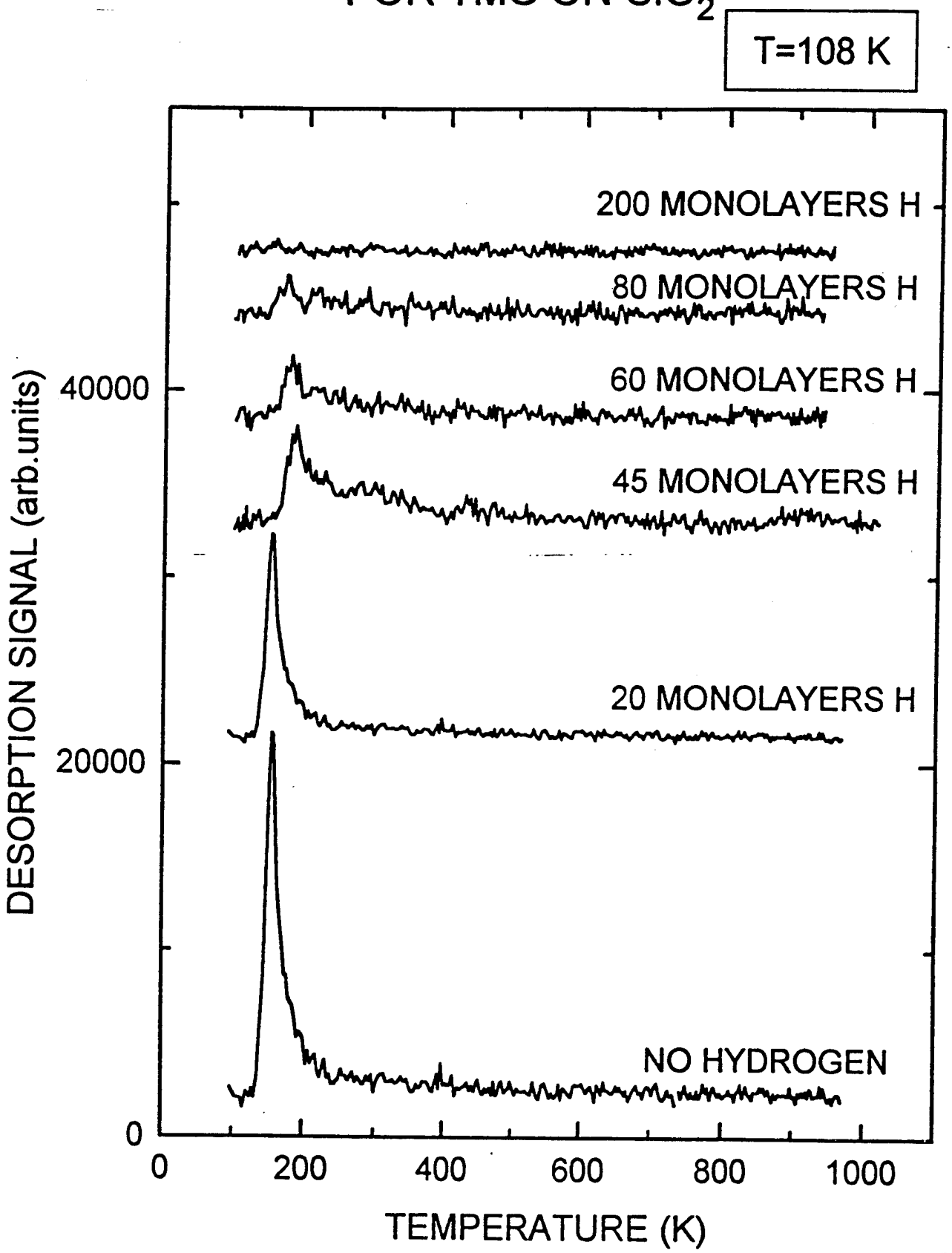

Lucas, et a

Figure 8

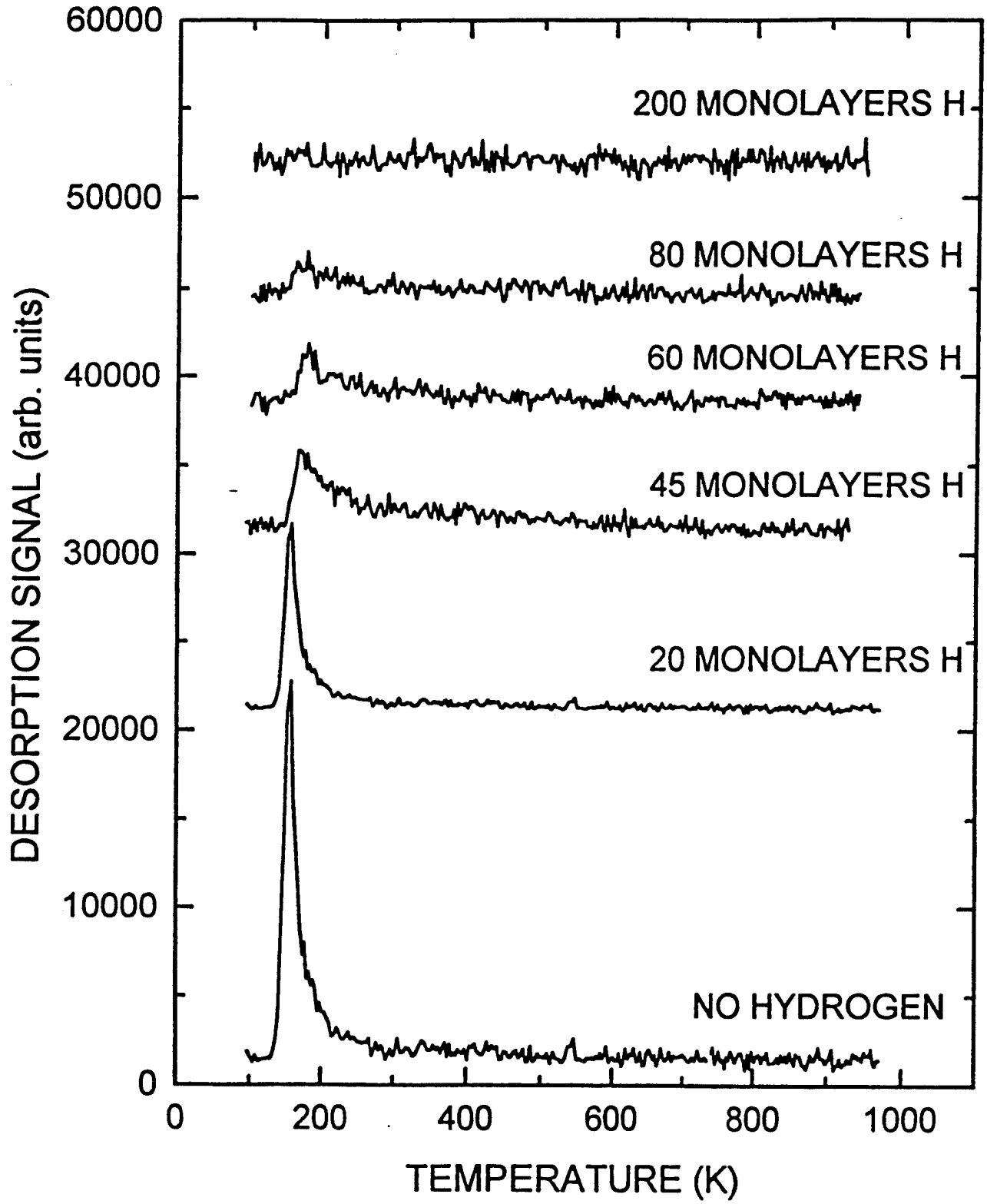

Lucas, et

Figure 9

Lucas, et al.

Figure 10

7. APPENDIX 2

"GaN Patterned Film Synthesis - Carbon Depletion by Hydrogen Atoms Produced From NH_3 Activated by Electron Impact", A. Hubner, S. R. Lucas, W. D. Partlow, W. J, Choyke, J. A. Schaefer, and J. T. Yates, Jr., Submitted to J. Vac. Sci. Technol., April, 1994.

Submitted: J. Vac. Sci. Technol. A

Date: 18 April 1994

GaN Patterned Film Synthesis - Carbon Depletion by Hydrogen Atoms Produced from NH_3 Activated by Electron Impact

A. Hübner,[a] S. R. Lucas, W. D. Partlow,[b] W. J. Choyke,[c] J. A. Schaefer,[a] and J. T. Yates, Jr.

Surface Science Center

Department of Chemistry

University of Pittsburgh

Pittsburgh, PA 15260

[a]Fachbereich Physik, Universität Kassel, D-34132 Kassel Germany

[b]Westinghouse Science and Technology Center

[c]Department of Physics, University of Pittsburgh, Pittsburgh, PA 15260

GaN Patterned Film Synthesis - Carbon Depletion by Hydrogen Atoms Produced from NH_3 Activated by Electron Impact

A. Hübner,[a] S. R. Lucas, W. D. Partlow,[b] W. J. Choyke,[c] J. A. Schaefer,[a] and J. T. Yates, Jr.

Surface Science Center

Department of Chemistry

University of Pittsburgh

Pittsburgh, PA 15260

[a]Fachbereich Physik, Universität Kassel, D-34132 Kassel, Germany

[b]Westinghouse Science and Technology Center

[c]Department of Physics, University of Pittsburgh, Pittsburgh, PA 15260

Abstract

The electron induced reaction of NH_3 with a surface layer produced by adsorption of trimethylgallium (TMG) on SiO_2 at 108 K has been investigated by Auger electron spectroscopy. It is shown that atomic hydrogen, produced by electron induced dissociation of NH_3, to form NH_X and H, efficiently extracts the methyl-groups from the layer leading to carbon removal from the GaN film which is formed. This process is non-thermal. A procedure for the synthesis of GaN is demonstrated and the layer-by-layer growth of a GaN film is shown. The method permits GaN to be deposited in a localized region which has been bombarded by the electron beam.

1. Introduction

GaN having a wide direct bandgap (3.4 eV at 300 K) is of great interest as an optoelectronic material applicable for blue and violet emitting devices working possibly at high temperatures [1,2]. Therefore the fabrication of high quality GaN films is required. Usually, GaN films are grown by metal organic molecular beam epitaxy (MOMBE) or metal organic chemical vapor deposition (MOCVD) methods. However, growth by these traditional techniques is accompanied by a variety of problems [2,3]. A possible major problem could be carbon contamination of the GaN films during the reaction of metal organics such as trimethylgallium (TMG) with NH_3, as seen for example in GaAs growth [4].

Previous studies have shown that atomic hydrogen extracts the methyl-groups from trimethylgallium-derived layers by producing either CH_3(g) or CH_4(g) [5]. This reaction is thought to be an Eley-Rideal process. The reaction occurs with an efficiency of 10^{-2} near 100 K and is non-activated [5]. Building on these first observations of the active role of atomic hydrogen in extracting CH_3 groups from the Ga-CH_3 bond, we have developed a second method which removes CH_3 groups efficiently while simultaneously synthesizing a GaN film. The source for atomic hydrogen is NH_3. It has been found previously that electron bombardment induces the dissociation of chemisorbed NH_3 to chemisorbed NH_2 [6] and chemisorbed NH [7] on Ni(110) producing atomic hydrogen at the surface. In addition Singh et al. [8] reported the dissociation of NH_3 to NH_2 on GaAs(100) following irradiation by 10 eV electrons at 150 K. This method has also been used successfully for low temperature electron-impact-induced nitridation of GaAs(100) [9] and SiO_2 thin films [10] using NH_3.

This study concerns the effect of electron impact on TMG-derived layers in the presence of adsorbed NH_3. The results provide a new method for the

production of GaN films under reaction conditions where carbon is directly eliminated from the surface. This new technique is utilized to grow monolayer and multilayer films of GaN and to show that direct writing of GaN features with an electron beam is possible, using the new technique.

2. Experimental

The experiments were carried out in an ultra-high vacuum (UHV) chamber with a base pressure of $p = 1\times10^{-10}$ Torr. The system is equipped with a cylindrical mirror analyzer (CMA) Auger electron spectrometer (AES), an Ar^+-ion sputter gun, a multiplexed quadrupole mass spectrometer, a reverse view low energy electron diffraction (LEED) apparatus and a calibrated microcapillary array doser [11-13]. The mounting procedure for the Si(100) crystal (p-type, B doped, 10 Ω·cm, $13\times13\times1.5$ mm^3) has been described previously [11, 13]. Final crystal cleaning is achieved by sputtering with Ar^+-ions ($E_i = 2$ keV, $I_{Ar^+} = 3.0$ μA) and subsequent heating to 1200 K. The heating is carried out resistively using a temperature programmer. SiO_2 films were prepared on the clean Si(100) crystal in the UHV chamber by a sputter-oxidation technique which employed approximately equal Ar and O_2 backing pressures ($p_{Ar} = p_{O_2} = 2\times10^{-5}$ Torr) [5] following the procedure of Chen et al., described previously [14]. An ion energy of 500 eV was employed. The thickness of the as-formed SiO_2 film was estimated to be 15-25 Å using the attenuation of the Si^0 (92 eV) Auger feature characteristic of the underlying Si(100) substrate and assuming an electron escape depth of 6.5 Å for SiO_2 [15]. Trimethylgallium (99.9999 % pure, Strem Chemicals) (TMG) was further purified by a freeze - pump - thaw cycle. The gas molecules were delivered to the crystal surface through the beam doser. Other studies indicate that almost pure TMG is emitted from the doser under the conditions of this experiment [16].

The adsorption/desorption kinetics for TMG on SiO_2 have been studied previously using Auger spectroscopy and temperature programmed desorption (TPD) [5] making it possible to estimate the layer thickness deposited in terms of monolayers.

All electron and ion beam currents (I) reported here were those measured between the crystal and ground and are uncorrected for secondary electron yield. The AES measurements were carried out with a 3 keV primary excitation electron beam which delivered $I_e = 3$ μA of current to the surface. The diameter of the electron beam was measured to be ~ 0.3 mm by translating the edge of the crystal through the electron beam and measuring the collected current. The modulation voltage was set at 6 V peak-to-peak for AES intensity measurements and 2 V peak-to-peak for AES line shape observations, respectively. The electron beam exposure used in these measurements was shown not to produce significant carbon depletion in control experiments carried out without a source of atomic hydrogen being present.

3. Results and Discussion

A. Electron-induced reaction of NH_3 with $Ga(CH_3)_X/SiO_2$

It has been shown by thermal desorption measurements that an adsorbed monolayer produced from TMG on SiO_2 probably consists of $Ga(CH_3)_2$, based on observations of the thermal desorption of this species at ~ 155 K [5].We designate this layer as $Ga(CH_3)_X$. The effect of NH_3 and electron impact on $Ga(CH_3)_X/SiO_2$ was measured by adsorbing approximately 1 monolayer of TMG on SiO_2/Si(100) at 108 K [5], backfilling the chamber with various pressures of NH_3 and exposing the crystal to a 3 keV electron beam for a pre-determined time. The electron

exposure was carried out in a duty cycle of 40 s active exposure time and 30 s with the crystal out of the electron beam to avoid large charging effects. Figure 1 shows the C (KLL) AES signal intensity (left side) and its natural logarithm (right side) versus the electron fluence for various NH_3 pressures.

While there is only a weak electron induced-desorption of carbon without NH_3 in the chamber, a strong decrease in the C (KLL) signal is observed when the NH_3 pressure is increased. Assuming first-order kinetics for the electron impact induced reaction, a cross section, $Q_{p_{NH_3}}$, for this process may be evaluated from the expression:

$$N_C = N_C^0 \exp[- (jt/e) Q_{p_{NH_3}}]. \qquad (1)$$

Here N_C and N_C^0 are the coverage of carbon atoms at the time t and at the time t = 0, respectively, j is the electron irradiation current density and e is the elementary charge. The cross section determined from this analysis, $Q_{p_{NH_3}}$, is dependent on the pressure of NH_3 because of the dependence of the rate of the electron-induced process on the steady state coverage of NH_3 achieved under dynamic conditions.

In addition to measurements of carbon depletion due to electron induced-processes, it was important to monitor Ga depletion effects also. In the Ga (LMM) Auger measurements (Figure 2), almost no difference between the "no NH_3"-curve (background pressure of ~ 1×10^{-10} Torr) and the curves at the various NH_3 pressures is seen. This clearly indicates that the major electron-induced process in the presence of NH_3 is the removal of the methyl-groups, while Ga remains on the surface. The Ga Auger intensity was shown to be stable up to ~ 900 K, as would be expected for GaN.

A control experiment with N_2 instead of NH_3 was employed to distinguish between the role of electron-induced formation of N and H in the reaction. Figure

3 shows clearly that even at a N_2 pressure of $p_{N_2} = 5 \times 10^{-8}$ Torr there is no influence (within the experimental uncertainty) on the rate of the C(KLL) and the Ga(LMM) loss processes. This leads to the conclusion that H derived from electron-induced dissociation of NH_3 (a) is needed for the extraction of the methyl-groups.

Previous studies on the effect of atomic hydrogen on TMG/SiO_2 [5] and the results presented here lead to the postulated mechanism shown schematically in Figure 4:

a) Electron-induced dissociation of adsorbed NH_3 [6,7,8] leads to the production of NH_X (a) and H species. Since we employ a 3 keV electron beam it is very likely that backscattered and/or secondary electrons returning from the bulk to the surface play an important role in this process.
b) Atomic hydrogen reacts with the methyl-groups of $Ga(CH_3)_X/SiO_2$ eliminating CH_3 groups efficiently.
c) During the irradiation with electrons GaN is formed. The GaN is thermally stable to 900 K.

The mechanism accounts for increase of the cross section, $Q_{p_{NH_3}}$, with increasing ammonia pressure, since the surface coverage of adsorbed NH_3 under dynamic conditions, and hence the supply of atomic hydrogen, will increase with increasing p_{NH_3}. Atomic hydrogen made from NH_3 removes the methyl-groups from TMG. The rate of extraction of the methyl-groups increases with the rate of production of hydrogen atoms from NH_3 on the surface. As indicated by linear semilog plots in Fig. 1, the reaction is first-order in the surface concentration of CH_3 groups at a given p_{NH_3}. The cross section, $Q_{p_{NH_3}}$, for depletion of carbon is of the order of 5×10^{-20} cm^2 at $p_{NH_3} = 5 \times 10^{-8}$ Torr.

It is of interest to compare the rate of the CH_3 depletion process with the flux of electrons and the flux of NH_3 onto the surface under these conditions. At

the beginning of the CH_3 extraction process, we assume that a monolayer of the $Ga(CH_3)_X$ consists of about 1×10^{14} species/cm^2 = N [5]. Then, for an electron flux,

$F_e \approx 2 \times 10^{16}$ e / (cm^2 s),

$$-dN/dt = N F_e Q_{p_{NH_3}} \cong 1 \times 10^{11} /(\text{cm}^2\ \text{s}) \qquad (2)$$

$$= \text{rate of } CH_3 \text{ loss.}$$

Under these conditions, the flux of NH_3, F_{NH_3}, from kinetic theory is ~ 200 times larger than the rate of the CH_3 loss, viz.

$$F_{NH_3} = p_{NH_3} / (2\pi\, m_{NH_3}\, k\, T_g)^{1/2} \approx 2 \times 10^{13}\ NH_3 / (\text{cm}^2\ \text{s}) \qquad (3)$$

Thus, under the conditions of the experiment, as shown by the information in equation (2), each electron has an efficiency of order 5×10^{-6} for causing a CH_3 extraction process. Assuming that electron stimulated desorption (ESD) effects have not caused significant depletion of NH_3 from a monolayer under the conditions of this experiment, a CH_3 extraction efficiency of 5×10^{-6} is reasonable on the following grounds:

a) Two inefficient processes work in series causing the extraction process. They are:

$$NH_3 + e^- \xrightarrow{\varepsilon_1} NH_x + H \qquad (4)$$

$$H + Ga(CH_3)_x \xrightarrow{\varepsilon_2} HGa(CH_3)_{x-1} + CH_3(g) \text{ or } CH_4(g) \qquad (5)$$

where ε_1 is the efficiency to produce one H per collision of one electron with NH_3 (a) and ε_2 is the efficiency of CH_3 extraction by the atomic H produced as described by equation (4).

b) We know, from previous studies of the CH_3 extraction process by atomic H, that an efficiency of order 10^{-2} is appropriate for ε_2 [5].

c) Thus, since the joint efficiency $\varepsilon_2\varepsilon_1$ is ~ 5×10^{-6} / electron, ε_1 is ~ 5×10^{-4}, corresponding to a cross section of order 5×10^{-19} cm^2 for breaking

the N-H bond in adsorbed NH_3 by electron impact using 3 keV electrons (assuming a NH_3 coverage of the order of 10^{15} /cm^2) .

A value of ~ 10^{-16} cm^2 for N-H bond breaking in chemisorbed NH_3 by 55 eV electrons has been measured on a Ni(110) surface [6].

B. GaN growth

Applying the above method, it is possible to grow GaN on SiO_2 as schematically shown in Fig. 4. GaN is produced from this treatment and the Ga(LMM) and the N(KLL) Auger intensities were observed to be stable to 900 K in the electron irradiated spot, while elsewhere (without electron exposure) the N(KLL) and the Ga(LMM) AES intensities fell to near zero at 900 K, as thermal desorption of non-reacted species occurred.

Figure 5 shows the N(KLL) Auger signal from Si_3N_4 [17], and also of a monolayer and a multilayer of the as-formed GaN on SiO_2. In addition the measured N(KLL) lineshape of a 1.23 μm thick GaN film on (0001)Al_2O_3 (grown by metal-organic chemical vapor deposition) was used as a reference. With increasing thickness of the GaN film grown by the process described in this paper, the N(KLL) lineshape becomes increasingly similar to that of the GaN reference; however, the characteristic nitride Auger lineshape was not observed.

In Fig. 5, a superposition of the GaN and a Si_3N_4 N(KLL) Auger signal is present. After adsorption of approximately 1 monolayer of TMG on SiO_2 and methyl-group extraction by NH_3 activated by electron impact, both GaN and Si_3N_4 will be detected by AES. With increasing thickness of the GaN film, the N(KLL) Auger lineshape will approach that of GaN, but as long as the thickness of the GaN film is in the order of the escape depth for Auger electrons (~ 10 Å for 380 eV electrons [18]) there will be a contribution from Si_3N_4 also, as seen in Figure

5. This may contribute to the lack of exact agreement in the N(KLL) Auger lineshape with the GaN standard.

The GaN film growth in three steps is shown in Figure 6 together with the corresponding C(KLL), N(KLL) and Ga(LMM) AES signals. In step one, approximately 1 monolayer of TMG is adsorbed on the SiO_2/Si(100) surface at 108 K [5] so that in addition to the Si and the O Auger signals, also the C and the Ga signals due to the TMG-derived layer are visible. In the second step the chamber is backfilled with $p_{NH_3}=5\times10^{-7}$ Torr of ammonia and the crystal is exposed to the 3 keV Auger electron beam (I = 3μA) for 15 min. The C(KLL) signal disappears due to the reaction of H atoms (produced from adsorbed NH_3) with the surface methyl-groups and the N(KLL) signal develops indicating that GaN and adsorbed NH_X are present; the Ga Auger intensity remains the same as in step one. In step three, subsequent heating to 300 K yields an Auger spectrum which indicates no carbon; only N and Ga are present. Auger spectra acquired on areas of the SiO_2 surface not subjected to electron irradiation in the presence of NH_3 (g) show that 300 K is sufficient to desorb NH_3 and the $Ga(CH_3)_X$, as shown at the bottom of Figure 6.

Repeated use of this procedure leads to a multilayer of GaN (Figure 7). After the growth of the first layer the crystal was heated to 300 K (2nd row) and after the growth of the second layer the crystal was heated up to 900 K (4th row). AES measurements outside the actual GaN dot (5th row) show almost no C, Ga or N, indicating that the GaN synthesis reaction takes place only where the crystal containing $Ga(CH_3)_X$ and NH_3 layers is exposed to electrons.

The procedure to produce a dot of GaN was modified to produce a line of GaN and an AES profile perpendicular to the line was then acquired (Figure 8). This line was grown at 108 K without heating subsequently, so that outside the line both $Ga(CH_3)_x$ and NH_3 remain adsorbed. The C(KLL) signal is low on the

GaN line due to the electron-induced reaction of atomic H from NH_3 with the surface methyl-groups. Off the line the C(KLL) signal is high, indicating the presence of adsorbed $Ga(CH_3)_x$ on both sides of the line. The N(KLL) signal shows opposite behavior. Outside the line adsorbed NH_3(low signal) is seen. In contrast, in the GaN line region the N(KLL) signal is quadrupled. The Ga(LMM) signal (not shown) exhibits a slight increase on the line as compared with its values acquired off the line. The data are arbitrarily fit to a Gaussian profile but the actual GaN lineshape cannot be determined in this experiment.

C. Extension to GaN Film Growth at Higher Substrate Temperatures

The SiO_2 substrate temperatures chosen for these studies was 108 K. This is done so that significant coverages of TMG and NH_3 can be maintained in ultrahigh vacuum, needed for the analytical procedure employed here. It is envisioned that growth of GaN by this method will work at higher substrate temperatures, using higher TMG and NH_3 pressures to maintain the appropriate surface coverage for efficient electron-impact induced GaN film growth.

4. Conclusions

Trimethylgallium and ammonia have been used as precursors for GaN formation, activated by electron impact. It is found that the methyl-groups are removed from TMG by a reaction with atomic hydrogen, formed by the electron-impact-induced dissociation of NH_3. This is consistent with earlier studies [5] in which atomic hydrogen, produced in the gas phase also efficiently removes methyl-groups. The mechanism has been applied to grow GaN on SiO_2 and it is shown that GaN-structure writing on SiO_2 is possible using the electron beam.

This synthesis method offers the possibility of producing GaN films which are less contaminated by carbon impurities than GaN films grown thermally from the same precursors.

Acknowledgment

The authors acknowledge with thanks the support of the work by AFOSR under contract F49620-91-C-0032. We thank Dr. D.K. Wickenden, Applied Physics Laboratory, Johns Hopkins University, for supplying the GaN/Al_2O_3 sample used for reference Auger spectral measurements.

Figure captions

Figure 1. Electron induced reaction of NH_3 with $Ga(CH_3)_X$ / SiO_2. Shown is the C(KLL) Auger signal (left side) and its normalized natural logarithm (right side) versus the number of electrons per cm^2. $Q_{p_{NH_3}}$ is the NH_3 pressure dependent cross section for the depletion of the methyl-groups
by the electron stimulated process.

Figure 2. Electron induced reaction of NH_3 with $Ga(CH_3)_X$ / SiO_2. Shown is the Ga(LMM) Auger signal (left side) and its normalized natural logarithm (right side) versus the number of electrons per cm^2.

Figure 3. Control experiment with N_2 instead of NH_3. Shown is the C(KLL) Auger signal and its normalized natural logarithm (top) and the Ga(LMM) Auger signal and its normalized natural logarithm (bottom) versus the number of electrons per cm^2.

Figure 4. Schematic mechanism for GaN production by an electron induced reaction of adsorbed $Ga(CH_3)_X$ with NH_3.

Figure 5. Normalized and superimposed lineshapes of the N(KLL) Auger signal with increasing thickness of the GaN film. A comparison to a reference thick film of GaN and a reference Si_3N_4 film is given. Modulation voltage = 2 V peak-to-peak.

Figure 6. Monolayer GaN synthesis on SiO_2 by an electron-induced reaction of $Ga(CH_3)_X$ with NH_3 at 108 K.

Figure 7. Multilayer GaN synthesis on SiO_2 by an electron-induced reaction of $Ga(CH_3)_X$ with NH_3 at 108 K.

Figure 8. Profile of C(KLL) and N(KLL) Auger signals across a GaN line grown according to the procedure of this paper by scanning the electron beam.

References

[1] J. I. Pankove, Mat. Res. Soc. Proc. **162**, 515 (1990).

[2] (a) S. Strite and H. Morkoç, J. Vac. Sci. Technol. B **10**, 1237 (1992); (b) M. Rubin, N. Newman, J.S. Chan, T.C. Fu and J.T. Ross, Appl. Phys. Lett. **64**, 64 (1994).

[3] R. F. Davis, Z. Sitar, B. E. Williams, H. S. Kong, H. J. Kim, W. Palmour, J. A. Edmond, J. Ryu, J. T. Glass, and C. H. Carter, Jr., Mater. Sci. Eng. B **1**, 77 (1988).

[4] (a) T. R. Gaw, F. Lee, R. Lin, A. L. Backman and R. I. Masel, Vacuum **41**, 954 (1990); (b) C. R. Flores, X-L. Zhou and J. M. White, Surf. Sci. **261**, 99 (1992); (c) S. P. DenBaars, B. Y. Maas, P. O. Dapkus, A. D. Danner and H. C. Lee, J. Cryst. Growth **77**, 188 (1986).

[5] S. Lucas, W. D. Partlow, W. J. Choyke and J. T. Yates, Jr., J. Vac. Sci. Technol., submitted.

[6] C. Klauber, M. D. Alvey, and J. T. Yates, Jr., Surf. Sci. **154**, 139 (1985).

[7] I. C. Bassignana, K. Wagemann, J. Küppers, and G. Ertl, Surf. Sci. **175**, 22 (1986).

[8] N. K. Singh, A. J. Murrell, and J. S. Foord, Surf. Sci. **274**, 341 (1992).

[9] Y.-M. Sun and J. G. Ekerdt, J. Vac. Sci. Technol. B **11**, 610 (1993).

[10] A. Glachant, B. Balland, A. Ronda, J. C. Bureau, and C. Plossu, Surf. Sci. **205**, 287 (1988).

[11] K. H. Bornscheuer, S. R. Lucas, W. J. Choyke, W. D. Partlow, and J. T. Yates, Jr., J. Vac. Sci. Technol. A **11**, 2822 (1993).

[12] C. C. Cheng, R. M. Wallace, P. A. Taylor, W. J. Choyke, and J. T. Yates, Jr., J. Appl. Phys. **67**, 3693 (1990).

[13] M. J. Bozack, L. Muehlhoff, J. N. Russell, Jr., W. J. Choyke, and J. T. Yates,

Jr., J. Vac. Sci. Technol. A **5**, 1 (1987).

[14] P. J. Chen, M. L. Colaianni, M. Arbab, and J. T. Yates, Jr., J. Non-Cryst. Solids **155**, 131 (1993).

[15] F. J. Himpsel, F. R. McFeely, A. Taleb-Ibrahimi, J. A. Yarmoff, and G. Hollinger, Phys. Rev. B **38**, 6084 (1988).

[16] R. Lin, L. Cadwell, R. I. Masel, J. Vac. Sci. Technol. A **12**, 179 (1994).

[17] The Si_3N_4 was prepared by an electron-induced nitridation of SiO_2, using NH_3 (see ref. 9).

[18] A. Zangwill, in *Physics at Surfaces* (Cambridge University Press, 1988).

Electron Induced Reaction of NH_3 with $Ga(CH_3)_X/SiO_2$

$I_{crystal}$ = 3μA

V_e = 3 kV

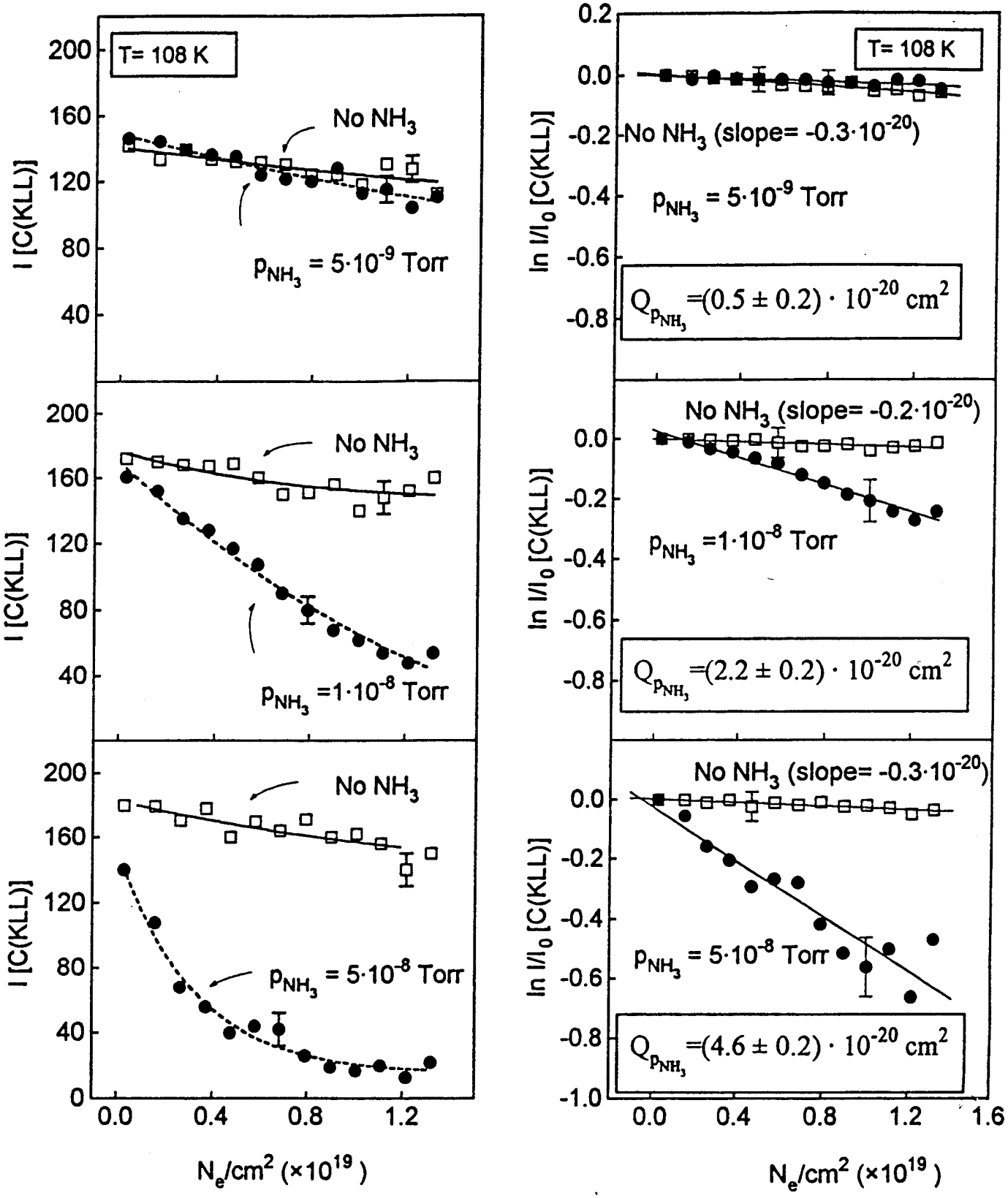

Hubner, et

Figure 1

Electron Induced Reaction of NH_3 with $Ga(CH_3)_X/SiO_2$

$I_{crystal}$= 3μA

V_e= 3 kV

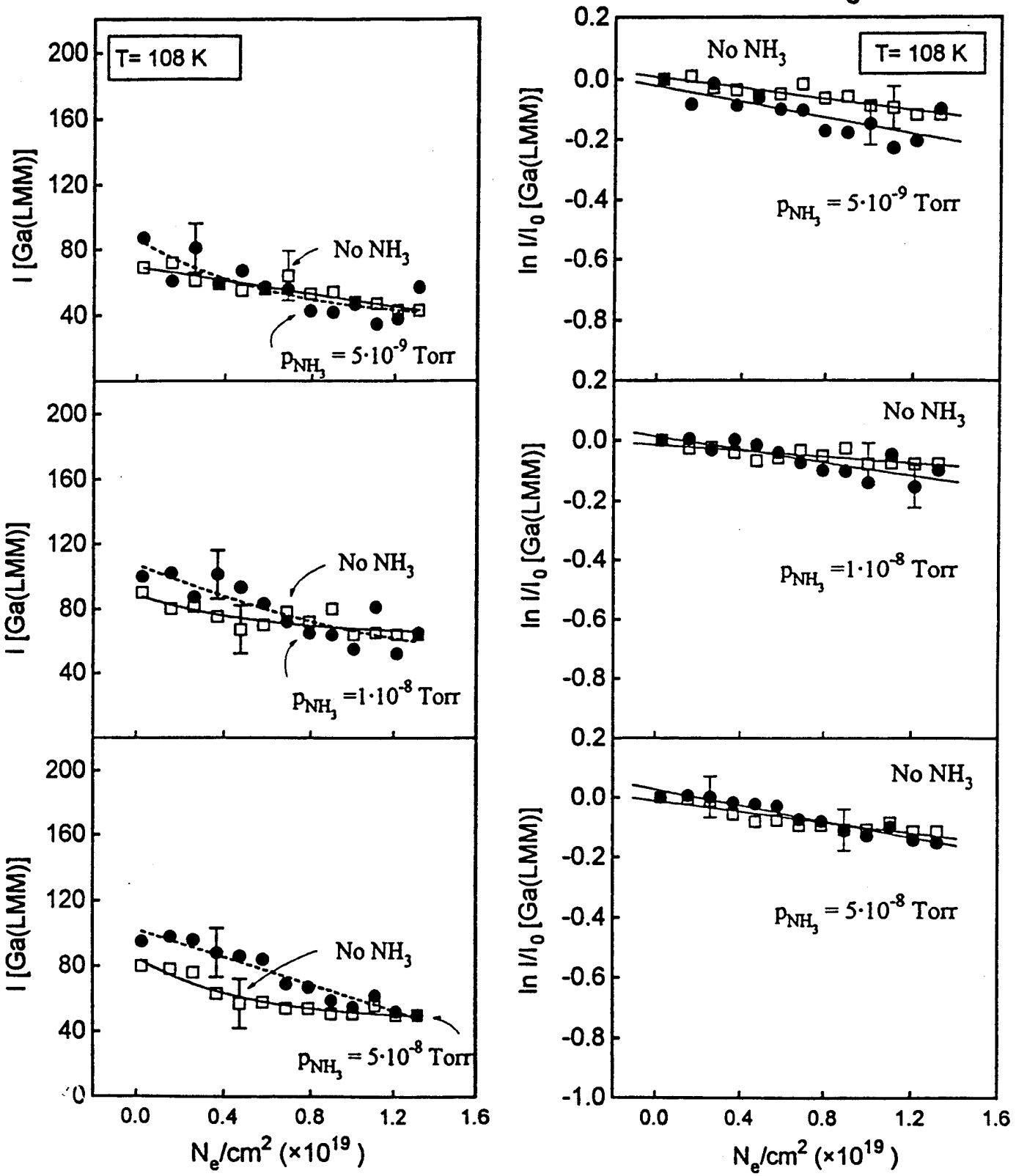

Hubner, et al

Figure 2

Control Experiment - Electron Induced Reaction of N_2 with $Ga(CH_3)_X/SiO_2$

$I_{crystal}$= 3μA

V_e= 3 kV

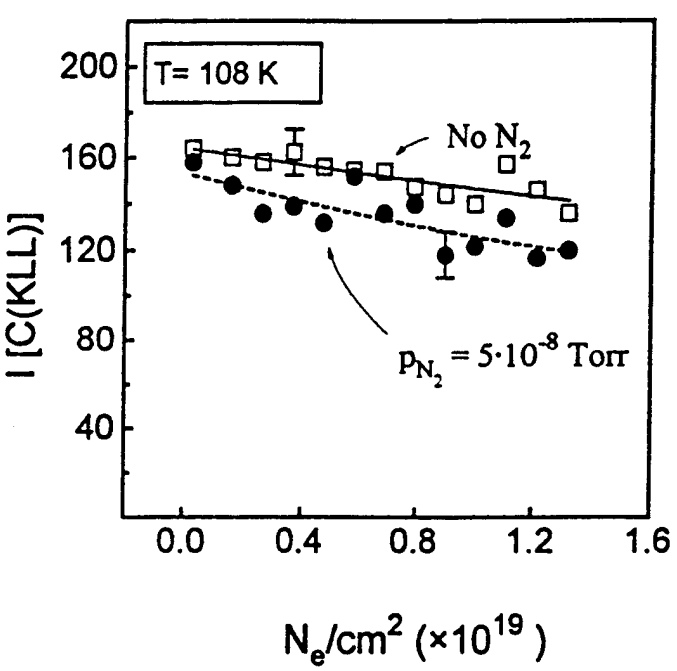

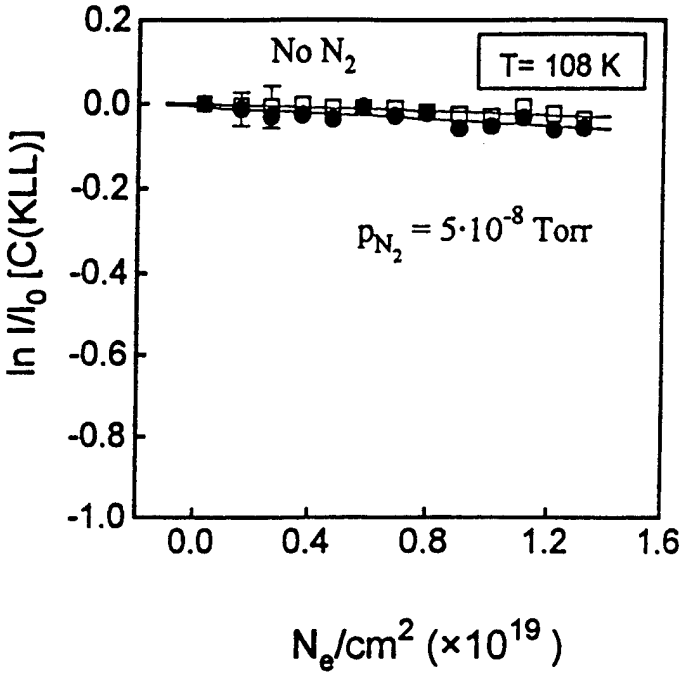

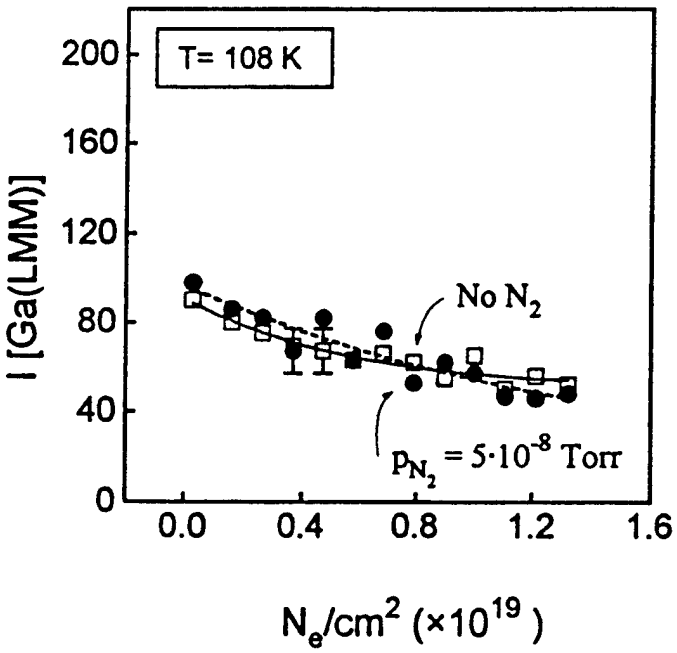

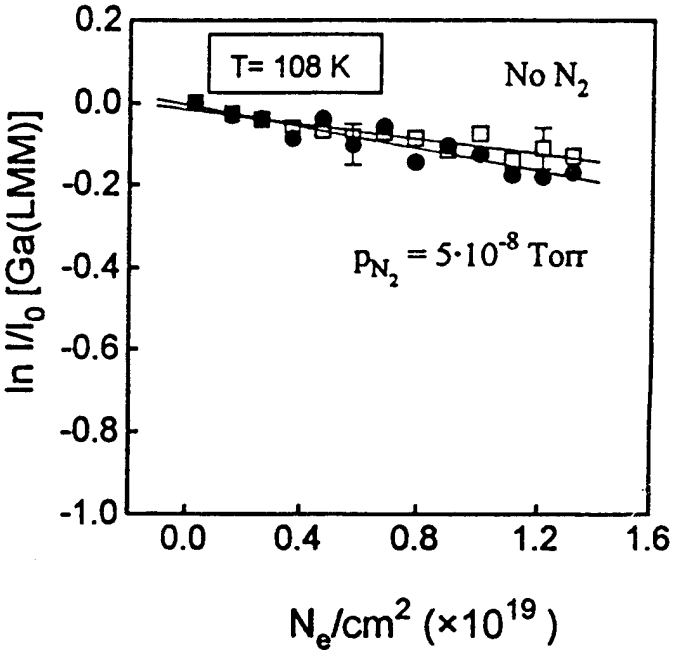

Hubner, et

Figure 3

Schematic Sequence of Reaction Events in Carbon Extraction and GaN Formation

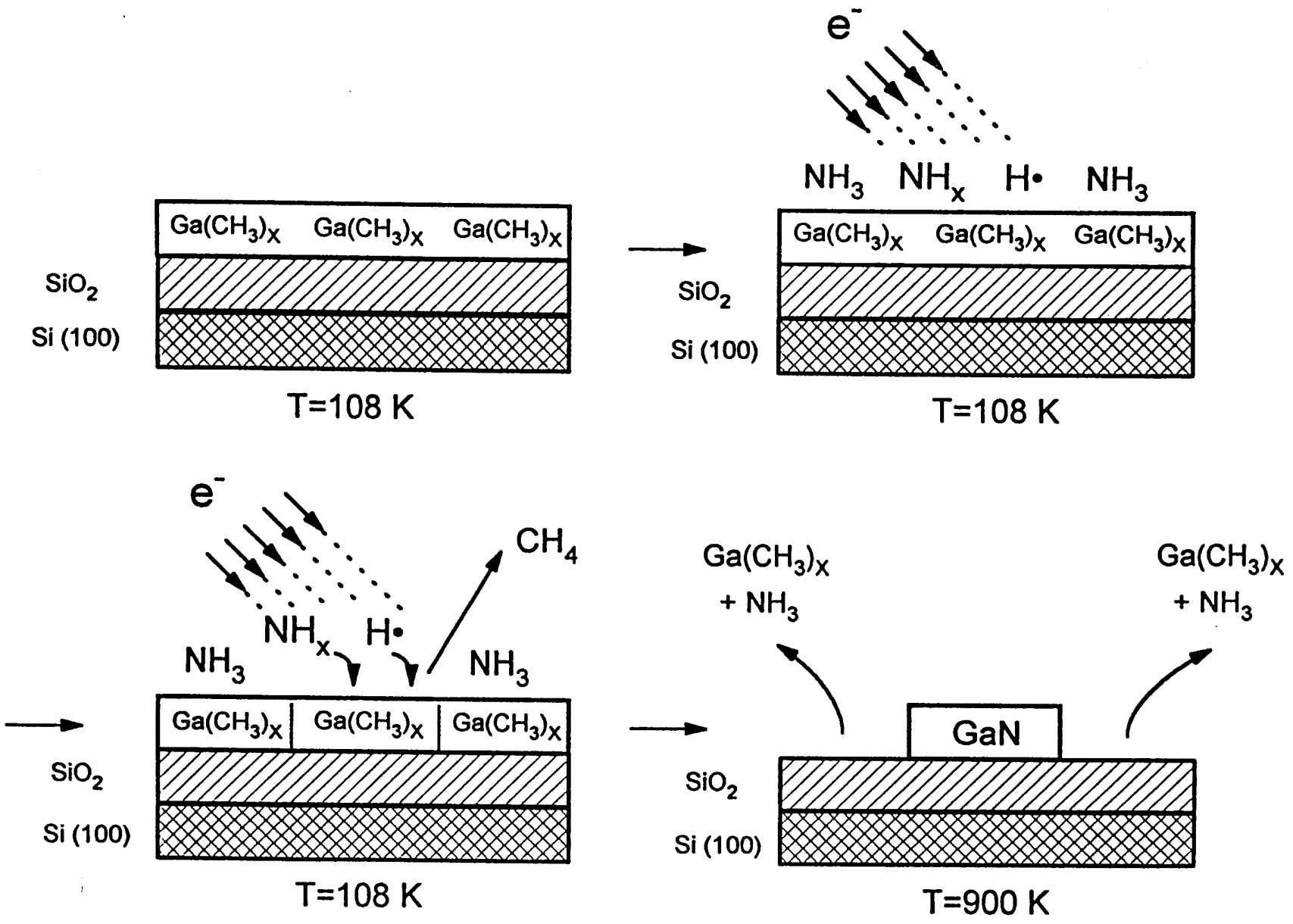

Hubner, et al.

Figure 4

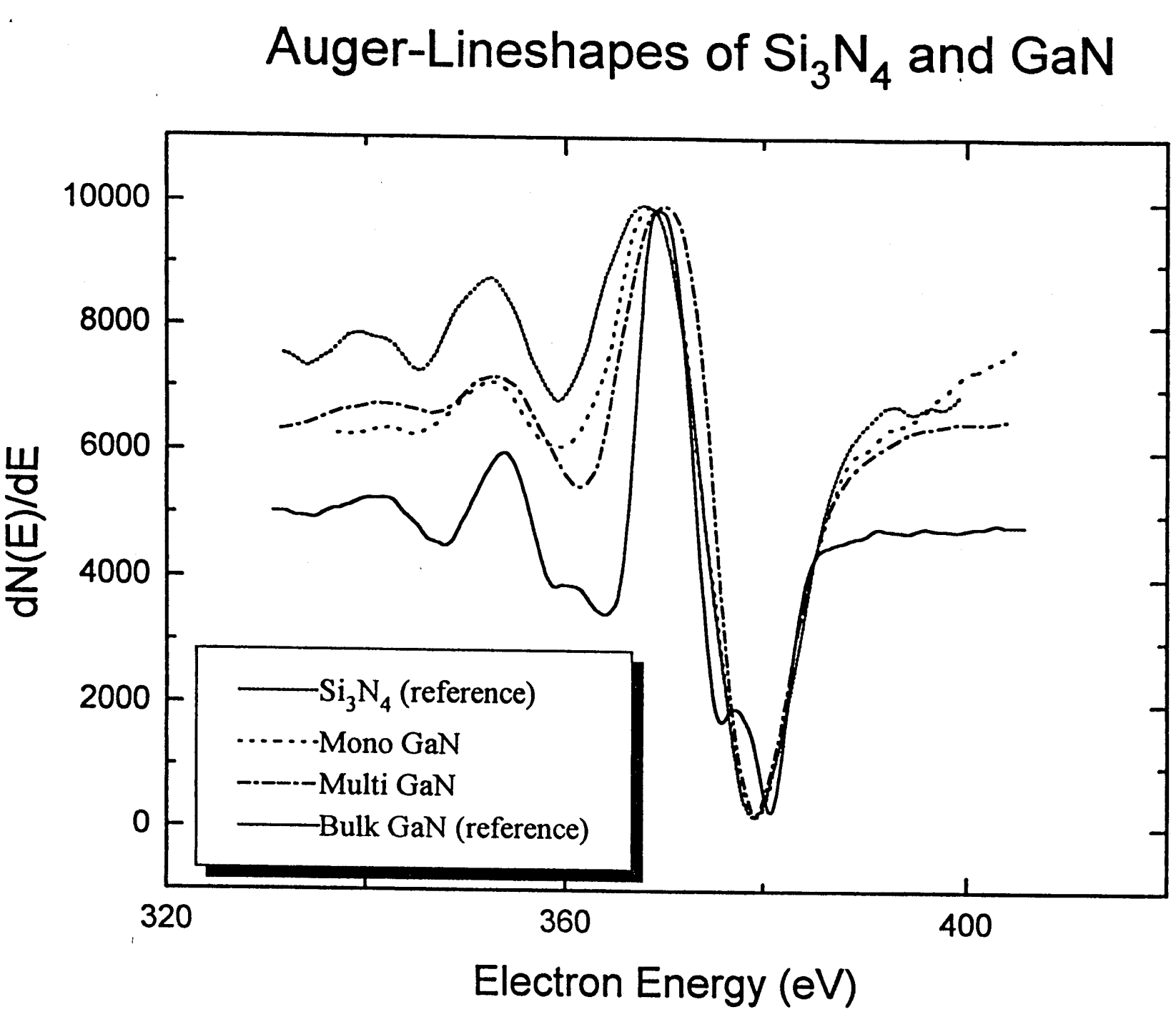
Auger-Lineshapes of Si_3N_4 and GaN
dN(E)/dE
10000
8000
6000
4000
2000
0
320
360
400
Electron Energy (eV)
Si_3N_4 (reference)
Mono GaN
Multi GaN
Bulk GaN (reference)

Monolayer GaN Synthesis on SiO_2 by using NH_3 + Electron Impact

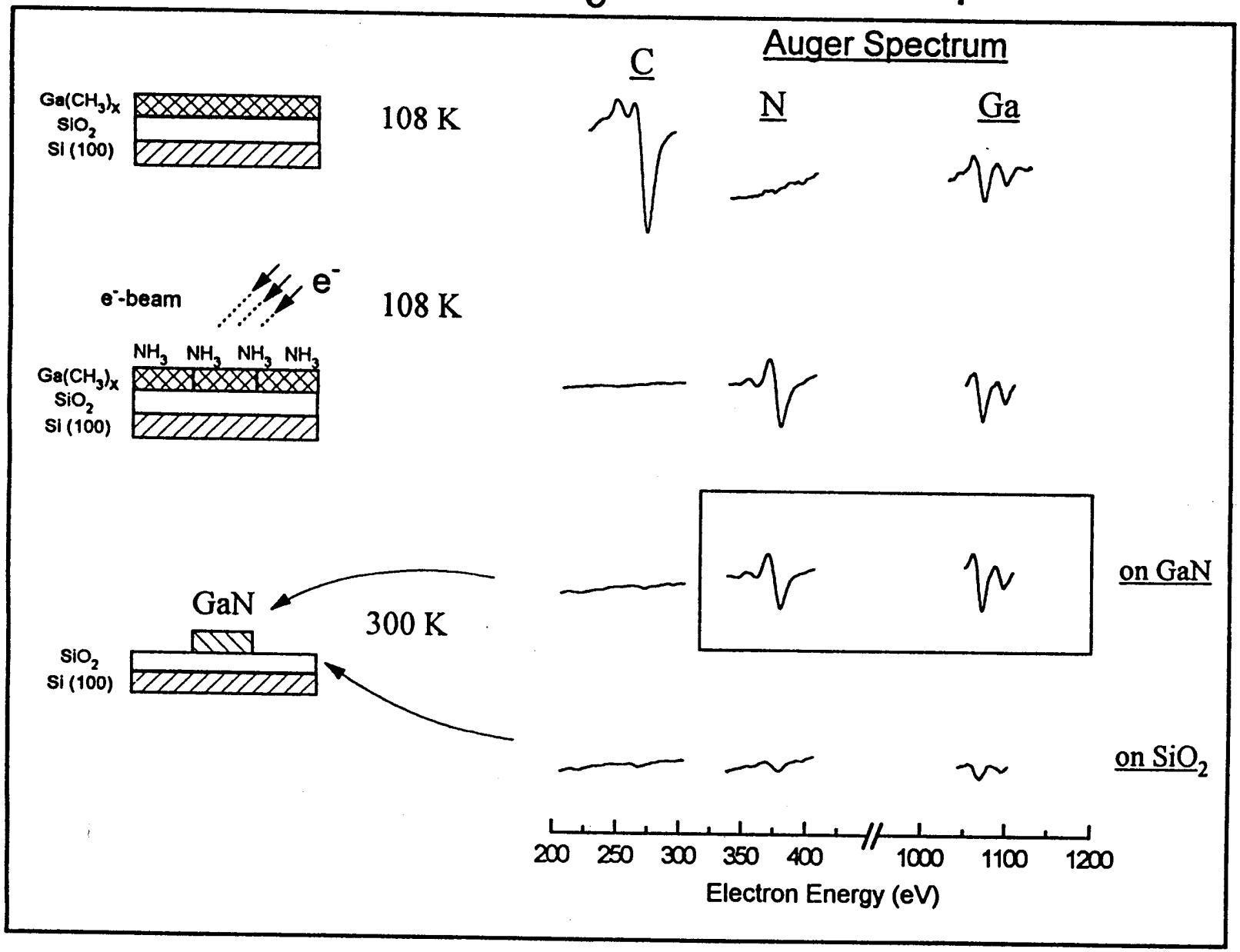

Hubner, et al.

Figure 6

Multilayer GaN Synthesis

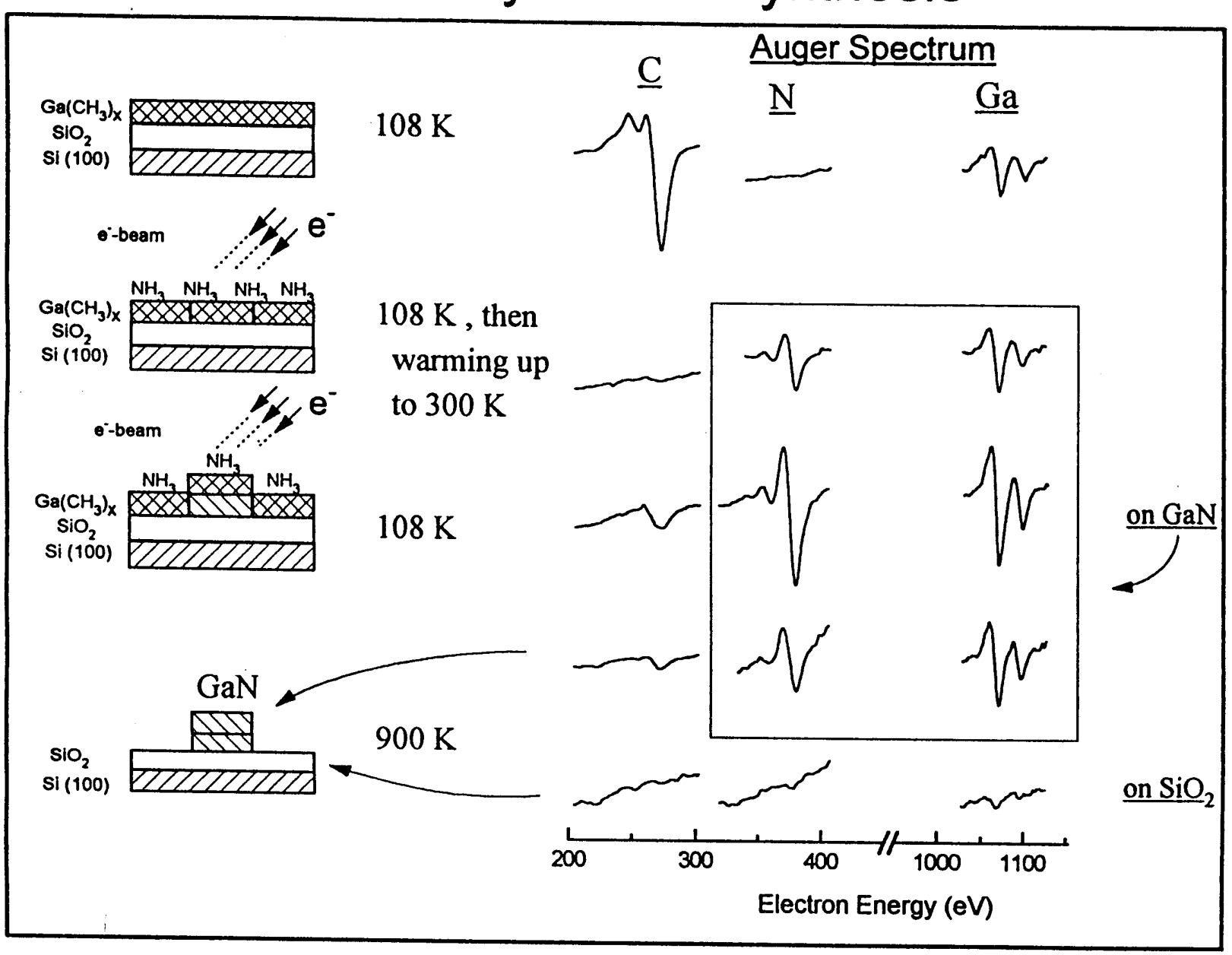

Hubner, et
Figure 7

Hubner, et al.

Figure 8

8. APPENDIX 3

"Cathodoluminescence and FTIR Reflectance of Thin AlN and GaN Films", M. F. MacMillan, R. P. Devaty, W. J. Choyke, A. Khan, M. E. Lin, H. Morkoc, W. A. Bryden, T. J. Kistenmacher, and S. Nakamura, to be published in Proceedings of the ICSCRM-93 Conference, Institute of Physics.

Cathodoluminescence and FTIR Reflectance of Thin AlN and GaN Films

M. F. MacMillan[a], R. P. Devaty,[a] W. J. Choyke[a], A. Khan[b], M. E. Lin[c], H. Morkoç[c], W. A. Bryden[d], T. J. Kistenmacher[d], and S. Nakamura[e]

a) Department of Physics and Astronomy, University of Pittsburgh, Pittsburgh, PA 15260
b) APA Optics, Inc., 2950 North East 84th Lane, Blaine, Minnesota 55434
c) Coordinated Science Laboratory, University of Illinois at Urbana-Champaign, Urbana, IL 61801-3082
d) Applied Physics Laboratory, The Johns Hopkins University, Laurel, Maryland 20723
e) Nichia Chemical Industries, Ltd., 491 Oka, Kaminaka, Anan, Tokushima 774 Japan

ABSTRACT: Cathodoluminescence has been measured at several temperatures (300, 77, and 6 K) for thin (0.1 to ≈ 5.0 μm) AlN and GaN films deposited on 6H SiC and sapphire substrates. Below band gap spectral features due to silicon in GaN and oxygen in AlN have been observed along with many other unexplained features. Room temperature infrared reflectance near the reststrahlen region has also been measured for these samples, providing information about the vibrational modes of the film material. These two optical techniques provide complementary characterization information for thin films.

Wide band gap nitride semiconductors are receiving a great deal of attention recently due to their possible applications for blue or ultraviolet solid state optical devices (Davis 1991). Two wide band gap nitrides currently under study are AlN and GaN, with band gaps of 6.2 eV (Maruska and Tietjen 1969) and 3.39 eV (Monemar 1974) respectively . Rapid characterization techniques are essential for the growth of high quality thin films. This paper presents data on thin AlN and GaN films deposited on 6H SiC and sapphire substrates using two characterization techniques, Fourier transform infrared (FTIR) reflectance and cathodoluminescence (CL), which provide complementary information.

The reflectance data from 400 - 5200 cm^{-1} are collected on a FTIR spectrometer using a KBr beamsplitter and a deuterated triglycine sulfate (DTGS) room temperature detector. The resolution of the spectra is 1 cm^{-1}. The data are collected at near normal incidence (5^0), using a 2000 Å thick platinum film deposited on a sapphire substrate as the reflectance standard (Mantese et al. 1986). The spectra are not corrected for the reflectance of the Pt film.

The reflectance data are compared to calculated reflectance spectra based on Lorentz oscillator models for the frequency dependent infrared dielectric functions of the film and substrate materials. For GaN we use the results of Barker and Illegems (1973). For 6H SiC we use the model of Spitzer et al. (1959) with ε_0 as given by Patrick and Choyke (1970). For sapphire we

use the multi-oscillator model of Barker (1963). Details of the reflectance calculation are given by MacMillan et al. (1993).

The CL spectra were collected at 6 K, 77 K, and 300 K on an instrument described in detail elsewhere (Partlow et al. (1990). The samples are mounted on a cold finger in a UHV chamber ($5x10^{-11}$ torr). The luminescence is excited by an electron beam with energy in the range 5 to 10 keV. The luminescence is passed through a 1 meter Ebert monochromator to a liquid nitrogen cooled photomultiplier connected to either a photon counter or a lock-in amplifier.

Figure 1 shows the room temperature reflectance spectrum in the reststrahlen region of a 0.96 μm thick GaN film deposited on a 6H SiC substrate. Similar reflectance spectra have been seen in thin AlN films deposited on 6H SiC substrates which were analysed in detail by Mac Millan et al. (1993) and will not be discussed in this paper. The complicated structure seen in the GaN film samples is a result of both the film and the substrate having reststrahlen bands in the same region. The triangular shape of the GaN reststrahlen peak is due to the thinness of the film. The sharp dip in the spectrum at 733 cm^{-1} indicates the LO (A_1) vibrational frequency of GaN. This value does not agree with the value of 744 cm^{-1} obtained by Barker and Illegems (1973). However, their values for the vibrational frequencies were obtained from thin GaN films deposited on (0001) sapphire, which has a significant lattice mismatch with GaN. The lattice constant of 6H SiC is much closer to that of GaN and so any strain effects would be less (Strite and Morkoç 1992). Fabry-Perot fringes seen at higher frequencies (not shown on the figure) were used to determine the GaN film thickness.

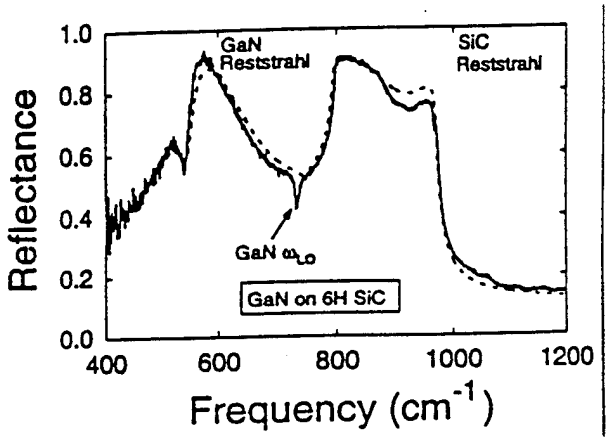

FIG. 1. Relative reflectance of a 0.96 μm thick GaN film on a (0001)-6H SiC substrate. The solid line represents the data and the dashed line the calculated spectrum.

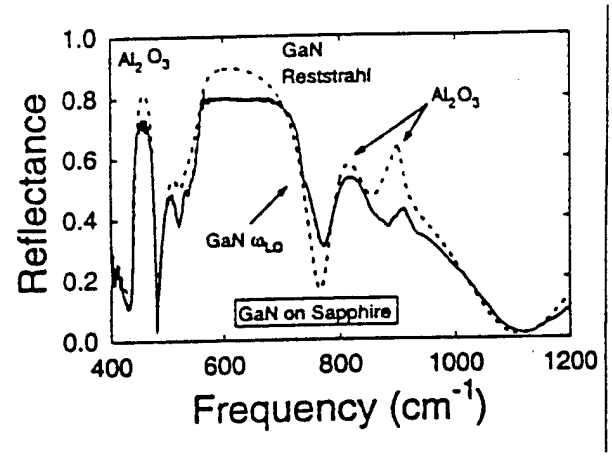

FIG. 2. Reflectance of a 4.52 μm thick GaN film on a sapphire substrate. The solid line represents the data and the dashed line the calculated spectrum.

Figure 2 shows the room temperature

reflectance spectrum in the reststrahlen region of a 4.52μm thick GaN film deposited on a sapphire substrate. Sapphire has several reststrahlen bands in this region, leading to the many reflectance peaks seen in the spectrum. For this film, the $LO(A_1)$ frequency is 743 cm^{-1}, which matches quite well with the Barker and Illegems (1973) value.

Figure 3 shows the low temperature (77 K) cathodoluminescence spectrum of a 4.48μm thick GaN film deposited on a sapphire substrate with a GaN buffer layer between the film and substrate. At this temperature the band gap of GaN is 3.5 eV (Monemar 1974). The small bump lying on the high energy side of the main emission peak at 3548Å has been attributed to free excitons (Dai et al. 1982). The main emission peak at 3567 Å is probably due to bound excitons (Dingle et al. 1971) The two side bands at 3646Å and 3751Å may be LO phonon replicas of the free exciton. This assignment was determined by using the LO phonon energy of 91.3 meV (737 cm^{-1}) obtained from the infrared reflectance spectrum of this sample.

Figure 4 shows the low temperature (77 K) cathodoluminescence spectrum of a 0.5 μm thick GaN film deposited on a 6H SiC substrate. This film was intentionally doped with Si to a level of 1.2×10^{18} cm^{-3}. Silicon acts as an acceptor in GaN with an estimated binding energy of 225 meV (Khan et al. 1986). The peak located at 3775 Å (216 meV) is due to the presence of Si in the sample, but the mechanism for the luminescence has not yet been established.

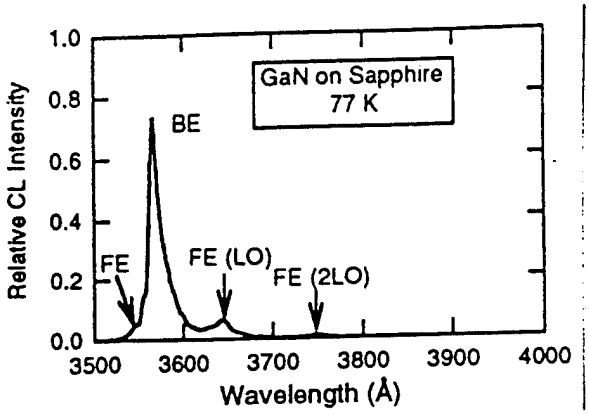

FIG. 3. Cathodoluminescence of a 4.48 μm thick GaN film deposited on a sapphire substrate with a GaN buffer layer

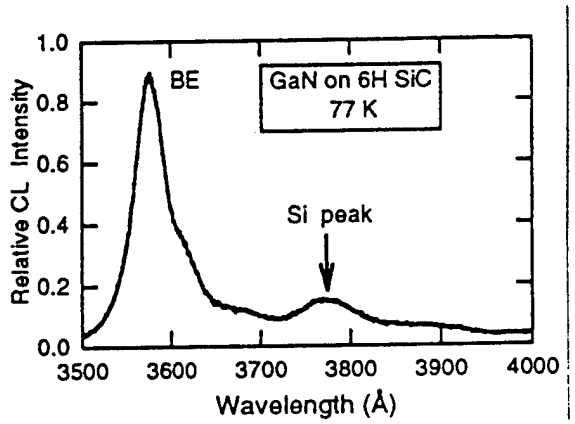

FIG. 4.Cathodoluminescence of a 0.5 μm thick GaN film doped with silicon deposited on a (0001) 6H SiC substrate.

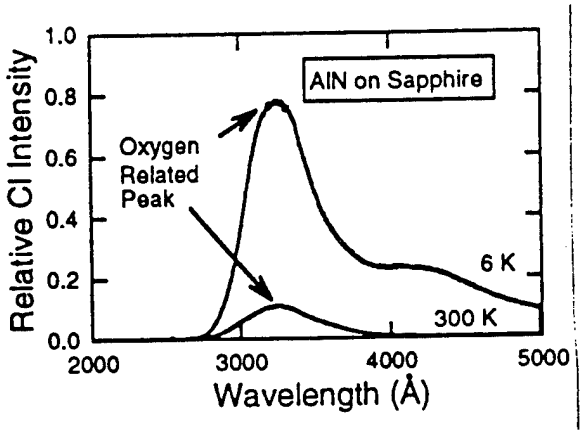

FIG. 5. Cathodoluminescence of a 0.58 μm thick AlN film deposited on a sapphire substrate.

Figure 5 shows both low temperature (6 K) and room temperature cathodoluminescence spectra of a 0.58μm thick AlN film deposited on a sapphire substrate in a UHV chamber. The peak centered at 3260Å is broad and does not shift with temperature. A similar peak was seen in polycrystalline AlN ceramics as well as one high purity single crystal AlN sample by Youngman et al. (1990), who attributed the feature to oxygen in the AlN.

Cathodoluminescence and room temperature reflectance spectra of thin GaN films deposited on SiC and sapphire substrates have been measured. Luminescence due to silicon impurities in GaN have been observed. Room temperature reflectance measurements on GaN films show that vibrational frequencies can be shifted for films deposited on different substrates. For GaN deposited on 6H SiC, $LO(A_1)$ = 733 cm^{-1}. For GaN deposited on sapphire with a buffer layer of either AlN or GaN, $LO(A_1)$ = 737 cm^{-1}. These values are quite different from the value $LO(A_1)$ = 744 cm^{-1} obtained from GaN films deposited directly on sapphire. The cause of this shift is probably strain effects in the film, but this has not been proven. Information about the vibrational frequencies of the film material obtained from the reflectance spectra can be used to understand some of the features seen in the cathodoluminescence spectra.

Acknowledgements

This research was supported under AFOSR Contract # F49620-91-C-0032 and the Materials Research Center, University of Pittsburgh under a grant from AFOSR : #91-0441.

References

A. S. Barker Jr. and M. Illegems, Phys. Rev B 7 , 743 (1973).
A. S. Barker Jr. Phys. Rev. 132 , 1474 (1963).
R. Dai, S. Fu, J. Xie, G. Fan, G. Hu, H. Schrey, and C. Klingshirn, J. Phys. C 15, 393 (1982).
R. F. Davis, Proc. of IEEE, 79, 702 (1991).
R. Dingle, D.D. Sell, S.E.Stokowski, and M. Illegems, Phys. Rev. B. 4, 1211, (1971).M. R.
H. Khan, Y. Oshita, N. Sawaki, and I. Akasaki, Solid State Commun. 57, 405 (1986).
M. F. Mac Millan, R. P. Devaty, W. J. Choyke, Appl. Phys. Lett. 62, 750 (1993).
J. V. Mantese, W. A. Curtin, and W. W. Webb, Phys. Rev. B 33, 9897 (1986).
H. P. Maruska, and J. J. Tietjen, Appl. Phys. Lett. 15, 327 (1969).
B. Monemar, Phys. Rev B 10 , 676 (1974).
W. D. Partlow, J. Ruan, R. E Witkowski, W. J. Choyke, and D. S. Knight, J. Appl. Phys. 67, 7019 (1990).
L. A. Patrick and W. J. Choyke, Phys. Rev. B 2, 2255 (1970).
W. G. Spitzer, D. Kleinman, and D. Walsh, Phys. Rev. 113 , 127 (1959).
S. Strite and H. Morkoç, J. Vac. Sci. Technol B 10, 1237 (1992).
R. A. Youngman and J. H. Harris, J. Am. Ceram. Soc. 73 , 3238 (1990).